Impact of Icelandic dust and volcanic ash on snow and ice

Monika Wittmann

Faculty of Earth Sciences
University of Iceland
2017

Impact of Icelandic dust and volcanic ash on snow and ice

Monika Wittmann (née Dragosics)

Dissertation submitted in partial fulfillment of a
Philosophiae Doctor degree in Earth Sciences

Advisor
Throstur Thorsteinsson

PhD Committee
Andreas Stohl
Finnur Pálsson
Gerrit de Leeuw
Outi Meinander

Opponents
Thorsteinn Thorsteinsson
Andreas Massling

Faculty of Earth Sciences
School of Engineering and Natural Sciences
University of Iceland
Reykjavik, 31 January 2017

Impact of Icelandic dust and volcanic ash on snow and ice
Impact of Icelandic dust on snow and ice
Dissertation submitted in partial fulfillment of a *Philosophiae Doctor* degree in Earth Sciences

Faculty of Earth Sciences
School of Engineering and Natural Sciences
University of Iceland
Sturlugata 7
101, Reykjavik
Iceland

Telephone: 525 4000

Abstract

Located on the mid-Atlantic ridge, Iceland has the largest volcaniclastic desert on Earth, created by glacio-fluvial processes and frequent volcanic eruptions. Due to its location along the North Atlantic Storm track, Iceland frequently experiences high winds. With an abundance of loose dust (particulate matter) from sandur plains and high winds, Icelandic glaciers are exposed to dust storms and redistributed ash. Deposited material is influencing glacier albedo and therefore the surface energy balance. The effects of deposited volcanic ash on ice and snow melt were examined using laboratory and outdoor experiments to find an insulating threshold and showed that ash insulated the ice at a thickness of 9-15 mm whereas maximum melt occurred at a thickness of ≤1-2 mm.

To estimate the frequency of dust events, the dispersion model FLEXDUST was used to simulate dust events on Brúarjökull, a north outlet of Vatnajökull for the year 2012. All simulated dust events showed a corresponding albedo drop at the weather stations. For the weather station B13, near the ELA on Brúarjökull, FLEXDUST produced 10 major dust deposition events and a total annual deposition of 20.5 g m^{-2}.

Surface snow samples from Vatnajökull were analysed for impurities to map the distribution over the ice cap in 2013 and 2015, as well as two 4.5 m deep firn cores on Brúarjökull were drilled in 2015. The cores reached down to the year 2006 and showed distinct dust layers for the years 2014, 2012, 2011 and 2008 and only very small amounts for the years 2007 and 2013.

Sonic sounder for snow elevation measurements at AWS site B13 on Brúarjökull, (picture taken by F. Pálsson in September 2001).

Útdráttur

Á Íslandi er að finna stærstu sanda heims úr basísku gjóskugleri. Þeir hafa myndast úr eldfjallaösku frá fjölda eldgosa og við jökul- og vatnsveðrun gosbergs. Mjög vindasamt er á Íslandi vegna legu landsins í brautum lægða eftir Norður Atlantshafi . Gnægð lausra efna (svifryks) í söndum landsins og vindasöm veðrátta gerir jökla á landsins útsetta fyrir sand- og öskufoki. Efnið sem sest á jöklana hefur áhrif á endurkast sólarljóss frá yfirborðinu. Yfirborðið verður dekkra og tekur upp meira af orku frá sólgeislun; það hefur áhrif á orkubúskap við jökulyfirborð, leysingu og þannig afkomu jöklanna.

Áhrif eldfjallaösku sem sests á snjó og ís voru rannsökuð með tilraunum, bæði á tilraunastofu og í náttúrunni. Fundin voru mörkin þar sem öskuþykkt er svo mikil að hún einangrar alveg og hindrar bráðnun íss og reyndust þau vera 9 - 15 mm. Hámarks aukning í bráðnunar varð hinsvegar þegar öskulagið er um ≤1-2 mm þykkt.

Reiknilíkanið FLEXDUST, sem reiknar dreifingu loftborinna efna, var notað til að herma sandfok á Brúarjökul í norður Vatnajökli árið 2012. Við öll tilvik sandfoks sem komu fram í líkanreikningum mældist samsvarandi lægra hlutfall endurkastaðs sólarljóss frá yfirborði við sjálfvirkar veðurstöðvar á jöklinum. Við veðurstöð nærri jafnvægislínu Brúarjökuls, voru 10 tilvik verulegs sandfoks og uppsafnað magn efnis var 20.5 g/m^2 samkvæmt líkanreikningunum.

Kort af dreifingu ryks á yfirborði Vatnajökuls voru gerð eftir mælingum á rykmagni í snjósýnum sem safnað var af yfirborði (við hausthvörf) Vatnajökuls haustin 2013 og 2015. Einnig var borað eftir tveimur 4.5 m löngum kjörnum úr efsta hluta hjarns á safnsvæði Brúarjökuls árið 2015. Kjarnarnir náðu aftur til ársins 2006 og greinileg ryklög í þeim rakin til hausthvarfa áranna 2014, 2012, 2011 og 2008, en aðeins fannst mjög lítið ryk árin 2007 og 2013.

Dedication

This work is dedicated to my late father Walter Dragosics †

Table of Contents

List of Figures

List of Tables

Abbreviations

a.s.l	Above sea level
AWS	Automatic Weather Station
BC	Black carbon
DOY	Day of the year
ECMWF	European Centre for Medium-Range Weather Forecasts
EDS	Energy dispersive spectrometer
ELA	Equilibrium line altitude
FMI	Finnish Meteorological Institute, Helsinki, Finland
GPR	Ground Penetrating Radar
IES	Institute of Earth Sciences, University of Iceland
MODIS	Moderate Resolution Imaging Spectroradiometer
ppm	Parts per million
w.e.	Water Equivalent

Acknowledgements

This thesis would never have been written without the supervision and help of Thröstur Thorsteinsson. I thank him for the opportunity to do a PhD in Iceland that included Nordic partners in addition to his comments and discussions. He was able to have a good overview of my research topic and main questions.

I am extremely grateful for one of my supervisors and friends, Outi Meinander. During my three months at FMI in Helsinki, she motivated me at a weak period in my PhD and helped me with her organised and structured manner to set the ball rolling. With her and Gerrit's help I was able to write and publish my first paper.

My work also greatly benefited from Finnur Pálsson. Finnur is a very jovial/cordial man and has great expertise in the field on the glacier; I am thankful for my discussions with him and the time on the glacier was great fun! He and his wife, Sjöfn, are one of the cutest couples I know and they work perfectly together in the field as well ☺

I am very pleased for the 3 years I could spend in Iceland. I became colleagues and friends with many lovely people: Izabela, Deirdre, Barbara, Hannah, Daniel Juncu, Vincent, Pavla, Louise, Joaquin, Mary, Paavo, Jed, Morgan, Harald – Mr. Arkímedes, Will[2], Becca, Gro, Ella, Tinna, Hrönn, Águst Þór, Rob, Kate, Sydney, Dave, Mathylda, Jónas, Svandís and the great strong technicians Steini, Sveinbjörn and Águst Pétursson.

Furthermore, I am glad to have won a very special friend. I had spent basically all my lunches and tea (for him coffee only) breaks with him and am sure will be in contact for a long time! Thanks goes to Tobi "the fox" Dürig.

While studying in Askja, I was lucky to meet my Bavarian colleague and now husband Werner <3 Thank you for the support and funny times you have given me these past couple of years.

I would like to thank Magnús Tumi, head of department and president of Jörfi, the Icelandic glaciological society, for his advice and enabling me to twice join the annual expedition to Vatnajökull in order to help take firn cores for my project.

In addition, I enjoyed our weekly glaciology meetings with Tolly, Finnur, Bergur, Águst, Joaquin, Louise, Helgi Eyfi and Sverrir, which were always fun and informative! And no, I did not forget a very valuable part of our glaciology team - Alex! It was great to have another Austrian in the boat. Alex Jarosch greatly assisted me with strategic, personal, but also technical problems.

I want to thank my whole PhD committee for their supervision, and especially my supervisor Andreas Stohl as well as Christine and Sabine for a great 3 months at NILU in Oslo/Kjeller, Norway and for their collaboration.

Last but not least, ich möchte auch ganz herzlich meiner Familie danken, die trotz der großen Entfernung von Österreich immer für mich da waren. Ohne die finanzielle

Unterstützung meines Vaters wäre meine ganze Studienlaufbahn mit Sicherheit anders verlaufen.

1 Introduction

Valley glaciers and small ice caps are known to contribute significantly to sea-level rise on a century time scale. Glaciers are, compared to the large ice sheets Greenland and Antarctica, in a warmer and wetter climate and therefore have fast response times and mass turnover rates, which makes them sensitive to climate change. (e.g. Oerlemans, 2001; Gardner et al., 2013). Icelandic glaciers have contributed ~0.03 mm a^{-1} to sea level rise since the mid-1990s which represents an average annual ice loss of 9.5±1.5 Gt a^{-1} (Björnsson et al., 2013). Fresh snow is one of the most reflective natural surfaces on Earth. Addition of dark impurities decreases its albedo, the reflectivity of the surface, and increases its absorption of solar energy. Therefore, trace amounts of black carbon, dust and other absorbing impurities in snow significantly affect glacier mass balance and regional to global climate (e.g. Hadley and Kirchstetter, 2012, Painter et al. 2007, 2013, Flanner et al. 2007, Hansen and Nazarenko, 2004). The contribution of dust from high-latitude sources is still an underestimated part of the global dust cycle (Bullard et al., 2016). Dust storms originating from high latitudes such as Iceland provide inputs of aeolian sediment to regions far from the subtropical dust belt. It is important to study and understand the potential impacts that the dust may have on wider environmental systems, such as the cryosphere (Baddock et al., 2016). Local dust sources such as from Iceland are very important in the Arctic. Groot Zwaaftink et al. (2016) show that 3% of global dust emission originates from the near-Arctic regions (>60°N).

1.1 Theoretical Background

1.1.1 Dust storms

Iceland is situated in the middle of the North Atlantic and has the largest volcaniclastic desert in the world which covers 22,000 km^2. Iceland is one of the most active aeolian areas and therefore an important dust source for the Arctic (Groot Zwaaftink et al., 2016). Arctic deserts with glacial sediments of riverbeds or ice-proximal areas are an important contribution to the dust cycle (Bullard, 2013; Bullard et al., 2016). The Icelandic desert has been mainly formed by glacio-fluvial processes as well as frequent volcanic eruptions.

Being located along the North Atlantic Storm track, Iceland frequently experiences high winds, resulting in dramatic wind erosion and dust production. Despite the generally moist Atlantic lows, dry winds occur on the lee side of Icelandic mountains and glaciers (Arnalds et al., 2016). Each year dust is transported to glaciers and snow surfaces during dust storms, lowering the albedo and therefore indicating a negative impact on glaciers and snow. The main dust sources are the proglacial areas and sandy deserts, covering more than 22% of the country (Arnalds et al., 2001). A long-term frequency analysis of atmospheric dust observations by Dagsson-Waldhauserova et al. (2014a) states, that on average 34.4 dust days per year occurred in Iceland. A *dust day* is defined as a day when at least one weather station recorded at least one dust observation (Dagsson-Waldhauserova et al., 2013). Airborne redistribution of dust has a strong influence on human health, climate, snow melt, Icelandic soils, and possibly ocean fertility. Satellite images have shown that dust particles can travel very far distances from Iceland and are transported over the Atlantic and Arctic Ocean, sometimes for more than 1000 km (Arnalds, 2010). The shortest distance to the Greenland ice

sheet is only 500 km, and Icelandic dust particles were found in ice-core samples in Central Greenland (Drab et al., 2002). Baddock et al. (2016) modelled trajectories of Icelandic dust transported into the Denmark Strait and towards Greenland, into the Norwegian, Greenland and Barents Seas, and there is potential for delivery to the North Atlantic Ocean in summer months. To reach the central Greenland Ice Sheet trajectories hardly ascend high enough. Icelandic dust is likely to contribute to Arctic and European air pollution and can affect the climate via dust deposition on Arctic glaciers or sea ice (Arnalds et al., 2016). How far particles are transported depends on grain size and wind speed. Smaller grains are more prone to get transported over long distances. The probability for dust events is high in areas with little vegetation and severe or extremely severe erosion. These areas are mainly located along Iceland's south coast and the glacier forefields in the volcanic zone (Arnalds et al., 2001). Volcanic eruptions can have a great effect on the annual averages. After the eruption 2010 in Eyjafjallajökull it was recorded that over 11 million tons of ash passed over a 1 m wide transect, and events such as these continued over extensive areas (Arnalds et al., 2013, Thorsteinsson et al., 2012). In contrast effusive eruptions creating a lava field, such as the Bárðabunga-Holuhraun in 2014-2015 can cause a prolonged emission decrease. In this eruption the new lava covered 85 km^2 of an area that was defined to be in an extreme erosion area (Gudmundsson et al., 2016). Jökulhlaups (glacial outburst floods) have the ability to deliver large amounts of sediment to the sandur plains and therefore were associated to periods of increased dust storm frequency (Prospero et al., 2012). Icelandic tephra origins from the mid ocean ridge basalt and consists therefore mainly of basaltic volcanic glass. The chemical composition of tephra varies depending on the volcanic system and even eruption. Deserts of this composition are globally unique (Arnalds, 2010). Generally phreatomagmatic basaltic eruptions occur in Iceland from subglacial, subaerial, and submarine volcanoes (Thordarson and Larsen, 2007).

Every year a considerable number of dust storms occur in Iceland with presumable deposition of dust or ash on the ice caps (Arnalds et al., 2014). About half of all dust storms that occur in south Iceland each year happen at temperatures around freezing; therefore, dust could be mixed together with snow influencing albedo and snow melt (Arnalds et al., 2016). The transported dust is volcanic in origin (Arnalds et al., 2013) but redistributed and deposited in the glacier forefield where it is mixing with glacial till. From the forefield, it can easily be re-suspended into the air by the action of wind and carried onto the glacier. Arnalds et al. (2014) roughly estimated the total deposition of dust on the Icelandic glaciers to be 4.5 million tons per year with a mean deposition of 400 g m^{-2} year^{-1}, only taking into account the distance to the source, not topography.

The deposition of dust on snow or ice has an important climatic effect due to influence on surface albedo reduction and enhanced snow melt. It has been hypothesized that Iceland's volcaniclastic desert will possibly expand due to glacier retreat, exposing more sediments to wind erosion and therefore increase magnitude and frequency of future dust storms (Thorsteinsson et al., 2011; Bullard, 2013).

1.1.2 Surface energy balance

Glacier melting is determined by the energy balance at the glacier surface. The energy balance is the balance between all positive (warming) and negative (cooling) energy flows to the surface and is controlled by physical properties of the glacier surface and meteorological conditions. The fluxes are expressed in W m^{-2} and are counted as positive if they provide energy to the surface (e.g. Oerlemans, 2001). The energy balance at the glacier-atmosphere boundary is controlled by weather conditions above the glacier and the physical properties of

the ice itself. The interactions between the atmosphere and glacier surface are complex because of feedback mechanisms. The atmosphere affects the energy balance and the atmosphere is affected in turn by the glacier due to the specific properties of snow and ice (Hock, 2005). Generally, snow and ice are characterized by defined surface temperatures during melting (0 °C), incident shortwave radiation, high and largely variable albedo, high thermal emissivity and variable surface roughness (Male, 1980; Kuhn, 1984).

The surface energy balance (Q_M) for a melting glacier surface is defined as the sum of all energy fluxes at the surface:

$$Q_M = Q_N + Q_H + Q_L + Q_G + Q_R \tag{1}$$

where Q_N is the net radiation, Q_H the sensible heat flux and Q_L the latent heat flux. Sensible and latent heat fluxes are known as turbulent heat fluxes. Q_G represents the ground heat flux, the change of the internal energy (temperature change) and Q_R is defined as the sensible heat flux of rain.

The net radiation is the balance between shortwave and longwave radiation flux

$$Q_N = G - R + L\downarrow - L\uparrow \tag{2}$$

where G is the incoming shortwave radiation from the sun (global radiation). It is a function of the solar constant, the solar geometry (e.g. zenith angle), topographic effects (inclination), clouds and atmospheric composition. R is defined as reflected shortwave radiation and a function of the albedo. $L\downarrow$ and $L\uparrow$ are the incoming and outgoing longwave radiation fluxes from the atmosphere.

$G - R$ is the shortwave radiation balance, where $R = \alpha \times G$, so $G - R = G(1 - \alpha)$ where α is the albedo, the ratio of reflected and incoming short wave radiation

$$\alpha = R/G \tag{3}$$

Albedo is dependent upon the material properties of the surface, such as grain size, liquid water content, solar zenith angle and snow layer thickness (Wiscombe and Warren 1980).

Energy for melting

If the sum of net radiation and turbulent fluxes is positive on a temperate glacier, then the energy goes towards:

- **warming** of snow or ice, when the snow or ice temperature at the surface is negative;

- **melting** when the snow or ice temperature at the surface is already zero.

But if the sum of net radiation and turbulent fluxes is negative, then the glacier cools and ablation is zero. The energy available for melt is converted to water equivalent melt, m, and calculated as

$$m = \begin{cases} \frac{Q_M}{\rho_w L_f}; Q_M \geq 0 \\ 0; \quad Q_M < 0 \end{cases} \tag{4}$$

where L_f is the latent heat of fusion ($L_f = 3.34 \cdot 10^5$ J kg^{-1}) and ρ_w the density of water (1000 kg m^{-3}) (e.g. Guðmundsson et al., 2006).

Net radiation is usually dominant in the energy balance of glaciers, contributing up to > 90% of the energy available for melt (Oerlemans et al., 1999). On the Icelandic outlet glacier Brúarjökull net radiation is occasionally equalled by turbulent fluxes. During the melting season, typically around two thirds of the melt energy is caused by radiation and one third by the turbulent fluxes (Figure 1) (Björnsson, 1972; Björnsson et al., 2005; Guðmundsson et al., 2006).
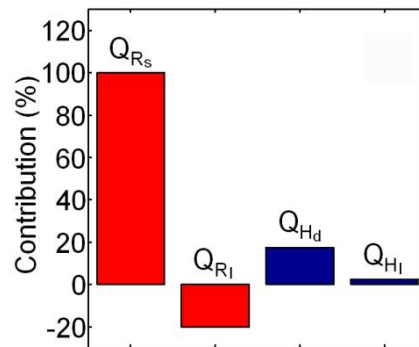
Figure 1: The relative contribution of various energy fluxes to the total energy provided for melting during the ablation season on Brúarjökull (N-Vatnajökull): Q_{Rs} the short wave radiation, Q_{Rl} the long wave radiation, Q_{Hd} the sensible heat and Q_{Hl} the latent heat (Björnsson and Pálsson, 2008; analysis by Sverrir Guðmundsson)

Albedo

Albedo (Eq. 3), the reflectivity of a surface, is a dominant part of the surface energy balance. Albedo of snow can vary from 0.9 to 0.4 or less, depending on snow condition and type, therefore it is an important term for melt rate. Albedo has an important and large influence on the shortwave radiation absorbed by the surface and hence on glacier melt (Cuffey and Paterson, 2010). Grain size, solar zenith angle, ratio of diffuse to direct incident radiation and snow layer thickness are all important parameters influencing albedo (e.g. Wiscombe and Warren, 1980; Meinander et al., 2014). Glacier ice typically has a lower albedo than snow, but ice albedos can span a large range (Table 1). Albedo increases as the solar zenith angle increases; in winter e.g. in Reykjavik the solar zenith angle exceeds 90°, compared to almost 40° in the summer (Sasaki et al., 2003, Figure 2).
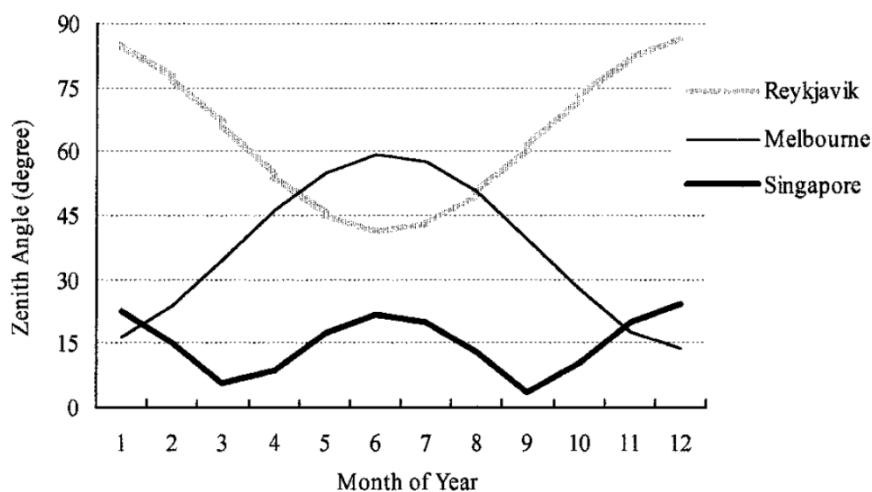
Figure 2: Monthly average of the solar zenith angle at noon for Reykjavík, Melbourne, and Singapore (Sasaki et al., 2003).

Because larger snow grains are more absorptive, albedo decreases as the grain radius or the age increases. Snow albedo as well decreases when the liquid water content increases because it replaces air between ice grains. Since the albedo of a thin snowpack depends on the albedo of the underlying surface, only when the snowpack becomes thick enough, the effects of the underlying surface negligible. Generally it is the topmost 10-20 cm of snow which determines the albedo (Wiscombe and Warren 1980). Albedo has a wavelength dependency of the radiation. AWS measurements used for this work (with Kipp and Zonen CM14, CNR1 or CNR4 sensors), measure at wavelengths from 0.3 – 2.8 μm and gives a relatively uniform spectral response over the range (Kipp & Zonen CNR1, 2002; Guðmundsson et al., 2009). Very low albedo values, dropping below 0.03 in late summer, are not unusual for the ablation area of Icelandic glaciers, such as the ablation area on Brúarjökull (N-Vatnajökull), because of the large amount of tephra layers melting out from below making the surface effectively black (e.g. Oerlemans 2001).

Table 1: Characteristic values for snow and ice albedo from a literature review by S.J. Marshall (Cuffey and Paterson, 2010).

| Surface type	Recommended	Minimum	Maximum
Fresh dry snow	0.85	0.75	0.98
Old clean dry snow	0.80	0.70	0.85
Old clean wet snow	0.60	0.46	0.70
Old debris-rich dry snow	0.50	0.30	0.60
Old debris-rich wet snow	0.40	0.30	0.50
Clean firn	0.55	0.50	0.65
Debris-rich firn	0.30	0.15	0.40
Superimposed ice	0.65	0.63	0.66
Blue ice	0.64	0.60	0.65
Clean ice	0.35	0.30	0.46
Debris-rich ice	0.20	0.06	0.30

Since albedo represents the amount of reflected versus incident radiation, it is a key variable in the surface energy balance and used to calculate melting. With the cryosphere being an important part of the earth climate system, small changes in absorbed radiation at snow or ice surfaces can cause feedbacks with impacts on the climate and hydrological cycle (e.g., Budyko, 1969, Flanner et al., 2007, Painter et al., 2013). The snow- or ice-albedo feedback is a positive feedback loop where a change in the area of snow-or ice-covered land or sea ice alters the albedo. Radiation absorption is enhanced due to impurity content in snow and ice and leads to increased melt (Hansen and Nazarenko, 2004; Myhre et al., 2013). Therefore it's important to estimate changes in snow albedo, to predict changes in seasonal snowmelt and runoff rates and for calculating the regional and global energy budget (Painter et al. 2007). Since Icelandic dust is mainly basaltic, its effect on albedo is somewhat similar to black carbon (Yoshida et al., 2016, Gölles et al., 2015) which has received much interest recently as a short-lived climate forcer, especially in the Arctic (e.g. Quinn et al., 2008; AMAP, 2015; Meinander et al., 2016; Di Mauro et al. 2015).

Temperatures in the Arctic have increased much faster in the past than the global mean temperature, an effect known as Arctic Amplification (e.g. Serreze and Barry, 2011). In Arrhenius, (1986) the Arctic Amplification was originally attributed to albedo feedback, i.e. initial warming induces melting of some of the highly reflecting snow and ice, thus exposing darker surface with stronger absorption of solar radiation which in turn leads to stronger warming. Also more recent research shows that Arctic Amplification is closely linked to the snow albedo feedback (Hadley and Kirchstetter, 2012).

1.2 **Research Objectives**

This thesis addresses current research gaps concerning the impact of dust and ash on snow and ice with the aim of improving our understanding of the amounts of dust getting deposited on Vatnajökull, frequencies of events and how that relates to changes in albedo. This thesis assesses the properties of an insulation effect of ash-covered ice or snow.

The following research questions were focused on:

- What is the influence of ash layers of variable thickness, as would result from dust storms or eruptions and how do they influence glacier surface mass balance?

    o Would they rather insulate the ice or enhance melting?

    o At what thickness is dust or ash insulating the ice and when is the melt maximised?

- How is dust distributed over the area of Vatnajökull?

- What is the impact of dust on glacier albedo?

- Can we quantify or estimate the impact of dust on energy balance?

- Are there variations of dust amounts from year to year and why?

- Is there a relation of dust storms with wind speed and wind direction from data of AWS in the glacier forefield?

1.3 **Outline of the dissertation**

This doctoral thesis is based on the results presented in three first-author papers (née: Dragosics), these are referred to by roman numbers (PAPER I– III). One paper is published in a peer-reviewed international journal, in a special dust issue of the Arabian Journal of Geosciences, where most often Saharan dust is considered and therefore it is an important contribution of Icelandic Arctic dust sources introduced into the Saharan dust research community. The second paper is in review and the third paper is in preparation. After the current introductory chapter 1 about dust storms and albedo, the thesis is structured as follows: in chapter 2, data and methods are presented and chapter 3 contains a summary and the main results based on the original papers. General conclusions are included in chapter 0.

The papers are:

I: Dragosics, M., Meinander, O., Jónsdóttir, T., Dürig, T., de Leeuw, G., Pálsson, F., Dagsson-Waldhauserová, P., and Thorsteinsson, Th. (2016): Insulation effects of Icelandic dust and volcanic ash on snow and ice. *Arabian Journal of Geosciences*, 9, 126, doi: 10.1007/s12517-015-2224-6

II: Dragosics, M., Groot Zwaaftink, Ch., Schmidt, L.S., Guðmundsson, S., Pálsson,F., Arnalds, O., Björnsson, H., Thorsteinsson, Th., Stohl, A.: Impact of dust deposition on the albedo of Vatnajökull ice cap, Iceland. Submitted to *The Cryosphere*.

III: Wittmann, M., Vogel, A., Groot Zwaaftink, C. D., Butwin, M., Pálsson, F., Thorsteinsson, Th.: Ground based measurements of dust deposition on Vatnajökull; Firn core analysis and surface dust samples. In preparation for *Jökull*.

2 Data and Methods

In this thesis, the main focus is data from automatic weather stations as well as ground based measurements sampled on Vatnajökull and analysed to estimate annual dust deposition and its impact. Experiments conducted at FMI, Helsinki, contribute to a better understanding of insulation characteristics of ash and dust deposition on Icelandic glaciers. They were carried out in the laboratory and outside of FMI in a fenced area on snow in natural conditions. Results from the application of the dispersion model FLEXDUST, developed by Groot Zwaaftink et al. (2016) gave an assessment of the frequency and amount of dust events deposited on Brúarjökull in 2012.

2.1 Study area

Iceland is an island situated in the North Atlantic Ocean with an area of 103,000 km^2. Even though it's situated close to the Arctic Circle, the Irminger ocean current causes mild climate and small seasonal variations in temperature (5 °C annual temperature). On the Icelandic south coast the average winter temperatures lie around freezing temperatures and summer temperatures average 11 °C in the warmest month (Einarsson, 1984; Björnsson and Pálsson, 2008). On the Icelandic northern coast the polar East Greenland Current affects the climate. The typical *Icelandic low* frequently forms in the North Atlantic over Iceland and brings heavy precipitation. Due to the maritime climate today ~11% of Iceland's area is glacierized (Figure 3) (Björnsson, 1978, 1979; Björnsson and Pálsson, 2008). Icelandic glaciers are warm-based and preserve a large reservoir of ice, turning into meltwater and feeding the main rivers which are harnessed for hydropower (Thorsteinsson et al., 2013). Jökulhlaups (glacier outburst floods), frequently occur due to geothermal and volcanic activity. Many active volcanoes are covered by glacierized areas. The main part of the precipitation falls as snow on top of the ice caps due to perennial freezing temperatures. Most of the glaciers in Iceland are located close the southern coast caused by prevailing southerly precipitation. Annual precipitation values can exceed 4,000-5,000 mm above 1300 m a.s.l. on the southern side of Vatnajökull and Mýrdalsjökull (Crochet et al., 2007). Around 1990 annual mass balance measurements were initiated on the large ice caps such as Hofsjökull, Vatnajökull, Langjökull and Drangajökull. These measurements are important to estimate the glacial meltwater contribution feeding the river systems as well as whether glaciers are growing or shrinking. In the melting season (approximately a 100-day period) on some of the ice caps several automatic weather stations (AWS) are operated, beginning in 1994 on Vatnajökull. At the AWSs radiation components are measured directly. Turbulent fluxes are calculated using wind, air temperature and humidity measurements in the boundary layer. Katabatic glacier winds are dominating the boundary layer, especially in the lower, steeper regions of the ice caps. Only strong winds can interrupt the glacier winds. (Björnsson and Pálsson, 2008)
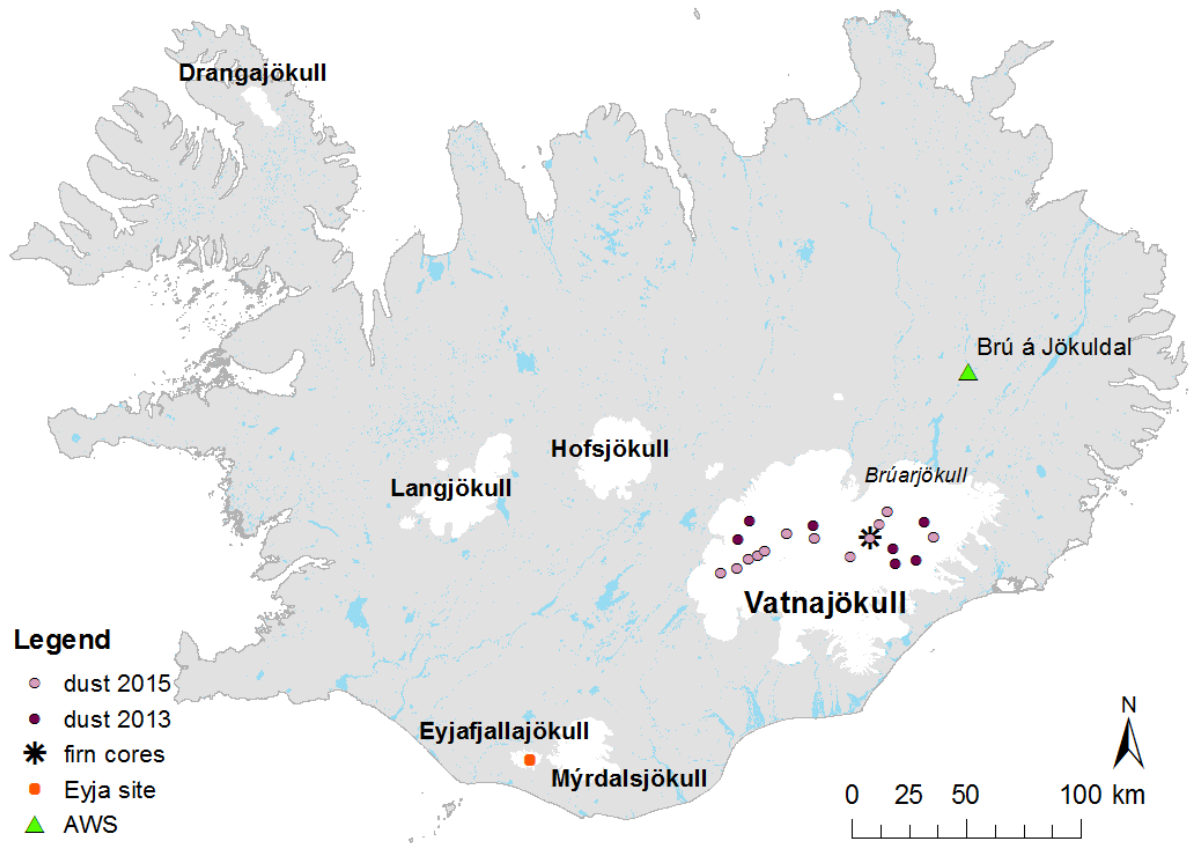
Figure 3: Iceland with glacier outlines and sample sites on Vatnajökull and Eyjafjallajökull (Eyja site) (base map by Landmælingar Íslands, 1993).

Vatnajökull

Vatnajökull is the largest ice cap in Iceland and Europe (by volume ~3,100 km³) with an area of 8,100 km². It is located in the south-east of Iceland and covers ~8% of the country. The ice thickness averages to ~400 m and reaches up to 1000 m in some areas. Except the year 2014/15 mass balance has been negative over Vatnajökull for the past two decades, and similar is true for all the larger ice caps in Iceland (e.g. Björnsson et al., 2013; Jóhannesson et al., 2013; Pálsson et al., 2012; Magnússon et al., 2016). For most of Vatnajökull the summer mass balance is negative, but might be slightly positive in the highest regions due to summer snow fall and therefore high surface albedo. Cold summer temperatures only allow 10-20 days of melting conditions, whereas in the ablation area ablation lasts for about three to four months. When ablation areas melted out and the pervious years melt layer comes to the surface, albedo can drop to values lower than 0.1 because of exposed tephra layers within the ice. Some of the outlet glaciers of Vatnajökull and Mýrdalsjökull reach very low elevation (100 m of less) and therefore even the winter balance is negative in those areas. The northern lee side of Vatnajökull counts to the dry central regions of Iceland and receive annual precipitation values of only 400-700 mm (Björnsson and Pálsson, 2008). Vatnajökull has about 30 outlet glaciers, one of them being Brúarjökull (Figure 4), the largest outlet of the ice cap. Brúarjökull is a north facing outlet with a current area of ~1500 km², ranging in elevation from ~600 to ~1900 m a.s.l. The ELA is situated at around 1200 m a.s.l. (Björnsson et al., 1998).
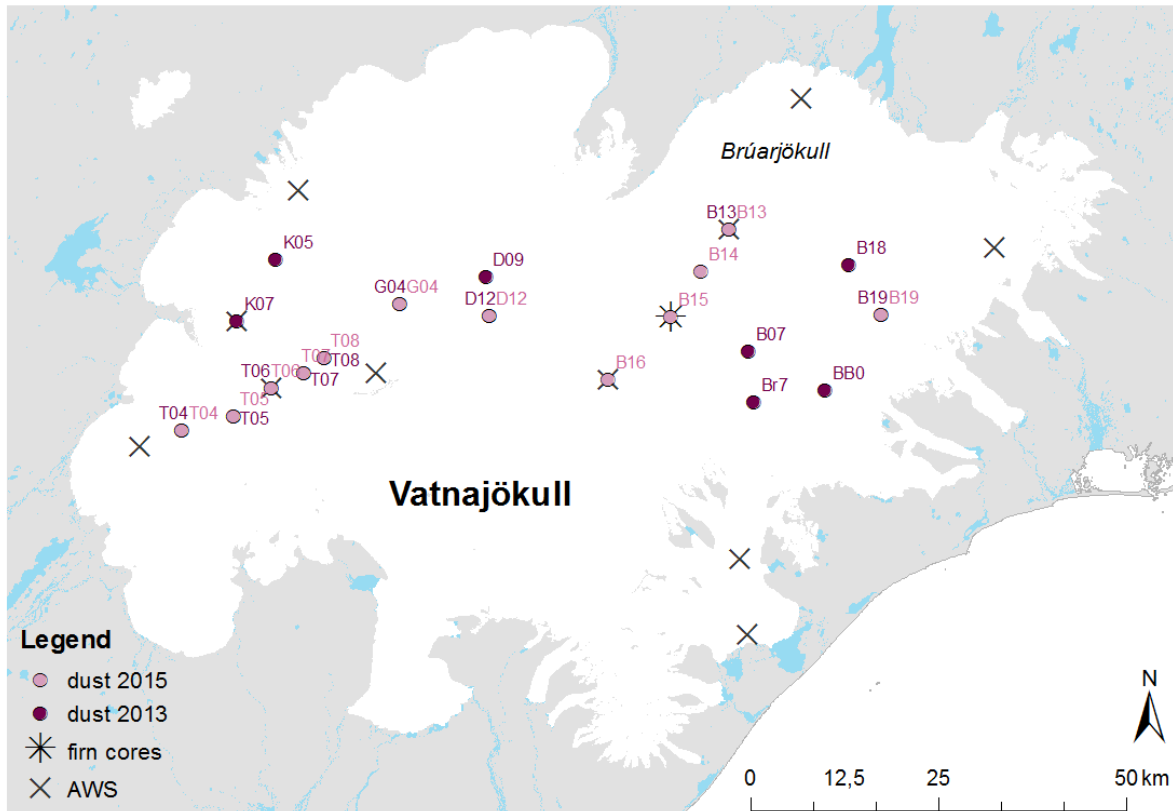
Figure 4: Sample sites and Automatic Weather Stations (AWS) on Vatnajökull ice cap (base map by Landmælingar Íslands, 1993).

Dyngjusandur

Dyngjusandur is located north of Vatnajökull (Figure 5), to the north bordered by the Askja volcano and to the east by the major glacial drainage system of Jökulsá á Fjöllum. Dyngjusandur covers about 170 km^2 and its sediment thickness reaches around 10 m. Glacier meltwater from Dyngjujökull is feeding numerous outlet streams merging into Jökulsá á Fjöllum (Baratoux et al., 2011). Arnalds et al. (2016) states that Dynjgusandur is Iceland's most extensive dust source area where several dust events can occur each day during dry summer periods. Most of the dust is transported to the north but dust directions range from south east to west, depending on dry wind directions. Over 300,000 tons of dust can be transported during a storm event, sometimes extending far into Arctic regions.
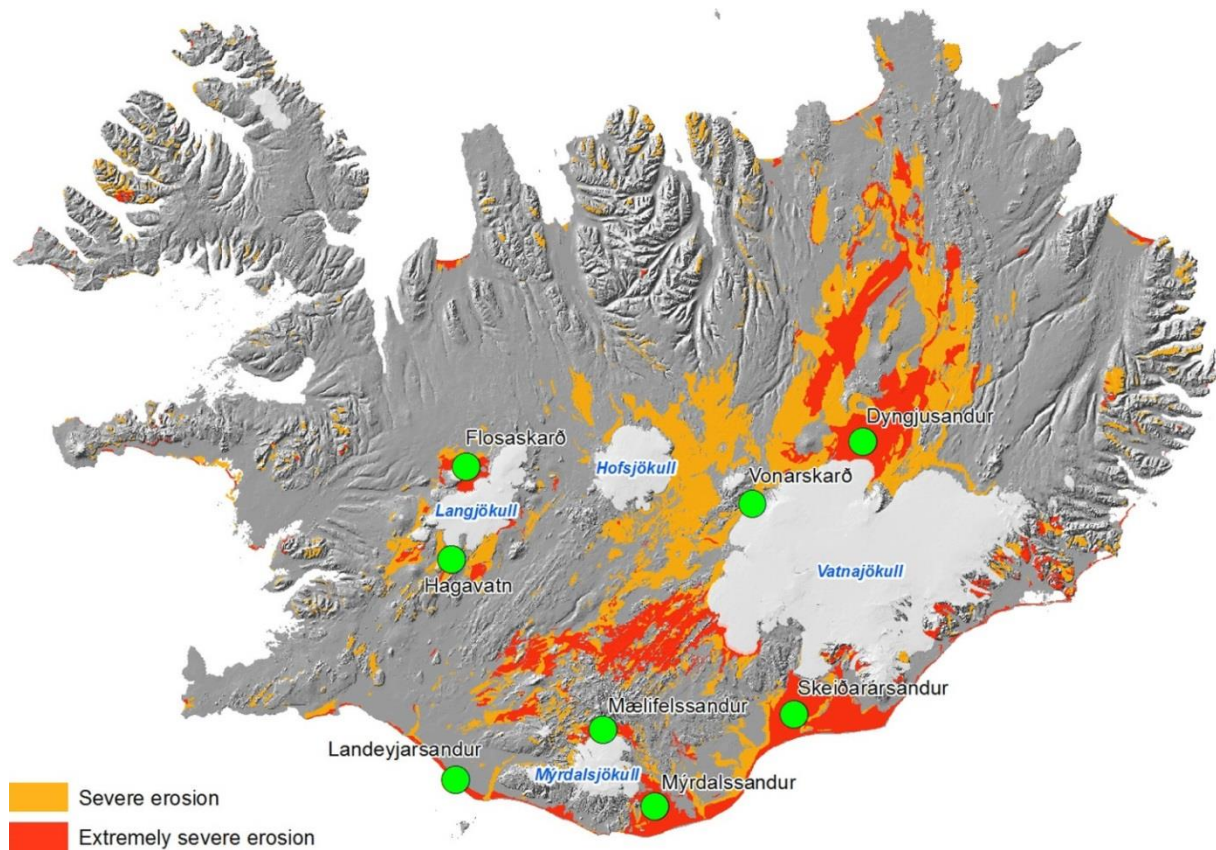
Figure 5: Sandy deserts in Iceland, in yellow severe erosion, in red extremely severe erosion. These sandur plains cover large proportions of the country and are mainly located at glacier margins. Highlighted with green circles are dust hot-spots, areas with most active dust emission. Figure by Arnalds et al. 2016.

2.2 Ground based measurements

2.2.1 Experiments at FMI

For the study on the impact of ash on surface melt, four outdoor and laboratory experiments with ash from the Eyjafjallajökull eruption 2010 (sample site in Figure 3, *Eyja site*), were carried out at the Finnish Meteorological Institute (FMI) at Kumpula Kampus in Helsinki, Finland. These experiments improved the understanding of insulation characteristics of ash and dust deposition on Icelandic glaciers or elsewhere.

In the first experiment, the Ash on Snow (AoS-2015) experiment, the effect of ash on snow in natural conditions outdoors was tested with an ash grain size of 1 ɸ (500 μm) and three different amounts of ash: 15 g, 85 g and 425 g (15 mm layer thickness). The ash was deposited on an area of $0.3{\times}0.3$ m^2 on a snow surface, and snow depth and temperature were then monitored for 17 days until the snow had melted naturally.

The second and third experiment (Roof-2015), with ash on ice (AoI-2015), was performed in the laboratory, and Roof-2015, performed outdoors in sunny conditions. Both experiments contained the same amounts of ash with grain site of 1 ɸ over a ~2.5 cm thick ice layer (frozen tap water): 3 g, 35 g (1 mm layer thickness), 71 g (3 mm layer thickness) and 283 g (9–13-mm layer thickness). In the roof experiment two different grain sizes were used: 1 and

3.5 ϕ. After the deposition of the material, the ice was transferred into white pots with holes in the bottom to measure the meltwater runoff.

The fourth experiment, the Ash in Container (AiC) experiment, was an evaluation experiment in a cold container at -10°C, to see the impact of cooling from above and melting temperatures only from the surface, a more realistic approach to a glacier surface. Inside a cold container, a big pot was filled at the bottom with a thick ice layer and on top of that an 8.5-cm thick layer of snow was deposited. Two different amounts of ash concentrations were deposited: 15 g and 425 g (15 mm thickness) of 1 ϕ grain size on a 0.3×0.3 m² area, and the snow depth was monitored.

2.2.2 Automatic Weather Stations

11 AWSs are deployed during summer at various locations on Vatnajökull, in a collaborative program of the National Power Company and Institute of Earth Sciences. The first AWS was installed in 1994. One to three AWSs have been operating on Brúarjökull since 1994 (Figure 4). The AWSs measure and archive incoming and outgoing shortwave radiation as well as incoming and outgoing longwave radiation at ~2 m above the glacier surface. Air temperature, relative humidity, wind speed and direction are measured at one to four levels above the surface (vertical profiles often at 2 and 4 m above the surface). The AWSs are operating approximately from May until October every year. A sonic echo sounder measures the daily surface changes due to melting (and snow accumulation), and with measurement based assumptions about the snow density, the corresponding ablation in water equivalent can be calculated. (Guðmundsson et al., 2006)

Since 1993/94 the mass balance has been conducted at ~15 survey sites on Brúarjökull. Each year in April or May, cores for measuring winter mass balance and snow density have been drilled through the winter layer. The summer mass balance is measured in September or October from readings at stakes or on wires, drilled into the glacier in April or May and left there over the summer (Björnsson et al., 1998, 2003). Figure 6 shows the mass balance (net balance in green) in m w.e. for Brúarjökull from 1993 to 2016 with most years being negative.
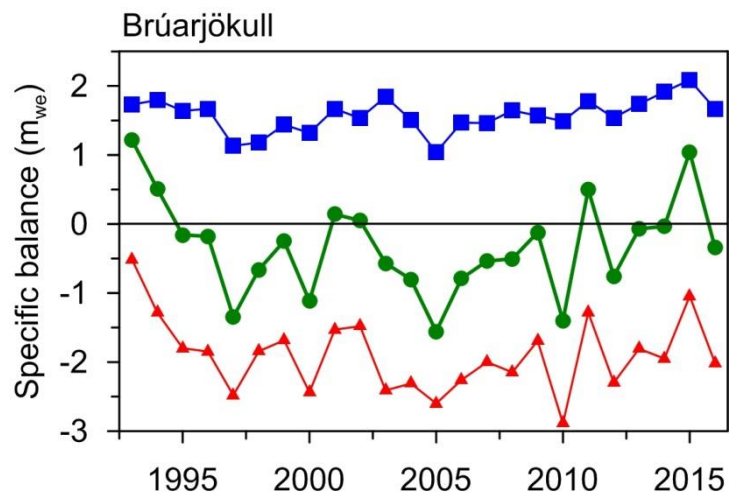
Figure 6: Mass balance records in m w.e. for station B13 at Brúarjökull for the years 1993 to 2016. In blue the winter balance, in red the summer balance and in green the net balance (data from IES Glaciology Group).

13

Albedo

Since 1996, the AWSs at B13 and B16 on Brúarjökull (Figure 4) have measured the energy balance components (Eq. 1). Albedo is estimated from the measured incoming and reflected short wave radiation (Eq. 3). Daily albedo values were calculated as the average over 10 minute data obtained between 13 and 14 UTC, when the solar zenith angle is smallest (Guðmundsson et al., 2006). The uncertainty has been estimated to be 3-5% on an ice sheet surface (e.g. Guðmundsson et al., 2009).

2.2.3 Surface snow samples

In October 2013 and 2015 surface snow samples on Vatnajökull were taken. The samples contain dust from the previous year melted out firn layer and enable us help to estimate the dust deposited during spring and summer on the snow and ice surface. The top ~8 cm (1-7 kg) of snow including impurities were brought back in plastic bags to the laboratory in Reykjavik, where they were cut into smaller segments, measured and then melted. Turbidity was measured for all samples in ppm with a MONITEK turbidity meter (galvanic.com). After the samples had evaporated, the mass of the dust was weighed in beakers. In 2015 the melted ice was filtered through quartz filters and the remaining mass on the filter was weighted, to achieve a better accuracy. In 2013, 16 locations on Vatnajökull were sampled, and in 2015, 12 samples have been taken the same way (Figure 3). Not all sample locations overlapped for both years, but 9 of the 12 samples were at the same location as in 2013. In 2015 the focus was more towards sites on Brúarjökull, therefore sites B13-16 were sampled.

The dust concentration was interpolated for Vatnajökull in g m^{-2} using the ArcGIS tool IDW (Inverse Distance Weighting) for a simple comparison approach, without taking topography into account. The southern part of Vatnajökull was not included in the interpolation since it is too far from the sample survey sites.

2.2.4 Firn cores

Within the framework of the spring expedition of the Icelandic Glaciological Society in 2015, it was possible for this work to drill two firn cores on Brúarjökull. On 3 June 2015 two cores at and close to site B15 on Brúarjökull (Figure 3) were drilled.

Figure 7: Firn core drilling on Brúarjökull with the Icelandic glaciological Society, Jörfi. On the right pictures: the drilled core, broken into segments with a close up with of sample A20, showing the 2011 dust layer.

The first core, core A was drilled close to (10 m) the mass balance survey site B15, and core B 650 m down glacier from B15, towards site B14. At the time of drilling, in spring 2015, all 590 cm of winter snow was still intact on top of the 2014 summer layer at core site A, and 530 cm at core site B. The denser layer of the summer surface of 2014 was defined as reference depth zero and sampling for the core analysis started from there. The total length of core A was 454 cm and of core B 455 cm (without the winter snow). The firn cores were drilled with the help of an engine driven snow corer, used for mass balance measurements (3" snow corer, Engineering & Science Research Support Facility, College of Engineering, University of Nebraska-Lincoln, USA) and automatically broke into pieces while drilling (Figure 7). The firn core pieces were weighted, measured (length and diameter) on the sample site before they were labelled and brought back frozen to the laboratory in Reykjavik. At the University of Iceland, they were cut in half longitudinally with a band saw; their dimensions were measured again, and the firn pieces were melted. Turbidity and filtering through quartz filters was measured in the same manner as used for the surface snow samples 2015. If the turbidity exceeded 10 ppm, the sample was considered as dusty and filtered through a quartz filter. The dust that remained on the filter was weighted by a scale with an accuracy of 0.1 mg. Depending on the depth of the core, the age of the firn could be allocated by density measurements and mass balance measurements from B15. For example when the mass balance (b) for the year 2014 was 148.8 cm and the measured density (ρ) in the top (~10 cm) of the firn core 0.62 g cm^{-3} this was multiplied ($b \times \rho$) and resulted in a layer thickness 92.8 cm corresponding to the year 2014. The whole core depth was calculated this way resulting in the oldest year being 2006.

2.2.5 FLEXPART

To simulate atmospheric dust concentrations and depositions on Vatnajökull, a dispersion model was used. The recently developed scheme, called FLEXDUST, described in detail in Groot Zwaaftink et al., 2016 is used to estimate dust emission. These emission estimates that can be imported directly into the Lagrangian particle dispersion model FLEXPART (Stohl et al., 1998, 2005) to estimate mineral dust transport, concentrations in the atmosphere and deposition on the surface. FLEXDUST is based on meteorological data from the European Centre for Medium-Range Weather Forecasts (ECMWF), land cover data by the Global Land Cover by National Mapping Organizations (GLCNMO) and additionally, for Iceland, a high-resolution land cover data set that identifies sandy deserts (Dagsson-Waldhauserova et al., 2014; Arnalds, 2015). Snow cover as well as precipitation inhibits the dust emission. It is assumed that emitted dust particles have a size between 0.2 and 18.2 µm and follow a size distribution after Kok (2011). In particular the areal distribution over Vatnajökull for the years 2012 and 2013 as well as dust events at the two AWS B13 and B16 situated on Brúarjökull outlet were simulated.

3 Presentation of papers

3.1 Paper I: Insulation effects of Icelandic dust and volcanic ash on snow and ice

3.1.1 Summary

Dust or volcanic ash is likely to be deposited on Iceland's ice caps during several dust storms every year (Arnalds et al., 2014). Volcanic tephra is also directly deposited from volcanic plumes during eruptions. Dust changes the glacier surface albedo and affects or even controls to a great extent the surface melt rates. Four outdoor and laboratory experiments with tephra have been conducted to study its influence on snow or ice melt. Basaltic ash from the eruption of Eyjafjallajökull (2010) in the grain sizes 1 and 3.5 ϕ have been used to identify an effective and critical thickness. The critical thickness characterizes the thickness of ash where the ablation rate equals that of clean snow; more ash would start to insulate. The effective thickness is the thickness where ablation is maximized (Brock et al., 2007). It is important to study different ash deposition amounts and their influence of glacier surface mass balance, such as after eruptions or dust storms, whether they insulate the ice or enhance melting. Results from our experiments show that a thin ash layer enhances snow and ice melt, but an ash layer exceeding a certain critical thickness insulates. Experiments showed that ash with a grain size of 1 ϕ insulated the ice at a thickness of 9-15 mm. For the finer grain size 3.5 ϕ it needs 13 mm to start insulating. Effective thickness was reached at a thickness of only 1 mm for both grain sizes.

3.1.2 Main results

- Four outdoor and laboratory experiments have been carried out at FMI in Helsinki. Results contribute to a better understanding of insulation characteristics of ash and dust deposition on Icelandic glaciers. Four outdoor experiments called AoS-2015, Roof 2015 and AiC-2015 as well as one laboratory experiment (AoI-2015) were carried out using snow (AoS-2015), ice (AoI-2015, Roof 2015) and snow over ice (AiC-2015).
- Our findings suggest that small concentrations, so very thin layer thicknesses, have the potential to increase snow or ice melt, but increasing thickness after a certain threshold would insulate.
- Table 2compares critical and effective thickness of different materials with the results of our experiments and shows very good agreement with e.g. thicknesses of Hekla or Grímsvötn tephra.

Table 2: Effective and critical thickness for different materials such as tephra, rock debris and dust in comparison (modified by Dragosics et al., 2016)

Material	Effective thickness [mm]	Critical thickness [mm]
Mt St Helens (1980) ash[1]	3	24
Hekla (1947) tephra[2]	2	5.5
rock debris [2]	~10	~15-50
Villarrica tephra (lapilli) [3]	-	<5
Dust (largely organic matter) [4]	-	1.33
Grímsvötn[5]	1-2	10
Eyjafjallajökull ash (2010, 1 φ)	1	9-15
Eyjafjallajökull ash (2010, 3.5 φ)	≤1-2	13

[1] Driedger (1981); [2] Kirkbride and Dugmore (2003); [3] Brock et al. (2007); [4] Adhikary et al. (2000); [5] Möller et al. (2016)

- In the Ash on Snow (AoS-2015, Figure 8) outdoor experiment ash concentrations with three different amounts, 15 g, 85 g and 425 g (15 mm layer thickness) in the size of 1 φ were deposited on natural snow on the ground. The effective thickness was reached at the medium concentration (85 g), and the critical thickness was achieved at the largest deposition of 15 mm layer thickness since the clean control snow took the same time to melt as the 15 mm deposition.
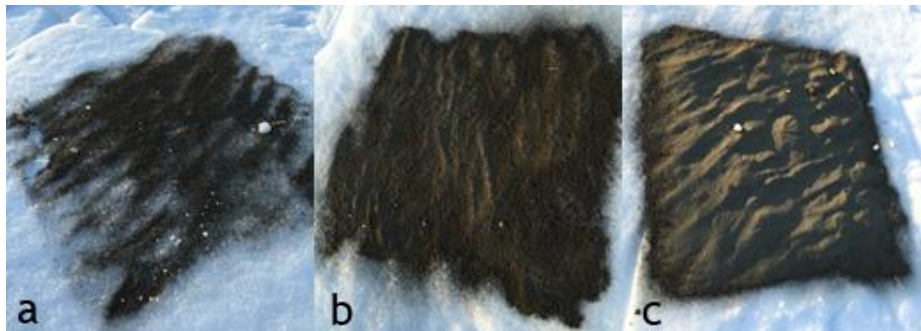
Figure 8: During the AoS-2015 experiment, different amounts of ash were deposited on a 0.3×0.3 m2 snow surface. a) 15 g, b) 85 g and c) 425 g (15 mm layer thickness) (Dragosics et al., 2016)

- The Roof-2015 experiment was a repeat of the Ash on Ice (AoI-2015) experiment from the laboratory to outside in sunny conditions with both grain sizes. The highest concentrations with 9 and 13 mm layer thickness were exceeding the critical thickness at both grain sizes because they were starting to melt later than the clean reference sample in the sun. The 1 mm thick layer (1 φ) was achieving the effective thickness.

- The two grain sizes showed different behaviours after the material was saturated. The finer material slipped off the ice, whilst the A-material stayed on the surface. The reason for this lies in the different surface morphologies. The coarser material shows clustering with fine adhesive particles and therefore a larger specific surface area than the finer particles with a smoother surface.

- The critical thicknesses are comparable and visible in all our experiments. In comparison, the effective thickness was reached at Hekla tephra at 2 mm and at Eyjafjallajökull ash at 1 mm, in the Roof experiment. The finer grain size needs a thickness of 13mm to start insulating as observed in the Roof experiment which also shows that only an ash thickness of 1–2 mm or smaller are enough to enhance melt to a maximum.

3.2 Paper II: Impact of dust deposition on the albedo of Vatnajökull ice cap, Iceland.

3.2.1 Summary

Dust deposition rates computed with the dispersion model called FLEXDUST (Groot Zwaaftink et al., 2016) for the surface of Vatnajökull were compared with ground based measurements and measured albedo values. Albedo used this study was determined from the two upper AWSs on Brúarjökull outlet, namely site B13 at ~1210 m a.s.l. and site B16 at ~1525 m a.s.l. A dust event is defined as: minimum modelled concentration of 6 µg m^{-3} over at least two days. In this paper the focus was on the year 2012, an exceptionally warm year with distinct modelled dust events and numerous observed low albedo values at the AWSs. The simulated dust events in 2012 were more striking and in better agreement with the albedo observations than in 2013.For the year 2012 no autumn surface snow samples were available, but they were for 2013, thus the spatial dust distribution for 2013 was also modelled by FLEXDUST for the same time period (until October 2013). The modelled and measured dust concentrations of 2013 were compared and show good agreement.

Meteorological parameters from the AWSs, such as albedo, temperature and wind were compared with dust concentration and deposition values from FLEXDUST as well as MODIS images for the measurement period in the year 2012. Four main dust events resulted from the simulations with concentrations as high as 6.6 g m^{-2} (deposited during a period of 14 days), and six smaller events occurred.

To estimate the impact of dust lowering the surface albedo, the energy balance for a clean glacier surface was simulated by the regional climate model HIRHAM5 for the weather conditions observed at the AWS B13 and B16 in 2012. By comparing the simulated HIRHAM5 albedo (the modelled albedo does not include the effect of dust, only that of the aging of the surface) with the measured albedo, we estimate the difference in snow melt with an increase by ~60% due to dust deposition, for both stations, and melting out of the dusty firn surface below at the lower site B13.
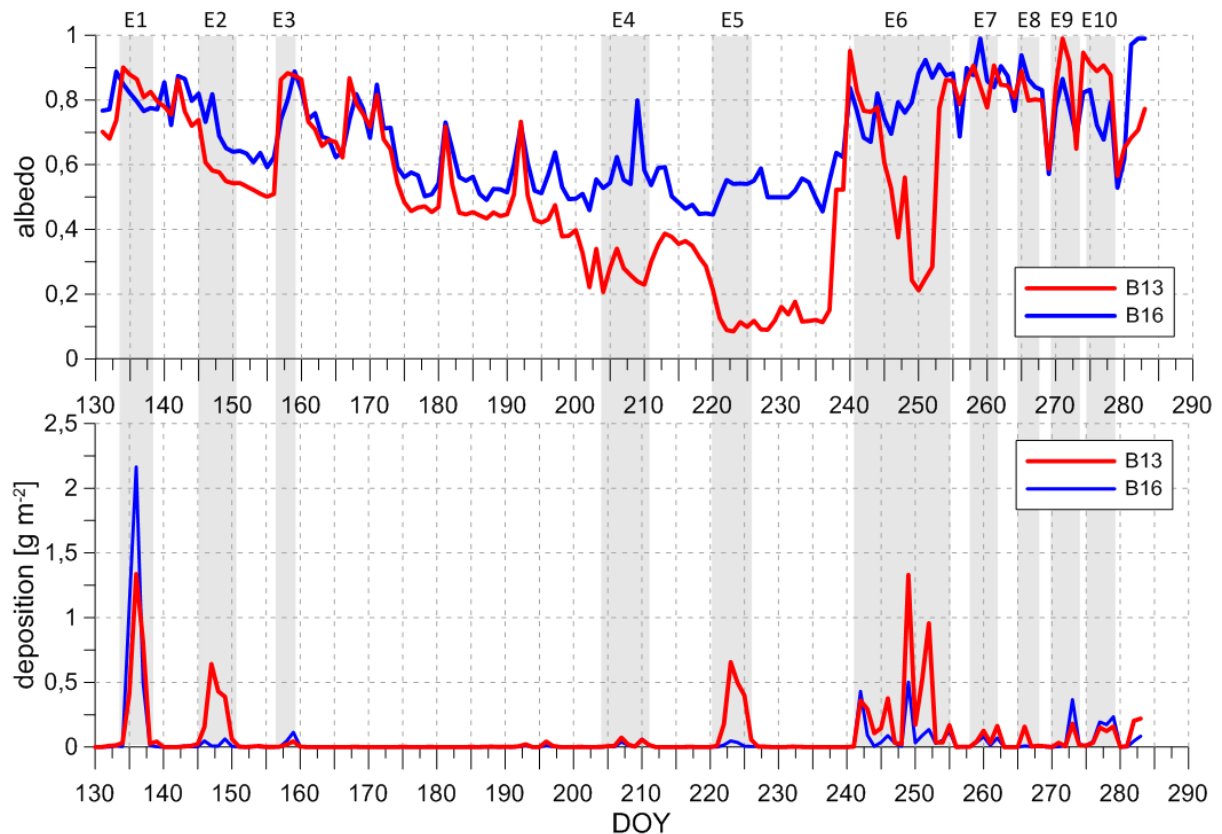
Figure 9: Upper graph: Albedo measurement in red from the AWS at station B13 and in blue station B16 for the measurement period in 2012. Lower graph: Simulated daily dust by FLEXDUST. Dust events are highlighted in beige and named E1-E10.

3.2.2 Main results

- The spatial dust distribution map produced by FLEXDUST, and the spatial distribution of the interpolated surface dust map, based on dust measured in the surface snow samples with impurities at 16 survey sites on Vatnajökull, show a similar pattern. The highest concentrations are found in the SW ice cap (Tungnaárjökull, Skaftárjökull, Síðujökull), followed by the north western and northern parts (Brúarjökull).

- FLEXDUST simulated ten dust events at the lower AWS, B13 during the measuring period (9 May to 14 October 2012). These dust events coincide with an observed albedo drop during each event at the AWS. Four main events with high dust concentrations and depositions, and six smaller events occurred (Figure 9).

- An average dust event at station B13 in 2012 had a duration of 6 days with a maximum dust concentration of 122 μg m^{-3} and a total deposition of 2 g m^{-2}. On average the albedo dropped during a dust event by 0.18. The average temperature occurring during a dust event was -2°C (at ~1210 m elevation) and in 80% of the events the prevailing wind direction was north, in 20% southwest (glacier wind). Precipitation of ~23 mm occurred on average during a dust event.

- The energy balance of a clean glacier surface was modelled by HIRHAM5 and compared to the observed energy balance with the only difference being the albedo.

20

- The total summer melt for a simulated dust-free surface at the lower site B13 in 2012 was estimated to be 1.7 m w.e., in comparison to measured values of 2.8 m w.e. Therefore, the melt rate due to impurities increased by 1.1 m w.e., or ~60%. At station B16, 1.0 m w.e. of snow melt was simulated for a dust free surface and 1.6 m w.e. for observed data. Therefore, melt rates increased as well by 60% (0.6 m snow melt) caused by dust on the surface. Reasons for the difference in albedo or melt were assumed to be dust deposited during dust storms and redistribution, as well as melting out of the dusty firn layer at station B13.

- The main wind direction at B13 was from a northerly direction during dust events which confirms the main dust source being Dyngjusandur, north of Vatnajökull.

3.3 Paper III: Ground based measurements of dust deposition on Vatnajökull; Firn core analysis and surface dust samples

3.3.1 Summary

In autumn 2013 and 2015 snow samples with impurities were collected on the surface of Vatnajökull. Samples from 16 locations in 2013 and 12 locations in 2015 were sampled and analysed for dust content. The sites did not completely overlap in both years: 9 of the 12 locations were the same in 2015 as in 2013. Overall surface dust was deposited in a very similar pattern, with most deposition in SW Vatnajökull, on Tungnaárjökull followed by Brúarjökull in the north. Amounts of dust deposition were in general larger in 2013 than 2015. Other ground based measurements, such as two firn cores have been taken on Brúarjökull close to the station B15 in spring 2015. Firn core A and B were drilled 650 m apart from each other with a depth of 4,5 m each, reaching as far back as the year 2006. In the cores dust layers for the years 2014, 2012, 2011 and 2008 have been identified. In 2007 and 2013 only very small dust amounts of 0.2 g m^{-2} were detected. The dust layers in 2011 were the largest deposition in both cores, but not located at the same depth. To demonstrate that those layers still belong to the same year and are due to the eruption of Grímsvötn, a volcano located beneath Vatnajökull, occurring in spring 2011, dust samples have been analysed on their chemical composition and compared to a reference sample taken from ash from the eruption. Chemical analysis confirmed that both dust layers originated from the eruption.

3.3.2 Main results

- The surface dust analysed from surface snow samples in 2013 and 2015 were overall smaller in 2015, but the spatial distribution over Vatnajökull was very similar in both years with most deposition south west and north of the ice cap.

- A comparison of the dust deposition modelled by the dispersion model FLEXDUST for the years 2012 and 2013 show a similar distribution pattern as observed from the surface snow samples. Most dust was deposited southwest of Vatnajökull and north of Brúarjökull. Generally dust amounts were larger in most areas in 2012 than 2013.

- The two firn cores, firn core A and B were taken close to station B15 on Brúarjökull in spring 2015 and the oldest firn sampled was calculated to be from 2006. Dust layers analysed by filtering as well as turbidity are shown in Figure 10.

- Distinct dust layers were found for the years 2014, 2012, 2011 and 2008, whereas dust layers in 2013 and 2007 are very small (0.2 g m^{-2}). The largest dust layer was identified for the year 2011 (Table 3; 12.4 g m^{-2} in core B), the year when the eruption in Grímsvötn occurred. With chemical analysis we confirmed that dust layers in both firn cores originate Grímsvötn 2011 ash even though dust layers were not located at the same depth beneath the surface.
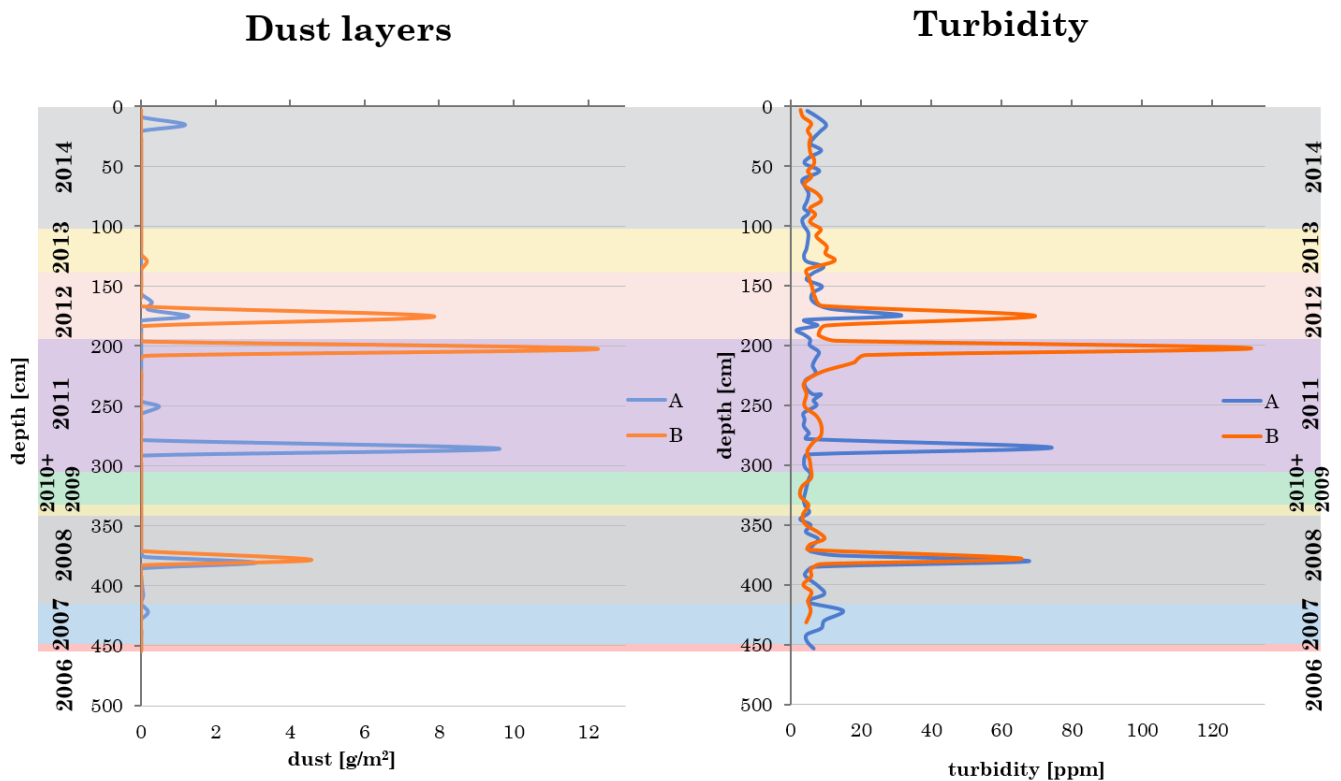
Figure 10: The left graph shows dust layers found in two firn cores, firn core A in blue and firn core B in orange. The different background colours indicated different years within the firn layer, from 2006 to 2014. The right graph shows the continuously measured turbidity of the firn cores.

- Due to a very negative mass balance in 2010, caused by a thin ash layer transported from the eruption at Eyjafjallajökull, accumulated winter snow melted away completely and melted together with the layer of 2009. In 2010 the lowest albedo of 0.058 occurred at station B13 on Brúarjökull. Due to the negative mass balance surface runoff must have removed the ash from the surface at the core sites, so no layer could be found.

Table 3: Dust amounts in firn cores A and B, taken in 2015 and snow surface sample dust from station B13, all on Brúarjökull.

year	2007	2008	2009	2010	2011	2012	2013	2014	2015
dust amount core A [g m^{-2}]	0.2	3.2	0.0	0.0	10.1	1.7	0.0	1.2	-
dust amount core B [g m^{-2}]	0.0	4.6	0.0	0.0	12.4	7.9	0.2	0.0	-
surface sample B13							2.0		0.9

- The second lowest albedo at station B13 was for the year 2012. This year showed as well distinct dust layers of 1.7 and 7.9 g m^{-2} in core A and B, respectively.

- The albedo in 2011 was lower at the upper station B16 (0.32) than at B13 (0.37) which is rather unusual because dust mostly accumulates closer to the source areas around the glacier.

- Dust deposited on Brúarjökull is expected to originate mostly from Dyngjusandur, the area north of the glacier. During strong winds dust gets airborne and the likelihood of dust deposition towards the glacier increases with the frequency of northerly winds.

4 General conclusions

Deposition of dust on the glacier surface greatly affects the surface albedo, and thus the surface energy balance and melt rates. Experiments with ash on snow and ice in natural conditions and in the laboratory show that small amounts of dust occurring e.g. during dust storms, amplify snow and ice melt. With an effective thickness of Eyjafjallajökull ash of ≤1-2 mm, melt rates are maximised, which is very similar to findings for Hekla tephra with maximum melt rates at 2 mm ash thickness (Kirkbride and Dugmore, 2003). Eyjafjallajökull ash insulated the ice at a thickness of 9-15 mm; these results are relevant in areas prone to dust storms very close to a dust source or by a deposition of volcanic ash from an eruption plume. Möller et al. (2016) produced very similar results from experiments with Grímsvötn tephra, deposited on a glacier surface. The effective thickness ranges from 1 to 2 mm with an increase up to ~25% compared to bare-ice conditions, and critical thicknesses are ~10 mm. Another finding of the experiments with different grain sizes of ash deposition on snow or ice was that finer ash (3.5 ϕ) with smooth particles are washed away easier by melt streams on the ice surface than coarser grains (1 ϕ) with a rough, irregular surface and high vesicularity. This could cause that coarser, vesicular material has a much greater effect on albedo.

Dust distribution on the surface of Vatnajökull was analysed from surface samples with impurities as well as simulated by the dispersion model FLEXDUST and shown the same pattern for several years (2012, 2013 and 2015). Most of the modelled dust was deposited in the southwestern part of the ice cap, followed by the northern part (Brúarjökull). FLEXDUST modelled in detail the dust events of summer 2012 (May-October) with dust deposited on Brúarjökull. The model simulated 10 dust events in total for the lower AWS station B13 (~1210 m a.s.l.); four distinct events with dust amounts reaching up to 6.6 g m^{-2} deposited during a single event (14 days long), and six smaller events. The total annual dust deposition summed up to 20.5 g m^{-2} at this location. An average dust event at AWS B13 in 2012 lasted for 6 days, had a maximum dust concentration of 122 µg m^{-3} and a total deposition of 2 g m^{-2}. The albedo during a dust event was lowered by 0.18 on average having a strong impact on the radiation and energy balance of the glacier. The average temperature at ~1210 m a.s.l during dust events was -2°C with a prevailing wind direction in 80% of the events being north. In 20% of the events wind direction was south west (glacier wind). The average precipitation during events was ~23 mm, which shows that quickly after a precipitation event the surface dries and emits dust. At B16, the AWS located higher on the glacier (~1525 m a.s.l.), FLEXDUST produced nine dust events, with one single event causing up to ~5 g m^{-2} (deposited during 3 days) of dust deposition and a total deposition of ~10 g m^{-2} yr^{-1}.

All simulated dust events were associated with an observed drop in albedo during the event measured at the AWSs. To estimate the contribution of the dust enforced albedo drop, the surface energy balance at the two AWS sites B13 and B16 was estimated from the AWS data in 2012 and compared to a simulated energy balance modelled by HIRHAM5 for a clean firn surface. The regional climate model HIRHAM5 simulated a clean glacier surface (albedo varies with aging of snow surface only) for the weather conditions occurring at the AWS B13 and B16 in 2012. When comparing the simulated clean surface albedo to the observed albedo including impurities, at AWS B13 the difference between dust free and real surface was 1.1 m w.e. of more snow melt (1.7 m w.e. snow melt for the clean surface and 2.8 m w.e. for the real surface), which is an increase of 60%. This is not only the influence of dust events lowering surface albedo, but also dust and tephra that was deposited during previous years melting out from below. At the higher B16 AWS, 0.6 m more snow melt was caused by dust on the surface. The increase in melt is similar to that in B13, i.e. additional 60% but in this case, there is no dust melting out from below since it's too far up in the accumulation area of the

glacier. These results show the remarkable impact of positive radiative forcing on snow melt of Icelandic glaciers caused by deposition of dust that strongly enhances absorption of light.

Ground based measurements on Vatnajökull were an important part in this project to estimate dust amounts deposited on the glacier and observe variations from year to year. Surface snow samples distributed over the glacier surface containing dust were collected in autumn 2013 and 2015, and results show larger dust amounts for 2013 than 2015. Two firn cores were drilled in 2015 on Brúarjökull (north east Vatnajökull outlet glacier), 650 m apart from each other with a depth of 4.5 m. The core represents the annual layers from 2014 back to the year 2006. Dust layers were detected for the years 2014, 2012, 2011 and 2008 and only very small amounts (0.2 g m^{-2}) for the years 2007 and 2013. The biggest dust layer found in both firn cores was for the year 2011 with 12.4 g m^{-2} of dust in core B. In core A there were two dust layers within the 2011 layer: a smaller and a bigger layer at the depths 250 and 286 cm. The two layers sum up to 10.1 g m^{-2}. Because the dust layers in 2011 in core A and B were not located at the same depth, chemical analysis was used to confirm their affiliation and the composition matching with tephra from the 2011 eruption of Grímsvötn, a big source of ash deposited on and around the glacier. Dust layers in 2012 and 2008 again were at the same depth in both cores. It is very likely that ash redistribution in the following year of the eruption caused the second largest dust amount found in firn cores. It has already been shown in past research that volcanic eruptions can have a great effect on ash or dust deposition rates on Icelandic glaciers; whether it is directly deposited during an eruption or redistributed in the following year (Arnalds et al., 2013; Thorsteinsson et al., 2012; Möller et al., 2013).

The main dust source for the study site Brúarjökull is identified to be Dyngjusandur, a dust hot spot with extremely severe erosion. Therefore, the likelihood of dust getting deposited on the northern side of Vatnajökull increases with the frequency of northerly winds. Most often continuous northerly winds for at least 10 hours in a row occurred in 2011 and 2012 (36 and 39 times, respectively in the snow free season), which are also the years with most dust deposition in the analysed firn cores. However, there is not a clear correlation between intensity of northerly winds and dust amounts for all years, but since very few wind events can be efficient enough to deposit more dust, a clear relationship cannot be expected.

References

Adhikary, S., Nakawo, M., Seko, K., and Shakya, B. (2000). Dust influence on the melting process of glacier ice: experimental results from Lirung Glacier, Nepal Himalayas. IAHS Publ. 264

AMAP Assessment (2015). Black carbon and ozone as Arctic climate forcers. Arctic Monitoring and Assessment Programme (AMAP), Oslo, Norway. vii + 116 pp, 2015.

Arnalds, O., Thorarinsdottir, E.F., Metusalemsson, S., Jonsson, A., Gretarsson, E., Arnason, A. (2001a). Soil erosion in Iceland. Soil Conservation Service and Agricultural Research Institute, Reykjavik (original edition in Icelandic 1997).

Arnalds, O., Gisladottir, F.O., Sigurjonsson, H. (2001b). Sandy deserts of Iceland: an overview. Journal of Arid Environments 47, 359–371.

Arnalds, O. (2010). Dust sources and deposition of aeolian materials in Iceland. Icelandic Agricultural Sciences 23: 3–21

Arnalds, O., Thorarinsdottir, E.F., Thorsson, J., Dagsson-Waldhauserova, P., Agustsdottir, A.M. (2013). An extreme wind erosion event of the fresh Eyjafjallajökull 2010 volcanic ash. Nat. Sci. Rep. 3, 1257. http://dx.doi.org/10.1038/srep01257

Arnalds, O., Olafsson, H., Dagsson-Waldhauserova, P. (2014). Quantification of ironrich volcanogenic dust emissions and deposition over ocean from Icelandic dust sources. Biogeosciences 11, 6623–6632. http://dx.doi.org/10.5194/bg-11-6623-

Arnalds, O., (2015). The soils of Iceland, 160 pp., Springer, Dordrecht, The Netherlands.

Arnalds, O., Dagsson-Waldhauserova, P., & Olafsson, H. (2016). The Icelandic volcanic aeolian environment: Processes and impacts—A review. Aeolian Research, 20, 176-195.

Baddock, M.C., Strong, C.L., Leys, J.F., Heidenreich, S.K., Tews, E.K., McTainsh, G.H. (2014). A visibility and total suspended dust relationship. Atmos. Environ. 89, 329–336.

Baratoux, D., Mangold, N., Arnalds, O., Bardintzeff, J.-M., Platevoet, B., Gregorie, M., Pinet, P. (2011). Volcanic sands of Iceland – diverse origins of aeolian sand deposits revealed at Dyngjusandur and Lambahraun. Earth Surf. Proc. Land. 36, 1789–1808.

Benn, D. and Evans, D. J. (2010). Glaciers and glaciation. Second edition. 802 pp. Routledge.

Björnsson, H. (1972). Bægisárjökull, North-Iceland. Results of glaciological investigations 1967–1968. Part II. The energy balance. Jökull 22, 44–61.

Björnsson, H. (1978). The surface area of glaciers in Iceland. Jökull 28, 31.

Björnsson, H. (1979). Glaciers in Iceland. Jökull 29, 74–80.

Björnsson, H., Pálsson, F., Guðmundsson, M. T. and Haraldsson, H. H. (1998). Mass balance of western and northern Vatnajökull, Iceland, 1991-1995. Jökull, 45, 35-58.

Björnsson, H., Pálsson, F., and Haraldsson, H. H. (2003). Mass balance of Vatnajökull (1991-2001) and Langjökull (1996-2001), Iceland. Jökull, 53, pp. 75-78.

Björnsson, H., Gudmundsson, S., and Pálsson, F. (2005). Glacier winds on Vatnajökull ice cap, Iceland, and their relation to temperatures of its lowland environs. Annals of Glaciology, 42(1), 291-296.

Björnsson, H., and Pálsson, F. (2008). Icelandic glaciers. Jökull, 58, 365-386.

Björnsson, H., Pálsson, F., Gudmundsson, S., Magnússon, E., Adalgeirsdóttir, G., Jóhannesson, T., Berthier, E., Sigurdsson, O. and Thorsteinsson, Th. (2013). Contribution of Icelandic ice caps to sea level rise: Trends and variability since the Little Ice Age. Geophysical Research Letters, Vol. 40, 1-5, doi:10.1002/grl.50278.

Bonadonna, C., Genco, R., Gouhier, M., Pistolesi, M., Cioni, R., Alfano, F. et al. (2011). Tephra sedimentation during the 2010 Eyjafjallajökull eruption (Iceland) from deposit, radar, and satellite observations. Journal of Geophysical Research: Solid Earth (1978–2012), 116(B12).

Brock, B., Rivera, A., Casassa, G., Bown, F., and Acuñn, C. (2007). The surface energy balance of an active ice-covered volcano: Villarrica Volcano, southern Chile. Annals of Glaciology, 45(1), 104-114.

Budyko, M. I. (1969). The effect of solar radiation variations on the climate of the earth. Tellus, 21(5), 611-619.

Bullard, J. E. (2013). Contemporary glacigenic inputs to the dust cycle. Earth Surface Processes and Landforms, 38(1), 71-89.

Bullard, J. E., Baddock, M., Bradwell, T., Crusius, J., Darlington, E., Gaiero, D., ... and Thorsteinsson, Th. (2016). High-latitude dust in the Earth system. Reviews of Geophysics.

Bursik, M., Jones, M., Carn, S., Dean, K., Patra, A., Pavolonis, M. et al. (2012). Estimation and propagation of volcanic source parameter uncertainty in an ash transport and dispersal model: application to the Eyjafjallajokull plume of 14–16 April 2010. Bulletin of volcanology, 74(10), 2321-2338.

Crochet, P., Jóhannesson, T., Jónsson, T., Sigurðsson, O., Björnsson, H., Pálsson, F., & Barstad, I. (2007). Estimating the spatial distribution of precipitation in Iceland using a linear model of orographic precipitation. Journal of Hydrometeorology, 8(6), 1285-1306.

Cuffey, K. M., and Paterson, W. S. B. (2010). The physics of glaciers, 693pp, Academic Press.

Dadic, R., Mullen, P. C., Schneebeli, M., Brandt, R. E., & Warren, S. G. (2013). Effects of bubbles, cracks, and volcanic tephra on the spectral albedo of bare ice near the Transantarctic Mountains: Implications for sea glaciers on Snowball Earth. Journal of Geophysical Research: Earth Surface, 118(3), 1658-1676.

Dagsson-Waldhauserova, P., Arnalds, O., and Olafsson, H. (2013). Long-term frequency and characteristics of dust storm events in Northeast Iceland (1949–2011). Atmospheric Environment, 77, 117-127.

Dagsson-Waldhauserova, P., Arnalds, O., Olafsson, H. (2014). Long-term variability of dust events in Iceland. Atmos. Chem. Phys. Discuss. 14, 17331–17358. http://dx.doi.org/10.5194/acpd-14-17331-2014

Dagsson-Waldhauserova, P., Arnalds, O., Olafsson, H., Skrabalova, L., Sigurdardottir, G. M., Branis, M., et al. (2014). Physical properties of suspended dust during moist and low wind conditions in Iceland. Icelandic Agricultural Sciences, 27, 25-39.

Dagsson-Waldhauserova, P., Arnalds, O., Olafsson, H., Hladil, J., Skala, R., Navratil, T., ... and Meinander, O.(2015). Snow–dust storm: unique case study from Iceland, March 6–7, 2013. Aeolian Research, 16, 69-74.

Dellino, P., Gudmundsson, M. T., Larsen, G., Mele, D., Stevenson, J. A., Thordarson, T. and Zimanowski, B. (2012). Ash from the Eyjafjallajökull eruption (Iceland): Fragmentation processes and aerodynamic behavior. Journal of Geophysical Research: Solid Earth (1978–2012), 117(B9).

Delmelle, P., Lambert, M., Dufrêne, Y., Gerin, P. and Óskarsson, N. (2007). Gas/aerosol-ash interaction in volcanic plumes: New insights from surface analyses of fine ash particles, Earth Planet. Sci. Lett., 259(1–2), 159–170, doi:10.1016/j.epsl.2007.04.052.

Di Mauro, B., Fava, F., Ferrero, L., Garzonio, R., Baccolo, G., Delmonte, B., and Colombo, R. (2015). Mineral dust impact on snow radiative properties in the European Alps combining ground, UAV, and satellite observations. Journal of Geophysical Research: Atmospheres, 120(12), 6080-6097.

Doherty, S. J., Warren, S. G., Grenfell, T. C., Clarke, A. D. and Brandt, R. E. (2010). Light-absorbing impurities in Arctic snow. Atmospheric Chemistry and Physics, 10(23), 11647-11680.

Dragosics, M., Groot Zwaaftink, Ch., Schmidt, L.S., Guðmundsson, S., Pálsson,F., Arnalds, O., Björnsson, H., Thorsteinsson, Th., Stohl, A. Impact of dust deposition on the albedo of Vatnajökull ice cap, Iceland, submitted to the Cryosphere.

Dragosics, M., Meinander, O., Jónsdóttir, T., Dürig, T., de Leeuw, G., Pálsson, F., Dagsson Waldhauserová, P., and Thorsteinsson, Th. (2016). Insulation effects of Icelandic dust and volcanic ash on snow and ice. Arabian Journal of Geosciences, 9, 126, doi:10.1007/s12517-015-2224-6

Driedger, C. L. (1981). Effect of ash thickness on snow ablation. In: Lipman, P. and D.R. Mullineaux (eds) The 1980 eruptions of Mount St Helens. USGS Professional Paper, 1250, 757–760.

Eerola, K. (2006). About the performance of HIRLAM version 7.0. HIRLAM Newsletter, 51:93–102.

Einarsson, M. Á. (1984). Climate of Iceland. In: van Loon, H., ed., Climates of the Oceans, Elsevier, Amsterdam, 673–697.

Flanner, M. G., Gardner, A. S., Eckhardt, S., Stohl, A., and Perket, J. (2014). Aerosol radiative forcing from the 2010 Eyjafjallajökull volcanic eruptions. J. Geophys. Res. 119, 9481-9491, doi:10.1002/2014JD021977.

Flanner, M. G., Zender, C. S., Randerson, J. T., and Rasch, P. J. (2007). Present-day climate forcing and response from black carbon in snow. Journal of Geophysical Research: Atmospheres, 112(D11).

Folch, A., Costa, A. and Basart, S. (2012). Validation of the FALL3D ash dispersion model using observations of the 2010 Eyjafjallajökull volcanic ash clouds. Atmospheric Environment, 48, 165-183.

Gabbi, J., Huss, M., Bauder, A., Cao, F. and Schwikowski, M. (2015). The impact of Saharan dust and black carbon on albedo and long-term mass balance of an Alpine glacier. The Cryosphere, 9(4), 1385-1400.

Gardner, A. S., Moholdt, G., Cogley, J. G., Wouters, B., Arendt, A. A., Wahr, J., ... and Ligtenberg, S. R. (2013). A reconciled estimate of glacier contributions to sea level rise: 2003 to 2009. science, 340(6134), 852-857.

Gislason, S. R., Hassenkam, T., Nedel, S., Bovet, N., Eiriksdottir, E. S., Alfredsson, H. A. et al. (2011). Characterization of Eyjafjallajökull volcanic ash particles and a protocol for rapid risk assessment. Proceedings of the National Academy of Sciences, 108(18), 7307-7312.

Gölles, T., Bøggild, C. E. and Greve, R. (2015). Ice sheet mass loss caused by dust and black carbon accumulation. The Cryosphere, 9(5), 1845-1856. doi:10.5194/tc-9-1845-2015

Greuell, W., Genthon, C. (2003). Mass Balance of the Cryosphere: Observations and Modelling of Contemporary and Future Changes, eds. Jonathan L. Bamber and Antony J. Payne. Published by Cambridge University Press. Cambridge University Press.

Groot Zwaaftink, C. D., Grythe, H., Skov, H. and Stohl, A. (2016). Substantial contribution of northern high-latitude sources to mineral dust in the Arctic, J. Geophys. Res. Atmos., 121, doi:10.1002/2016JD025482

Gudmundsson, M. T., Thordarson, T., Höskuldsson, Á., Larsen, G., Björnsson, H., Prata, F. .J, et al. (2012). Ash generation and distribution from the April-May 2010 eruption of Eyjafjallajökull, Iceland. Scientific reports, 2.

Guðmundsson, S., Björnsson, H., Pálsson, F. and Haraldsson, H. H. (2006). Energy balance of Brúarjökull and circumstances leading to the August 2004 floods in the river Jökla, N-Vatnajökull (Vol. 55, pp. 1-18). Jökull.

Guðmundsson, S., Björnsson, H., Pálsson, F., & Haraldsson, H. H. (2009). Comparison of energy balance and degree-day models of summer ablation on the Langjökull ice cap, SW-Iceland. Jökull, 59, 1-18.

Gudmundsson, S., Pálsson, F., Björnsson, H., Magnússon, E., Thorsteinsson, T. and Haraldsson, H. H. (2012). The impact of volcanic aerosols on the energy-and mass balance of Langjökull ice cap, SW-Iceland. In AGU Fall Meeting Abstracts (Vol. 1, p. 0659).

Gudmundsson, M. T., Jónsdóttir, K., Hooper, A., Holohan, E. P., Halldórsson, S. A., Ófeigsson, B. G. and Einarsson, P. (2016). Gradual caldera collapse at Bárdarbunga volcano, Iceland, regulated by lateral magma outflow. Science, 353(6296), aaf8988.

Hansen, J., and Nazarenko, L. (2004). Soot climate forcing via snow and ice albedos. Proceedings of the National Academy of Sciences of the United States of America, 101(2), 423-428.

Hock, R. (2005). Glacier melt: a review of processes and their modelling. Progress in physical geography, 29(3), 362-391.

IPCC: Climate change (2013). The physical science basis. In: Working Group I, Contribution to the IPCC 5th Assessment Report – summary for policy makers.

Jóhannesson, T., Björnsson, H., Magnússon, E., Guðmundsson, S., Pálsson, F., Sigurðsson, O., ... and Berthier, E. (2013). Ice-volume changes, bias estimation of mass-balance measurements and changes in subglacial lakes derived by lidar mapping of the surface of Icelandic glaciers. Annals of Glaciology, 54(63), 63-74.

Kerminen, V. M., Niemi, J. V., Timonen, H., Aurela, M., Frey, A., Carbone, S., Saarikoski, S., Teinilä, K., Hakkarainen, J., Tamminen, J., Vira, J., Prank, M., Sofiev, M. and Hillamo, R. (2011). Characterization of a volcanic ash episode in southern Finland caused by the Grimsvötn eruption in Iceland in May 2011, Atmos. Chem. Phys., 11(23), 12227–12239, doi:10.5194/acp-11-12227-2011.

Kipp & Zonen Instruction Manual for Pyranometer/Albedometer CNR1 (2002). www.kippzonen.com/Download/85/Manual-CNR-1-Net-Radiometer-English

Kirkbride, M.P. and Dugmore, A.J. (2003). Glaciological response to distal tephra fallout from the 1947 eruption of Hekla, south Iceland. J. Glaciol., 49(166), 420–428.

Kok, J. F. (2011). A scaling theory for the size distribution of emitted dust aerosols suggests climate models underestimate the size of the global dust cycle. Proceedings of the National Academy of Sciences, 108(3), 1016-1021.

Kuhn, M. (1984). Physikalische Grundlagen des Energie- und Massenhaushalts der Schneedecke. In Brechtel, H., editor, Schneehydrologische Forschung in Mitteleuropa, volume 7, DVWK (Deutscher Verband für Wasserwirtschaft und Kulturbau), 5–56.

Langen, P. L., Mottram, R. H., Christensen, J. H., Boberg, F., Rodehacke, C. B., Stendel, M., van As, D., Ahlstrøm, A.P., Mortensen, J., Rysgaard, S., Petersen, D., Svendsen, K. H. , Aðalgeirsdóttir, G. and Cappelen J. (2015). Quantifying Energy and Mass Fluxes Controlling Godthåbsfjord Freshwater Input in a 5-km Simulation (1991–2012). Journal of Climate, 28(9), 3694-3713.

Lieke, K. I., Kristensen, T. B., Korsholm, U. S., Sørensen, J. H., Kandler, K., Weinbruch, S., Ceburnis, D., Ovadnevaite, J., O'Dowd, C. D. and Bilde, M. (2013). Characterization of volcanic ash from the 2011 Grímsvötn eruption bymeans of single-particle analysis, Atmos. Environ., 79, 411–420, doi:10.1016/j.atmosenv.2013.06.044.

Lucas-Picher, P., Wulff-Nielsen, M., Christensen, J. H., Adalgeirsdóttir, G., Mottram, R. H. and Simonsen, S. B. (2012). Very high resolution regional climate model simulations over Greenland: Identifying added value. Journal of Geophysical Research, 117:2108.

Magnússon, E., Muñoz-Cobo Belart, J., Pálsson, F., Ágústsson, H., and Crochet, P. (2016). Geodetic mass balance record with rigorous uncertainty estimates deduced from aerial photographs and lidar data–Case study from Drangajökull ice cap, NW Iceland. The Cryosphere, 10(1), 159-177.

Male, D.H. (1980). The seasonal snow cover. In Colbeck, S., editor, Dynamics of snow and ice masses, New York: Academic Press, 305–91.

Marticorena, B. and Bergametti, G. (1995). Modeling the atmospheric dust cycle: 1. Design of a soil-derived dust emission scheme. Journal of Geophysical Research: Atmospheres, 100(D8), 16415-16430.

Meinander O, Kazadzis S, Arola A, Riihelä A, Räisänen P, Kivi R, et al. (2013). Spectral albedo of seasonal snow during intensive melt period at Sodankylä, beyond the Arctic Circle. Atmospheric Chemistry and Physics, 13(7), 3793-3810.

Meinander O, Kontu A, Virkkula A, Arola A, Backman L, Dagsson-Waldhauserová P et al. (2014). Brief communication: Light-absorbing impurities can reduce the density of melting snow. The Cryosphere, 8(3), 991-995.

Meinander, O., Dagsson-Waldhauserova, P. and Arnalds, O. (2016). Icelandic volcanic dust can have a significant influence on the cryosphere in Greenland and elsewhere. Polar Research, 35.

Möller, R., Möller, M., Björnsson, H., Guðmundsson, s., Pálsson, F., Oddsson, B., Kukla, P. A., Schneider, C. (2013). MODIS-derived albedo changes of Vatnajökull (Iceland) due to tephradeposition from the 2004 Grímsvötn eruption. International Journal of Applied Earth Observation and Geoinformation 26, 256-269.

Möller, R., Möller, M., Kukla, P. A., Schneider, C. (2016). Impact of supraglacial deposits of tephra from Grímsvötn volcano, Iceland, on glacier ablation. J. of Glaciology 62.235, 933-943.

Mountney, N. P., Russell, A. J. (2004). Sedimentalogy of cold-climate aeolian sandsheet deposits in the Askja region of northeast Iceland. Sediment. Geol. 166, 223–244.

Myhre, G., Shindell, D., Bréon, F. M., Collins, W., Fuglestvedt, J., Huang, J., ... and Nakajima, T. (2013). Anthropogenic and Natural Radiative Forcing. In: Climate Change 2013: The Physical Science Basis. Contribution of Working Group 1 to the Fifth Assessment Report of the Intergovernmental Panel on Climate Change. Table, 8, 714.

Nielsen-Englyst, P. (2015). Impact of albedo parameterizations on surface mass balance and runoff on the Greenland Ice Sheet. Master's thesis University of Copenhagen, unpublished.

Oerlemans, J., and Knap, W. H. (1998). A 1 year record of global radiation and albedo in the ablation zone of Morteratschgletscher, Switzerland. Journal of Glaciology, 44(147), 231-238.

Oerlemans, J., Björnsson, H., Kuhn, M., Obleitner, F., Palsson, F., Smeets, C. J. P. P., ... and De Wolde, J. (1999). Glacio-meteorological investigations on Vatnajökull, Iceland, summer 1996: An overview. Boundary-Layer Meteorology, 92(1), 3-24.

Oerlemans, J. (2001). Glaciers and climate change. CRC Press, 160p.

Oerlemans, J., Giesen, R. H., and Van den Broeke, M. R. (2009). Retreating alpine glaciers: increased melt rates due to accumulation of dust (Vadret da Morteratsch, Switzerland). Journal of Glaciology, 55(192), 729-736.

Painter, T. H., A. P. Barrett, C. C. Landry, J. C. Neff, M. P. Cassidy, C. R. Lawrence, K. E. McBride, and G. L. Farmer: Impact of disturbed desert soils on duration of mountain snow cover, Geophys. Res. Lett., 34, L12 502, doi:10.1029/2007GL030284, 2007.

Painter, T. H., Skiles, S. M., Deems, J. S., Bryant, A. C., Landry, C. (2012). Dust radiative forcing in snow of the Upper Colorado River Basin: Part I. A 6 year record of energy balance, radiation, and dust concentrations. Water Resour. Res. http://dx.doi.org/10.1029/2012WR011985

Painter, T. H., Flanner, M. G., Kaser, G., Marzeion, B., VanCuren, R. A., and Abdalati, W. (2013). End of the Little Ice Age in the Alps forced by industrial black carbon. Proceedings of the national academy of sciences, 110(38), 15216-15221.

Pálsson, F., Guðmundsson, S., Björnsson, H., Berthier, E., Magnússon, E., Guðmundsson, S., and Haraldsson, H. H. (2012). Mass and volume changes of Langjökull ice cap, Iceland, 1890 to 2009, deduced from old maps, satellite images and in situ mass balance measurements. Jökull, 62, 81-96.

Pálsson, F., Björnsson, H., Guðmundsson, S. and Haraldsson, H. H. (2013). Vatnajökull: Mass balance, meltwater drainage and surface velocity of the glacial year 2010-11. Institute of Earth Sciences, University of Iceland and National Power Company, December 2013, RH-24.

Peltoniemi, J., Hakala, T., Suomalainen, J. and Puttonen, E. (2009). Polarised bidirectional reflectance factor measurements from soil, stones, and snow. Journal of Quantitative Spectroscopy and Radiative Transfer, 110(17), 1940-1953.

Petersen, G. N., Bjornsson, H., Arason, P., & Löwis, S. V. (2012). Two weather radar time series of the altitude of the volcanic plume during the May 2011 eruption of Grímsvötn, Iceland. Earth System Science Data, 4(1), 121-127.

Quinn, P. K., Bates, T. S., Baum, E., Doubleday, N., Fiore, A. M., Flanner, M., ... and Shindell, D. (2008). Short-lived pollutants in the Arctic: their climate impact and possible mitigation strategies. Atmospheric Chemistry and Physics, 8(6), 1723-1735.

Roeckner, E., Bäuml, G., Bonaventura,L., Brokopf, R., Esch, M.,Giorgetta, M., Hagemann, S., Kirchner, I.,Kornblueh, L., Manzini, E., Rhodin, A., Schlese, U., Schulzweida, U. and Tompkins , A. (2003). The atmospheric general circulation model ECHAM 5 PART I: Model description. Technical Report 349, Report / MPI für Meteorologie.

Sasaki, H., Kawakami, Y., Ono, M., Jonasson, F., Shui, Y. B., Cheng, H. M., ... and Sasaki, K. (2003). Localization of cortical cataract in subjects of diverse races and latitude. Investigative ophthalmology & visual science, 44(10), 4210-4214.

Schmidt, L.S., Aðalgeirsdóttir, G., Pálsson, F., Björnsson, H., Guðmundsson, S., Langen, P.L., Mottram, R., Gascoin, S. Evaluating the Surface Energy Balance in the HIRHAM5 Regional Climate Model Over Vatnajökull, Iceland, Using Automatic Weather Station Data, submitted to the cryosphere.

Stohl, A., Forster, C., Frank, A., Seibert, P., and Wotawa, G. (2005). Technical Note: The Lagrangian particle dispersion model FLEXPART version 6.2. Atmos. Chem. Phys. 5, 2461-2474.

Stohl, A., Hittenberger, M., and Wotawa, G. (1998). Validation of the Lagrangian particle dispersion model 515 FLEXPART against large-scale tracer experiment data. Atmospheric Environment, 32(24), 4245-4264.

Thordarson, T. and Larsen, G. (2007). Volcanism in Iceland in historical time: Volcano types, eruption styles and eruptive history. Journal of Geodynamics, 43(1), 118-152.

Thorsteinsson, T., Gísladóttir, G., Bullard, J., McTainsh, G. (2011). Dust storm contributions to airborne particulate matter in Reykjavík, Iceland. Atmos. Environ. 45, 5924–5933. http://dx.doi.org/10.1016/j.atmosenv.2011.05.023.

Thorsteinsson, T., Johannsson, T., Stohl, A., Kristiansen, N.I. (2012). High levels of particulate matter in Iceland due to direct ash emissions by the Eyjafjallajökull eruption and resuspension of deposited ash. J. Geophys. Res. 117, B00C05. http://dx.doi.org/10.1029/2011JB008756.

Thorsteinsson, T., Jóhannesson, T., and Snorrason, Á. (2013). Glaciers and ice caps: Vulnerable water resources in a warming climate. Current Opinion in Environmental Sustainability, 5(6), 590-598.

Vogel, A., Diplas, S., Durant, A. J., Azar, A., Rose, W. I., Sytchkova, A., Bonadonna, C., Krüger, K. and Stohl, S. Reference dataset of volcanic ash physicochemical and optical properties for atmospheric measurement retrievals and transport modelling, J. Geophys. Res. Atmos., 2016, submitted.

Wiscombe, W. J., and Warren, S. G. (1980). A model for the spectral albedo of snow. I: Pure snow. Journal of the Atmospheric Sciences, 37(12), 2712-2733.

Yoshida, A., Moteki, N., Ohata, S., Mori, T., Tada, R., Dagsson-Waldhauserová, P., and Kondo, Y. (2016). Detection of light-absorbing iron oxide particles using a modified single-particle soot photometer. Aerosol Science and Technology, 50(3), 1-4. DOI: 10.1080/02786826.2016.1146402.

Zhao, C., Hu, Z., Qian, Y., Ruby Leung, L., Huang, J., Huang, M., .. and Yan, H. (2014). Simulating black carbon and dust and their radiative forcing in seasonal snow: a case study over North China with field campaign measurements. Atmospheric Chemistry and Physics, 14(20), 11475-11491.

Papers

Insulation effects of Icelandic dust and volcanic ash on snow and ice

Dragosics, M., Meinander, O., Jónsdóttir, T., Dürig, T., de Leeuw, G., Pálsson, F., Dagsson Waldhauserová, P., and Thorsteinsson, Th.

CrossMark

ORIGINAL PAPER

Insulation effects of Icelandic dust and volcanic ash on snow and ice

Monika Dragosics[1] · **Outi Meinander**[2] · **Tinna Jónsdóttír**[1] · **Tobias Dürig**[1] ·
Gerrit De Leeuw[2,3] · **Finnur Pálsson**[1] · **Pavla Dagsson-Waldhauserová**[1,4,5,6] ·
Throstur Thorsteinsson[1]

Abstract In the Arctic region, Iceland is an important source of dust due to ash production from volcanic eruptions. In addition, dust is resuspended from the surface into the atmosphere as several dust storms occur each year. During volcanic eruptions and dust storms, material is deposited on the glaciers where it influences their energy balance. The effects of deposited volcanic ash on ice and snow melt were examined using laboratory and outdoor experiments. These experiments were made during the snow melt period using two different ash grain sizes (1 ϕ and 3.5 ϕ) from the Eyjafjallajökull 2010 eruption, collected on the glacier. Different amounts of ash were deposited on snow or ice, after which the snow properties and melt were measured. The results show that a thin ash layer increases the snow and ice melt but an ash layer exceeding a certain critical thickness caused insulation. Ash with 1 ϕ in grain size insulated the ice below at a thickness of 9–15 mm. For the 3.5 ϕ grain size, the insulation thickness is 13 mm. The maximum melt occurred at a thickness of 1 mm for the 1 ϕ and only 1–2 mm for 3.5 ϕ ash. A map of dust concentrations on Vatnajökull that represents the dust deposition during the summer of 2013 is presented with concentrations ranging from 0.2 up to 16.6 g m^{-2}.

Introduction

The physical and optical properties of snow are influenced by the presence of impurities, in particular by absorbing material such as aerosol particles deposited on the snow surface (e.g., Doherty et al. 2010 and Painter et al. 2012). Effects of aerosol particles on, for instance, snow melt and albedo (e.g., Meinander et al. 2013) and bidirectional reflection (Peltoniemi et al. 2009) have been studied for natural snow and during campaigns where impurities were deposited on snow in different quantities (e.g., Meinander et al. 2014). Commonly, the effects of impurities, such as black carbon, are studied, which are transported from their source regions to the snow-covered northern latitudes. The properties of snow and ice on the surface of glaciers in Iceland are influenced by the deposition of dust (Arnalds et al. 2014) and, during volcanic eruptions, by volcanic ash. The 2010 eruption of Eyjafjallajökull (Thorsteinsson et al. 2012) not only influenced the whole global air traffic by tephra release into the atmosphere up to 10 km a.s.l. reaching as far as the southern parts of Europe (e.g., Bonadonna et al. 2011; Bursik et al. 2012; Gudmundsson et al. 2012a) but also drastically influenced the albedo of glaciers in Iceland (Gudmundsson et al. 2012b and Pálsson

et al. 2013). The majority of Icelandic tephra is basaltic in origin resulting from the mid ocean ridge basalt, but the chemical composition of tephra varies between different volcanic systems and even eruptions. Phreatomagmatic basaltic eruptions are typical in Iceland and occur from subglacial, subaerial, and submarine volcanoes (Thordarson and Larsen 2007). Therefore, Icelandic ash and dust is mainly basaltic volcanic glass which is deposited in Iceland's sandy deserts which cover an area over 22.000 km^2. Deserts of this composition are globally unique (Arnalds 2010). The ash from Eyjafjallajökull 2010 was of andesitic composition, slowly progressing from benmorite to thrachyte as the eruption proceeded with a silicic content ranging from ~58–69 % SiO$_2$. (Gislason et al. 2011 and Gudmundsson et al. 2012a)

Several dust storms occur in Iceland every year with deposition of dust or ash on the ice caps (Arnalds et al. 2014) with varying amounts at different altitudes which influence their melting behaviour. These dust storms are as well volcanic in origin (Arnalds et al. 2013) but redistributed and deposited in the glacier forefield where it is mixing with glacial till. From the forefield, it can be resuspended into the air by the action of wind and carried onto the glacier. After the 2010 eruption, the entire Eyjafjallajökull ice cap and most of the neighbouring Mýrdalsjökull were covered with a thick tephra layer, insulating the glacier surface whereas a thin tephra layer on Vatnajökull, Hofsjökull and Langjökull significantly increased the absorption of shortwave radiation and therefore enhanced melting (Gudmundsson et al. 2012b and Pálsson et al. 2013). In this paper, effective and critical thicknesses for Eyjafjallajökull (2010) ash are studied and compared with the help of outdoor and laboratory experiments. The effective thickness is the thickness when the material-covered ablation is maximized The critical thickness is the thickness of the material

covering the ice or snow where the ablation rate of the material-covered ice or snow equals that of clean snow or ice; more material will start to insulate. (Brock et al. 2007).

The aim was to study the influence of ash layers of variable thickness, as would result from dust storms or eruptions and how they influence glacier surface mass balance, whether they insulate the ice or enhance melting. The thickness of dust layers in dust storms is rather thin and is expected to enhance melting, whereas during eruptions layers can be very thick. In Gudmundsson et al. (2012a), it was reported that the maximum thickness of the ash layer from the Eyjafjallajökull 2010 eruption exceeded 30 m close to the vent and 1 m thickness 2 km away from the vent, whereas on SW Vatnajökull it was reported to be a 0.1 mm thick tephra layer covering the ice. In the 2011 eruption of Grímsvötn, observations showed ash thicknesses on Tungnaárjökull (W-Vatnajökull) in a cm to mm scale.

Effective and critical thicknesses for Mt St Helens (1980) tephra are 3 and 24 mm, respectively (Driedger 1981). For the Icelandic volcano Hekla (1947), where tephra was covering ice at Gígjökull, these values were 2 and 5.5 mm, respectively (Kirkbride and Dugmore 2003). For rock debris effective and critical thicknesses are much thicker than for tephra (usually ~10 and ~15–50 mm, respectively) due to its low thermal conductivity. Because of the typically darker colour of tephra, small concentrations can dramatically reduce snow or ice albedo and increase ablation rates (Driedger 1981).

No previous scientific papers were found on the insulation effect of the tephra from the 2010 Eyjafjallajökull eruption, and only one previous paper on insulation effect of Icelandic tephra was found (Kirkbride and Dugmore 2003). Our results were compared with earlier works as described in Table 1.

Table 1 Effective and critical thickness for different materials such as tephra, rock debris and dust

Material	Effective thickness (mm)	Critical thickness (mm)
Mt St Helens (1980) ash[a]	3	24
Hekla (1947) tephra[b]	2	5.5
Rock debris[b]	~10	~15–50
Villarrica tephra (lapilli)[c]	–	<5
Dust (largely organic matter)[d]	–	1.33
Eyjafjallajökull ash (2010, 1 ϕ)	1	9–15
Eyjafjallajökull ash (2010, 3.5 ϕ)	≤1–2	13

[a] Driedger (1981)

[b] Kirkbride and Dugmore (2003)

[c] Brock et al. (2007)

[d] Adhikary et al. (2000)

Materials and methods

Four outdoor and laboratory experiments have been carried out at the Finnish Meteorological Institute (FMI) at Kumpula Kampus in Helsinki, Finland. These experiments contribute to a better understanding of insulation characteristics of ash and dust deposition on Icelandic glaciers. The modalities of different experiments are related to natural conditions, which are described below.

Dust distribution 2013 on Vatnajökull

Dagsson-Waldhauserova et al. (2014) suggest that about half of all dust storms in south Iceland each year occur at temperatures at or below 0 °C; therefore, dust can be mixed together with snow. The deposition of dust on snow or ice has an important climatic effect due to influence on surface albedo reduction and enhanced melt.

Arnalds et al. (2014) calculated the total deposition of dust on the Icelandic glaciers to be 4.5 million tons per year with a mean deposition of 400 g m^{-2} years^{-1}. To compare this number with in situ measurements, snow samples from 16 locations on the surface of Vatnajökull (Fig. 1) were sampled in October 2013. Vatnajökull is Iceland's biggest ice cap with an area of more than 8.000 km^2 (Björnsson and Pálsson 2008). These samples represent dust that was deposited during one summer on the glacier surface. The top 8 cm of the snow surface (about 1–2 kg of snow) was collected from an area of approx. 57.2×10^{-3} m^2 for each sample. The 16 snow samples were brought back frozen in plastic bags to the laboratory in Reykjavík where they were melted, evaporated and the mass of the dust was weighed.

### Origin and properties of ash used in the experiments

Material used for experiments at FMI was ash from the 2010 Eyjafjallajökull eruption in Iceland. The material was collected on Eyjafjallajökull (sample site in Fig. 1) at 1420 m a.s.l., about 3 km east of the vent. It was collected just after the eruption ended in late May 2010.

The transport distance of different grain sizes depends on wind speed. The smaller the grain size the easier it is transported over long distances. Because of reconstruction of the main mode of the Eyjafjallajökull tephra fall out (Bonadonna et al. 2011 and Folch et al. 2012), ash has been used in the grain sizes 1 ϕ (500 μm) and 3.5 ϕ (90 μm) in the experiments. The bulk density for the 1 ϕ ash was measured as 2.57 g cm^{-3} and for 3.5 ϕ 2.46 g cm^{-3}. The particles of both grain sizes were investigated by SEM analysis. The ash

Fig. 1 Iceland with glacier outlines and sample sites on Vatnajökull and Eyjafjallajökull (base map by Landmælingar Íslands, 1993)

Fig. 2 SEM images of representative ash particles. **a** Particles of the fraction 1 ϕ are of blocky shape with angular or **b** stepped surfaces, **c** partly featuring indications of high vesicularity. **d** The surfaces of these coarse grains are mostly covered by adhesive ash particles of the smaller fractions which considerably affect their overall shape. **e** A blocky shape is also the key characteristic of the particles from the 3.5 ϕ fraction. **d-g** Both, angular and **h** stepped surface features can be identified
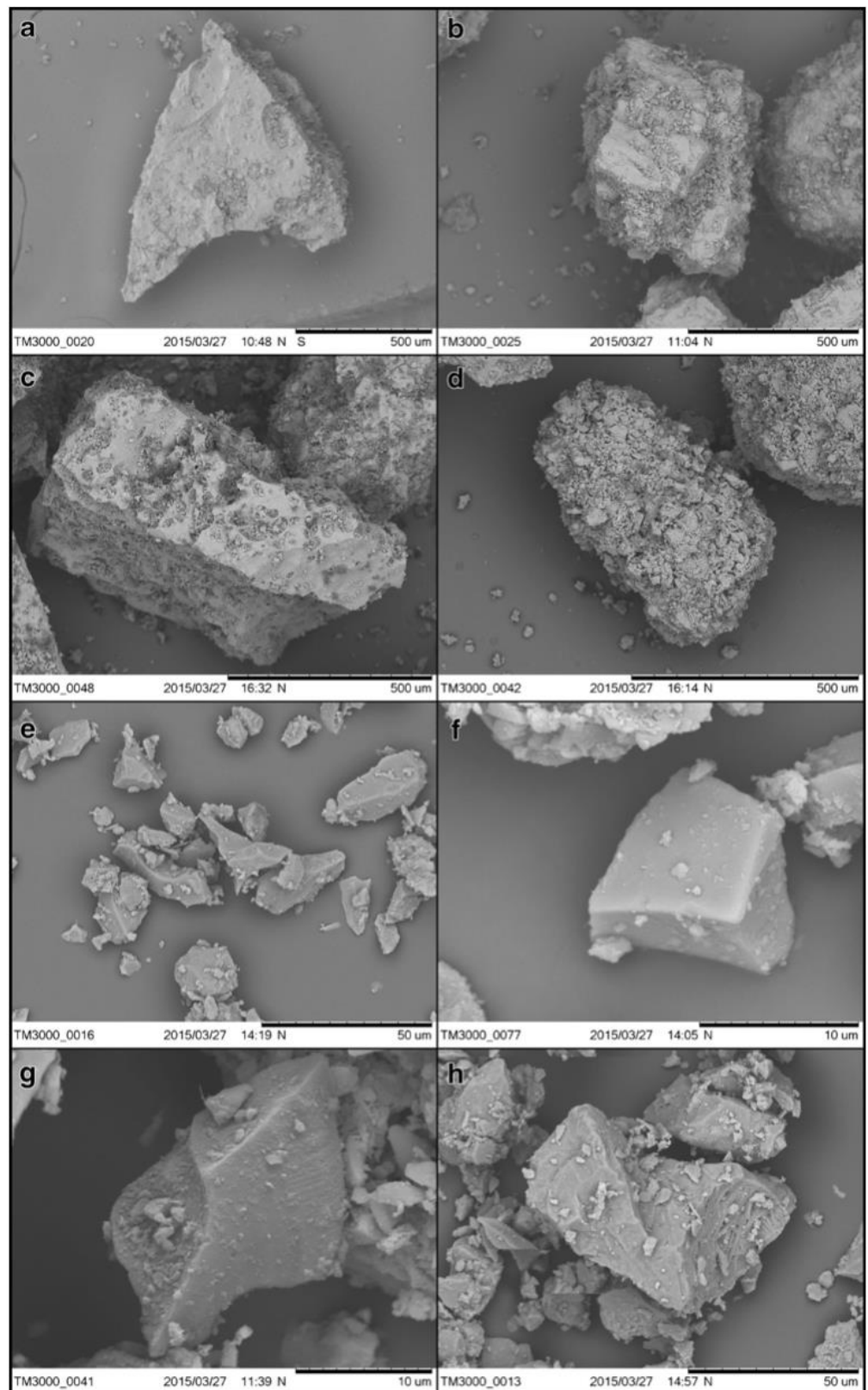
population is dominantly characterized by blocky shaped particles with stepped features and blocky angular particles with clustered clasts with smaller adhesive particles (Fig. 2) and is in agreement with former investigations of the ash (Dellino et al. 2012). However, this research includes as well proximal samples of the vent that have not been yet investigated before.

Experiments

Four outdoor (AoS-2015, Roof 2015 and AiC-2015) and laboratory (AoI-2015) experiments were carried out using snow (AoS-2015), ice (AoI-2015, Roof 2015) and snow over ice (AiC-2015). Ash of 1 ϕ grain size was used for the AoS-2015, AoI-2015 and AiC-2015 experiments, whereas ash of 1 and 3.5 ϕ was used for Roof 2015 experiment. Layer thicknesses were measured above 1 mm and in dry condition of the ash.

AoS-2015

The Ash on Snow (AoS-2015) experiment is an outdoor experiment on the effect of ash on snow in natural conditions. The experiments started on 6 February 2015 using natural snow in a fenced area, i.e., unperturbed by direct human interference. There are some impurities due to deposition of atmospheric aerosol particles from the air, with an unknown concentration; however, their concentration is negligible compared to the ash applied to the surface. Three different amounts of ash, 15 g (166 g m^{-2}), 85 g (944 g m^{-2}) and 425 g (4722 g m^{-2}, 15 mm layer thickness) with grain size 1 ϕ, were deposited on an area of 0.3×0.3 m^2 on a snow surface (Fig. 3) with a snow density of 280 kgm^{-3}.

Snow depth and temperature were then monitored for 17 days when the snow was melted naturally.

AoI-2015

A controlled experiment with ash on ice was made both indoors (AoI-2015) and outdoors (Roof-2015), to identify and separate the effects of temperature and solar irradiance.

Ash on Ice (AoI-2015) were laboratory experiments to examine the effect of ash layer thickness on ice melting, in a temperature-stabilized environment kept at +24 °C. For these experiments, small, transparent plastic boxes (Fig. 4) were filled with 200 ml of tap water and frozen (surface area 84 cm^2). This resulted in an ice layer with a depth of 25–28 mm. To find the insulating threshold of ash on ice, four different amounts of the 1 ϕ impurity were deposited: 3 g

(1.3 ml, 366 g m^{-2}), 35 g (15 ml, 4219 g m^{-2}, 1 mm layer thickness), 71 g (30 ml, 8437 g m^{-2}, 3 mm layer thickness) and 283 g (120 ml, 33,749 g m^{-2}, 9–13-mm layer thickness). After deposition of material, the ice was transferred into white pots with holes in the bottom to measure the meltwater runoff.

Roof 2015 experiment

The laboratory experiments were repeated outside on the roof of the FMI building in sunny conditions to study effects of solar irradiance in addition to that of temperature above zero. The experiment was repeated with the same volume of impurities, but using two different grain sizes of the Eyjafjallajökull 2010 ash: 1 ϕ (samples A) and 3.5 ϕ (samples B). The concentrations for the 3.5 ϕ B-samples were: 2.46 g (1 ml, 292 g m^{-2}); 36.8 g (15 ml, 4385 g m^{-2}, 1-mm layer thickness), 73.7 g (30 ml, 3–5-mm layer thickness, 8772 g m^{-2}) and 294.7 g (120 ml, 35,086 g m^{-2}, 9–13-mm layer thickness). The concentrations for the 1 ϕ ash were the same as used in AoI-2015.

AiC-2015

The Ash in Container (AiC) experiment was performed in a cold container where ash was deposited on snow over ice. This experiment should evaluate to see if the ash starts insulating as in the outdoor experiments even with a slight different setup of snow over ice. This setup shows more realistically the surface of a glacier with ice below and therefore cooling from above and melting temperatures only from the surface.

A big pot, inside a cold container, was filled at the bottom with a thick ice layer and on top of that an 8.5-cm thick layer of snow was deposited (Fig. 5). Two different amounts of impurities were used as in the outdoor experiments (Fig. 5): 15 g (166 g m^{-2}) and 425 g (4722 g m^{-2}, 15 mm thickness) of 1 ϕ Eyjafjallajökull ash on a 0.3×0.3 m^2 area. The experiment started at a temperature of −10 °C inside the container; then, the cooling system was shut down, and it adapted to outdoor temperatures up to +4 °C. Snow depth and behaviour of the ash were monitored.

Fig. 3 During the AoS-2015 experiment, different amounts of ash were deposited on a 0.3×0.3-m^2 snow surface. **a** 15 g (166 g m^{-2}), **b** 85 g (944 g m^{-2}) and **c** 425 g (4722 g m^{-2}, 15-mm layer thickness)
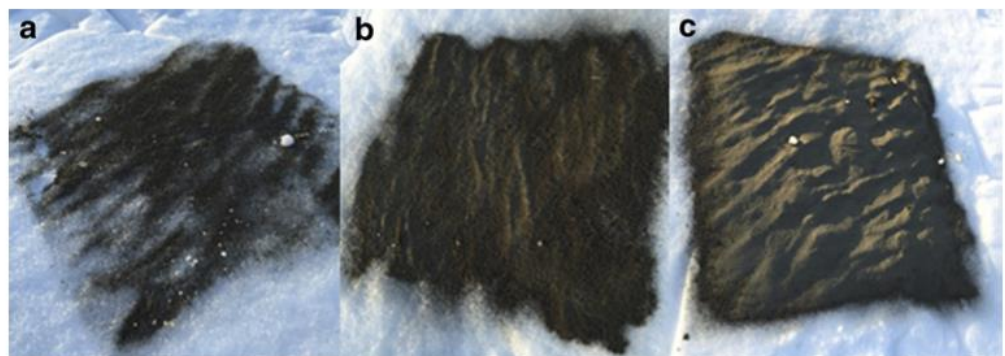
Fig. 4 During the AoI-2015 experiment, different ash concentrations were applied to ice indoors

Results

Results from the outdoor and indoor snow experiments with Icelandic ash at FMI are presented in this chapter as well as in situ measurements on Vatnajökull depicted in the dust distribution map (Fig. 6). Experiments have helped to understand impacts of deposited amounts on glaciers as in the example of the dust distribution map.

Dust distribution map 2013

Figure 6 shows a map representing the spatial distribution of dust concentration deposited in the summer 2013 on Vatnajökull, a year without volcanic eruptions. This should show that very small amounts of dust or ash are getting deposited on the glacier. The map in Fig. 6 shows the location points (called *stations*) where dust samples were collected, and the colours show the spatial distribution of the dust concentration obtained by interpolation of the measured values (interpolation with the geostatistical analyst method Inverse Distance Weighting (IDW) in ArcMap). Topography was not taken into account in the interpolation. The point locations are not evenly distributed over the glacier area, and the southern part of Vatnajökull was not included in the interpolation due to

Fig. 5 During the Ash in Container (AiC-2015) experiment, two different amounts of ash were deposited on snow over of ice. Bottom 15 g (166 g m^{-2}) and top 425 g (4722 g m^{-2}, 15 mm layer thickness) of 1 ϕ ash

too large distance from the measurement stations. The southern part of Vatnajökull was left out mainly due to the course of watersheds and snow line at Breiðamerkurjökull.

More dust was deposited in the western part of Vatnajökull than in the north eastern part (Fig. 6). The highest concentration, 16.6 g m^{-2}, was found at station T05 on Tungnaárjökull (SW Vatnajökull). Much lower amounts were found on the upper part of the ice cap, namely at D09, Br7 and BB0. As observed in nature, the highest amounts of dust do not necessary have to be at the lowest altitudes of the glacier (closest to the dust source). Whether the material stays on the surface or is accumulated at a certain spot depends on the local topography, the exposure to wind, the material properties, local weather and melt conditions.

AoS 2015

The Ash on Snow (AoS-2015) outdoor experiments were started on 6 February (day 0) and lasted for 17 days, until all the snow had melted.

The effective thickness was reached at the medium concentration (turquoise curve, Fig. 7) of ash (85 g), where the snow depth was the lowest, which means that melt was maximized. The ash is absorbing solar irradiance and warming up the snow. The medium concentration seems to be able to absorb more heat than the small concentration (15 g). However, the snow with the two thinnest layers of ash had melted completely in 14 days below the ash, so also faster than the control snow. The snow with the thickest layer of ash (425 g; 15 mm layer thickness) was still 2 cm deep after 14 days and it took 3 more days (day 17) before it had completely melted. Therefore, critical thickness was achieved with the largest deposition of 15 mm layer thickness (7 mm layer thickness in wet conditions at the end of the experiment remained) since the control snow took as long to melt as the large deposition. This observation supports the hypothesis that ash starts insulating the snow when its thickness exceeds a certain limit.

AoI-2015

During AoI-2015, the indoor ice experiment, melting started after 43 min. The clean ice and the two smallest impurities
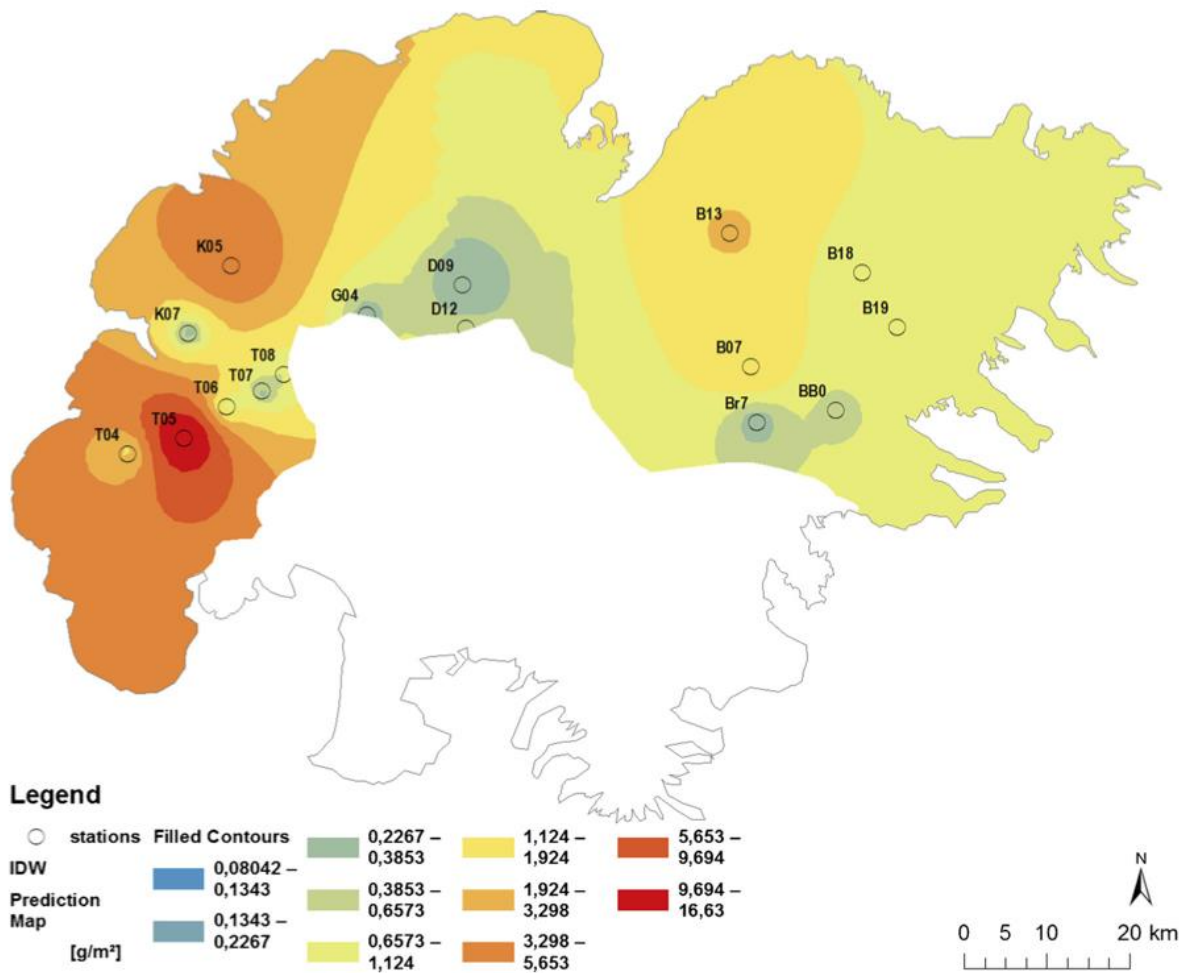
Fig. 6 Inferred dust distribution on Vatnajökull in 2013. The *circles* are the stations where surface snow was collected and the results from these point samples were used for interpolation over the wider area

showed very similar melt behaviour. The onset of the 8437 g m^{-2} (3 mm layer thickness) and 33,749 g m^{-2} (9–13 mm layer thickness) melt took longer; 75 min passed until runoff started at the 8437 g m^{-2} deposition and 125 min for the 33,749 g m^{-2}. The data in Fig. 8 show that once melt had started, the melt rate was similar for all samples. Until

saturation at 95 min for the 33,749 g m^{-2} ash, all the melt water was absorbed by the ash, after that it drains as melt water. Also, at the largest deposition, the ice had completely melted after 365 min, earlier then at the other depositions, because the large amount of ash was down wasting the ice and absorbed all the meltwater.

Fig. 7 Outdoor experiment (AoS-2015) with ash concentrations with three different amounts, 15 g (166 g m^{-2}), 85 g (944 g m^{-2}) and 425 g (4722 g m^{-2}, 15-mm layer thickness) in the size of 1 ϕ of impurities on natural snow on the ground
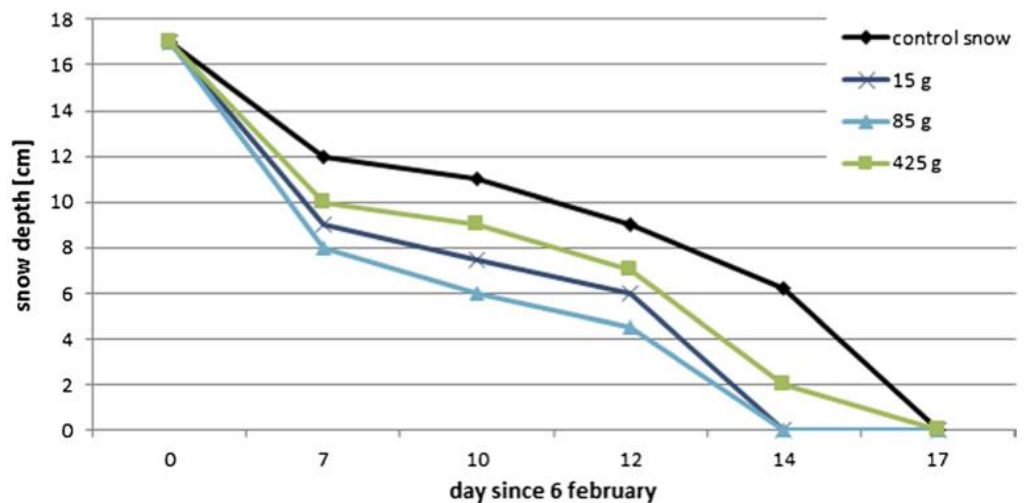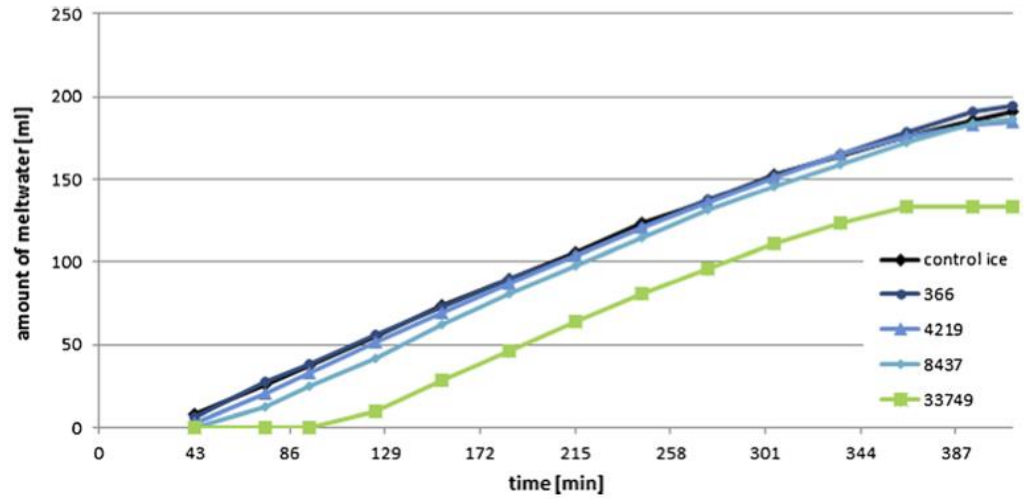
Fig. 8 Experiment with Ash on Ice (AoI) at indoor temperatures of +24 °C with four different concentrations. The amounts in g m^{-2} are indicated by different *colours* as indicated in the legend

Roof-2015

The indoor ice experiment was repeated outside in sunny conditions to study the insulating properties of ash with solar radiation. The results are presented in Fig. 9, which shows the measured amount of meltwater as a function of time for 10 different experiments. Two of these, A1 and B1, are reference measurements with clean reference ice: A1 was left in the shadow where the influence of radiation on temperature and melt is minimized, and B1 was the clean reference sample in the sun.

The highest concentrations A5 and B5 (9 and 13-mm layer thickness) were exceeding the critical thickness because they were starting to melt later (after 170 min) than the reference sample B1 in the sun. A3 with the deposition of 4219 g m^{-2} was achieving the effective thickness, with 1-mm thick layer, visible in the steepest curve and maximum melt rate. The two grain sizes showed different behaviours. After saturation of the fine B-material (87 min), it slipped off the ice (B5 in Fig. 10b) whilst the A-material stayed on the surface. Samples A2 (Fig. 10a) and B2 were forming cryoconite holes where the ash was collecting and melting into the ice.

Fig. 9 Experiment with melt behaviour of different amounts of ash deposited on ice (Roof-2015 experiment) including the influence solar radiation. A-samples with 1 ϕ tephra grain sizes, B-samples with 3.5 ϕ grain sizes. A1 and B1 reference measurement (A1 in the shadow, B1 in the sun); A2 366 g m^{-2}; A3: 4219 g m^{-2}, 1-mm layer thickness; A4 8437 g m^{-2}, 3–5-mm layer thickness; A5 33,749 g m^{-2}, 9 mm layer thickness; B2 292 g m^{-2}; B3 4385 g m^{-2}; B4 8772 g m^{-2}, 1–2 mm layer thickness; B5 35,086 g m^{-2}, 13 mm layer thickness
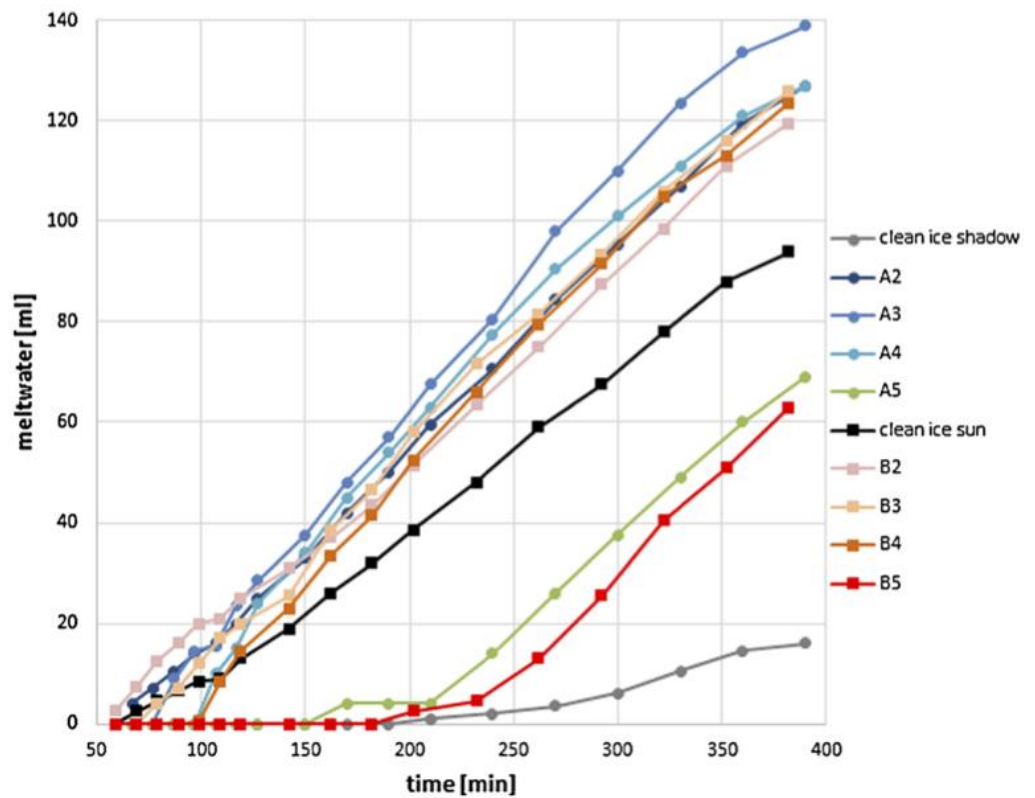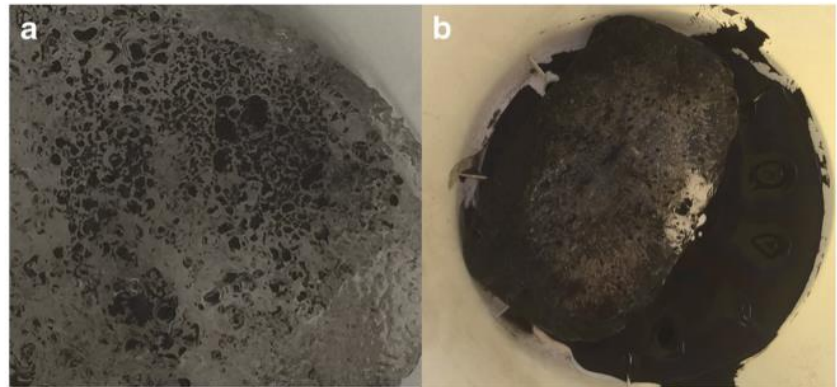
Fig. 10 An example of the ice surface at **a** sample A2 (after 360 min) where ash was melting in cryoconite holes. **b** Sample B5 (after 430 min) where the finer ash slipped off the ice

AiC-2015

The snow on top of the ice had melted inside the container after 1 week. When the control snow was in some parts totally melted, only snow spots of 5 mm thickness were left. In contrast, below the large impurity (425 g) snow of 15 mm thickness with a 5 mm ash layer (wet condition) on top remained. Therefore, the high concentration ash layer supported our assumption to insulate the snow from melt even with temperature influence only. The difference to the other ash on ice experiments was that there was ice beneath the snow so it was cooling from below and the container temperature influenced from above on the snow.

Discussion and conclusions

Our findings suggest that if the ash concentration on snow or ice is small, so the layer thickness is very thin, it has the potential to increase snow melt, but after a threshold the insulation effect begins, and the snow melt is decreased compared to clean ice.

In Table 1, critical and effective thickness of different materials is shown in comparison with the results of our experiments. The two grain sizes of the Eyjafjallajökull 2010 ash behave differently in terms of insulation. The Eyjafjallajökull ash has similar values for effective thickness to the thicknesses of the Icelandic volcano Hekla, it is in the range of 1–2 mm thickness. The critical thicknesses are comparable and visible in all our experiments: in the experiments AoS (at the large deposition with 425 g and 15 mm layer thickness), in the AoI experiment (deposition of 283 g, 120 ml, 33,749 g m^{-2} and 9–13 mm layer thickness), in the Roof 2015 experiment (A5 with 33,749 g m^{-2} and 9 mm layer thickness) as well as in the AiC experiment (425 g deposition and 15 mm layer thickness). The effective thickness was reached at Hekla tephra at 2 mm and at Eyjafjallajökull ash at 1 mm, in the Roof experiment (at A3 with a deposition of 4219 g m^{-2}). The 3.5 ϕ grain size needs a thickness of 13 mm to start insulating as observed in the Roof experiment (B5 with a deposition of 35,086 g m^{-2}). The Roof 2015 experiment shows as well that only 1–2 mm (B4) or smaller (B3, too thin layer to measure) are enough to enhance melt to a maximum for a grain size of 3.5 ϕ.

Different redistribution behaviours of the two grain sizes at the AoI-2015 experiments were observed. The smaller ash particle fraction of 3.5 ϕ slipped off the ice, whilst the layer of 1 ϕ ash stayed on the ice in-tact. It is suggested that the reason for this difference is to be found in the different surface morphologies. Due to the considerable clustering with fine adhesive particles (see e.g., Fig. 2b and d), the coarser material shows a larger specific surface area than 3.5 ϕ particles which feature smooth surfaces (see Fig. 2f and g). Hence, it is likely that the coarse grains are characterized by a larger coefficient of friction than the finer particles. This effect is even increased by the fact that 1 ϕ grains often feature a high vesicularity (Fig. 2c), which facilitates the absorption of water and is expected to enhance static friction. The majority of 3.5 ϕ particles however is blocky and shows no vesicles (see Fig. 2e). Furthermore, the 1 ϕ grains often feature vesicles, which facilitate the absorption of water. This is not the case for the blocky 3.5 ϕ particles characterized by smooth surfaces. This finding implies that finer, smooth particles, are washed away easier by melt streams on the glacier surface than coarser grains with a rough, irregular surface and high vesicularity. Hence, coarser material could have a much greater effect on the albedo.

The highest concentration of dust deposited on Vatnajökull was 16.6 g m^{-2}, which represents dust collection over the summer of 2013. This value is much lower than the mean deposition of 400 g m^{-2} years^{-1} suggested by Arnalds et al. (2014). As the results of the Roof 2015 experiments show for both grain sizes that very small amounts (1–2 mm or smaller) of ash (or dust) deposition are enough to enhance melt, it is possible that the small amounts of dust or ash deposited on Vatnajökull have a comparable melt effect. Similar experiments with volcanic particles of different origins would help to clarify.

References

Adhikary S, Nakawo M, Seko K, Shakya B (2000) Dust influence on the melting process of glacier ice: experimental results from Lirung Glacier, Nepal Himalayas. IAHS Publ. 264

Arnalds O (2010) Dust sources and deposition of aeolian materials in Iceland. Icel Agric Sci 23:3–21

Arnalds O, Thorarinsdottir EF, Thorsson J, Waldhauserova PD, Agustsdottir AM (2013) An extreme wind erosion event of the fresh Eyjafjallajokull 2010 volcanic ash. Sci Rep 3

Arnalds O, Olafsson H, Dagsson-Waldhauserova P (2014) Quantification of iron-rich volcanogenic dust emissions and deposition over the ocean from Icelandic dust sources. Biogeosciences 11(23):6623–6632

Björnsson H, Pálsson F (2008) Icelandic glaciers. Jökull 58:365–386

Bonadonna C, Genco R, Gouhier M, Pistolesi M, Cioni R, Alfano F et al (2011) Tephra sedimentation during the 2010 Eyjafjallajökull eruption (Iceland) from deposit, radar, and satellite observations. J Geophys Res Solid Earth (1978–2012), 116(B12)

Brock B, Rivera A, Casassa G, Bown F, Acuñn C (2007) The surface energy balance of an active ice-covered volcano: Villarrica volcano, southern Chile. Ann Glaciol 45(1):104–114

Bursik M, Jones M, Carn S, Dean K, Patra A, Pavolonis M et al (2012) Estimation and propagation of volcanic source parameter uncertainty in an ash transport and dispersal model: application to the Eyjafjallajokull plume of 14–16 April 2010. Bull Volcanol 74(10): 2321–2338

Dagsson-Waldhauserova P, Arnalds O, Olafsson H (2014) Long-term variability of dust events in Iceland. Atmos Chem Phys Discuss 14:17331–17358. doi:10.5194/acpd-14-17331-2014

Dellino P, Gudmundsson MT, Larsen G, Mele D, Stevenson JA, Thordarson T, Zimanowski B (2012) Ash from the Eyjafjallajökull eruption (Iceland): fragmentation processes and aerodynamic behavior. J Geophys Res Solid Earth (1978–2012), 117(B9)

Doherty SJ, Warren SG, Grenfell TC, Clarke AD, Brandt RE (2010) Light-absorbing impurities in arctic snow. Atmos Chem Phys 10(23):11647–11680

Driedger CL (1981) Effect of ash thickness on snow ablation. In: Lipman P, Mullineaux DR (eds) The 1980 eruptions of Mount St Helens. USGS Professional Paper, 1250, 757–760

Folch A, Costa A, Basart S (2012) Validation of the FALL3D ash dispersion model using observations of the 2010 Eyjafjallajökull volcanic ash clouds. Atmos Environ 48:165–183

Gislason SR, Hassenkam T, Nedel S, Bovet N, Eiriksdottir ES, Alfredsson HA et al (2011) Characterization of Eyjafjallajökull volcanic ash particles and a protocol for rapid risk assessment. Proc Natl Acad Sci 108(18):7307–7312

Gudmundsson MT, Thordarson T, Höskuldsson Á, Larsen G, Björnsson H, Prata FJ, et al (2012) Ash generation and distribution from the April-May 2010 eruption of Eyjafjallajökull, Iceland. Sci Rep 2

Gudmundsson S, Pálsson F, Björnsson H, Magnússon E, Thorsteinsson T, Haraldsson HH (2012) The impact of volcanic aerosols on the energy-and mass balance of Langjökull ice cap, SW-Iceland. In AGU Fall Meeting Abstracts (Vol. 1, p. 0659)

Kirkbride MP, Dugmore AJ (2003) Glaciological response to distal Tephra fallout from the 1947 eruption of Hekla, south Iceland. J Glaciol 49(166):420–428

Meinander O, Kazadzis S, Arola A, Riihelä A, Räisänen P, Kivi R et al (2013) Spectral albedo of seasonal snow during intensive melt period at Sodankylä, beyond the Arctic circle. Atmos Chem Phys 13(7): 3793–3810

Meinander O, Kontu A, Virkkula A, Arola A, Backman L, Dagsson-Waldhauserová P et al (2014) Brief communication: light-absorbing impurities can reduce the density of melting snow. Cryosphere 8(3):991–995

Painter TH, Skiles SM, Deems JS, Bryant AC, Landry C (2012) Dust radiative forcing in snow of the upper Colorado River basin: part I. A 6 year record of energy balance, radiation, and dust concentrations. Water Resour Res. doi:10.1029/2012WR011985

Pálsson F, Björnsson H, Guðmundsson S, Haraldsson H (2013) Vatnajökull: mass balance, meltwater drainage and surface velocity of the glacial year 2010-11. Institute of Earth Sciences, University of Iceland and National Power Company, December 2013, RH-24-2013

Peltoniemi J, Hakala T, Suomalainen J, Puttonen E (2009) Polarised bidirectional reflectance factor measurements from soil, stones, and snow. J Quant Spectrosc Radiat Transf 110(17):1940–1953

Thordarson T, Larsen G (2007) Volcanism in Iceland in historical time: volcano types, eruption styles and eruptive history. J Geodyn 43(1): 118–152

Thorsteinsson T, Jóhannsson T, Stohl A, Kristiansen NI (2012) High levels of particulate matter in Iceland due to direct ash emissions by the Eyjafjallajökull eruption and resuspension of deposited ash. J Geophys Res Solid Earth (1978–2012), 117(B9)

Paper II

Impact of dust deposition on the albedo of Vatnajökull ice cap, Iceland

Dragosics, M., Groot Zwaaftink, Ch., Schmidt, L.S., Guðmundsson, S., Pálsson,F., Arnalds, O., Björnsson, H., Thorsteinsson, Th., Stohl, A.

Impact of dust deposition on the albedo of Vatnajökull ice cap, Iceland.

Monika Dragosics [1], Christine D Groot Zwaaftink [2], Louise Steffensen Schmidt [1] , Sverrir Guðmundsson [1,3], Finnur Pálsson [1], Olafur Arnalds [4], Helgi Björnsson [1], Throstur Thorsteinsson [1], Andreas Stohl [2]

[1] Institute of Earth Sciences, University of Iceland, , Reykjavik, Iceland; [2] NILU - Norwegian Institute for Air Research, Kjeller, Norway, [3] Keilir, Institute of Technology, Reykjanesbær, Iceland; [4] Agricultural University of Iceland, Hvanneyri, Iceland

Correspondence to: Monika Dragosics (mod3@hi.is)

Abstract

Deposition of small amounts of airborne dust on glaciers causes positive radiative forcing and enhanced melting due to the reduction of surface albedo. To study the effects of dust deposition on the mass balance of Brúarjökull, an outlet glacier of the largest ice cap in Iceland, Vatnajökull, a study of dust deposition events in the year 2012 was carried out. The dust-mobilization module FLEXDUST was used to calculate spatiotemporally resolved dust emissions from Iceland and the dispersion model FLEXPART was used to simulate atmospheric dust dispersion and deposition. We used albedo measurements at two automatic weather stations on Brúarjökull to evaluate the dust impacts. Both stations are situated in the accumulation area of the glacier, but the lower station is close to the equilibrium line. For this site (~1210 m a.s.l.), the dispersion model produced 10 major dust deposition events and a total annual deposition of 20.5 g m^{-2}. At the station located higher on the glacier (~1525 m a.s.l.), the model produced nine dust events, with one single event causing ~5 g m^{-2} dust deposition and a total deposition of ~10 g m^{-2} yr^{-1}. The main dust source was found to be the Dyngjusandur floodplain north of Vatnajökull; northerly winds prevailed 80% of the time at the lower station when dust events occurred. In all of the simulated dust events, a corresponding albedo drop was observed at the weather stations. The influence of the dust on the albedo was estimated by using the regional climate model HIRHAM5 to simulate the albedo of a clean glacier surface without dust. By comparing the measured albedo to the modelled albedo, we determine the influence of dust events on the snow albedo and the surface energy balance. We estimate that the dust deposition caused an additional 1.1 m w.e. (water equivalent) of snow melt (or 42% of the 2.8 m w.e. total melt) compared to a hypothetical clean glacier surface at the lower station, and 0.6 m w.e. more melt (or 38% of the 1.6 m w e. melt in total) at the station located further upglacier. Our findings show that dust has a strong influence on the mass balance of glaciers in Iceland.

Key words: dust events, glacier, energy balance, snow melt, surface melt, FLEXPART, albedo

1. Introduction

The cryosphere is an important part of the global climate system. Small changes in reflected and absorbed radiation at snow or ice surfaces can have large impacts on the state of the cryosphere, and on Earth's climate and its hydrological cycle (e.g., Budyko, 1969, Flanner et al., 2007, Painter et al., 2013). Albedo, the reflectivity of a surface, is a dominant component of the surface energy balance. The albedo of snow depends e.g. on the snow grain size, wetness and impurities in the near-surface snow layer (e.g. Wiscombe and Warren, 1980; Meinander et al., 2014). Estimation of snow albedo is important to predict seasonal snowmelt

and runoff rates and for calculating the regional and global energy budget. The snow-albedo feedback, where radiation absorption is enhanced due to impurity content in snow and ice is indicated by complex processes (Hansen and Nazarenko, 2004; Myhre et al., 2013). This initiates a positive feedback loop, i.e. more snow melt results in more absorbed radiation which in turn amplifies the melting. Even though direct global radiative forcing of mineral dust in the atmosphere is calculated as negative in the IPCC report (IPCC, 2013), regionally this depends on both the optical properties of the dust, deposited amounts and the albedo of the underlying surface. Icelandic volcanic dust (mostly from basaltic material) is darker and more absorbing than mineral dust from most other regions. It is expected to cause positive radiative forcing, due to its dark colour, the high albedo of snow and ice, and a *clumping mechanism*, where fine dust impurities in snow form larger particles (Dagsson-Waldhauserova et al., 2015) and accelerate snow melt. In this study, the term *radiative forcing* means the instantaneous surface enhanced absorption due to deposited dust (Painter et al., 2007). In its effect on snow albedo, dust is somewhat similar to black carbon (Yoshida et al., 2016, Goelles et al., 2015) which has received much interest recently as a short-lived climate forcer, especially in the Arctic (e.g. Quinn et al., 2008; AMAP, 2015; Meinander et al., 2016). Other studies, e.g. Di Mauro et al. (2015) and Zhao et al. (2014), have shown the impact of dust and black carbon and their effect on radiative forcing and energy balance. Painter et al. (2007) has shown that snow cover duration in a mountain range in the United States was shortened through surface shortwave radiative forcing by deposition of desert dust. Similarly, Flanner et al. (2014) have shown that the snow albedo effect of deposited volcanic ash from an eruption in Iceland could counteract the otherwise negative radiative forcing of volcanic eruptions caused by sulphur emissions.

Sources of dust in Iceland are the proglacial areas and sandy deserts which cover more than 22% of Iceland (Arnalds et al., 2001). Iceland is one of the most active aeolian places on Earth, even though it is not situated in an arid climate (Arnalds et al., 2016). Due to the large area of sandur plains and strong winds resulting in numerous dust events. On average, 135 dust days per year occurred in Iceland, with 101 dust days in south Iceland and 34 dust days in northeast Iceland, where a *dust day* is defined as a day when at least one weather station recorded at least one dust observation. (Dagsson-Waldhauserova et al., 2013). Airborne redistribution of dust has a strong influence on climate, snowmelt and Icelandic soils. Satellite images have shown that dust particles can be transported over the Atlantic and Arctic Ocean, sometimes for more than 1000 km (Arnalds, 2010). Therefore, Icelandic dust is likely to contribute to Arctic or European air pollution and can affect the climate via dust deposition on Arctic glaciers or sea ice (Arnalds et al., 2016). Icelandic glaciers cover about 11% of the country and the focus area of this study is Vatnajökull, Iceland's largest glacier with an area of more than 8000 km^2 (Figure 1) (e.g. Björnsson and Pálsson, 2008).

In this study we explore what impact dust events in Iceland have on the glacier surface albedo, how often they occur and what their impact on the energy balance of glaciers in Iceland is. Therefore, dust deposition rates were calculated with a dispersion model and compared with albedo measurements on an Icelandic glacier.

2. Methods

    2.1. Dust transport modelling

A recently developed scheme for dust mobilization, called FLEXDUST (Groot Zwaaftink et al., 2016) is used to estimate dust emission. The model can be applied globally, but in this study we only included dust emission from Icelandic sources. FLEXDUST produces dust emission estimates that can be imported directly into the Lagrangian particle dispersion model

FLEXPART (Stohl et al., 1998, 2005) to estimate mineral dust transport, concentrations in the atmosphere and deposition on global and regional scales. FLEXDUST is based on meteorological data from the European Centre for Medium-Range Weather Forecasts (ECMWF), land cover data by the Global Land Cover by National Mapping Organizations (GLCNMO) and additionally, for Iceland, a high-resolution (~1 arcsec) land cover data set that identifies sandy deserts is used (Dagsson-Waldhauserova et al., 2014; Arnalds, 2015). In FLEXDUST, dust can be emitted in regions where mineral dust is available according to the land cover data set. Snow cover inhibits the dust emission. Dust emission is initiated in regions with erodible materials if a threshold friction velocity is exceeded. Contrary to the standard version of FLEXDUST, for this study dust mobilization was assumed not to be influenced by soil moisture. The reason for this is because the source regions are more sediment-like than actual soils, therefore, the functioning of the soil moisture model is questionable for these sources. The exclusion of dust emission during precipitation is better describing the process therefore dust emission is inhibited in case of precipitation. For the dust sources in Iceland, that are sediments rather than soils, this appears to be a better approach. We further used a combination of the erosion classes described by Arnalds et al. (2010) and the threshold values observed by Arnalds et al. (2001) to estimate threshold friction velocity. Once mobilization thresholds are exceeded, dust emission rates are calculated following Marticonera and Bergametti (1995). It is assumed that emitted dust particles have a size between 0.2 and 18.2 μm and follow a size distribution after Kok (2011). Dust emission rates were calculated on a grid with 0.1˚x0.1˚ resolution for Iceland, and with a time resolution of 3 hours.

Using the dust emission rates provided by FLEXDUST, dispersion of the dust in the atmosphere was simulated with FLEXPART version 10. Our simulations were driven with ECMWF operational analysis data with a resolution of 1˚x1˚ globally and a nest over Iceland with 0.2˚x0.2˚ resolution. FLEXPART simulates dispersion by transporting particles using both resolved winds and stochastic motions representing turbulence. Dust was carried in 10 size classes and was subject to both wet and dry removal. Further details about dust simulations with FLEXPART are provided by Groot Zwaaftink et al. (2016). In the current study, dust concentrations and depositions during so-called dust events, i.e., events with strong dust deposition on Vatnajökull simulated by FLEXPART, were analysed. A minimum modelled concentration of 6 μg m^{-3} over at least two days was defined as dust event. In particular, we studied simulated dust events at two automatic weather stations (AWS) situated on Brúarjökull outlet (NE Vatnajökull, Figure 1), namely station B13 at ~1210 m a.s.l. and station B16 at ~1525 m a.s.l.

2.2. Measurements

For this paper, we chose the year 2012, which was characterized by warm temperatures and exceptionally low glacier albedo on Brúarjökull. This year was chosen for analysis because it was not directly influenced by dust deposition from volcanic eruptions, and albedo data from weather stations were available. Dust events modelled by FLEXPART were more distinct in 2012 and agreed better with the albedo observations than in 2013. We used dust measurements in snow for the year 2013, since no measurements were available for 2012, and compared them for the same time period (until October 2013) with the simulated spatial dust distribution over Vatnajökull by FLEXPART.

Since 1996, AWS B13 and B16 at Brúarjökull have been used to measure the incoming (Q_i) and outgoing (Q_o) solar radiation, incoming (I_i) and outgoing (I_o) longwave radiation, wind direction, wind speed, air temperature and relative humidity at 2 m elevation above the

surface (Guðmundsson et al., 2006). Albedo is estimated from measured incoming and reflected short wave radiation as $\alpha = Q_o/Q_i$. Daily albedo values were calculated as the average over 10 minute data obtained between 13 and 14 UTC, when the solar zenith angle is smallest.

The AWS data, specifically albedo, temperature and wind, were compared with dust concentration and deposition values from FLEXPART as well as MODIS images for the measurement period in the year 2012 (dates in this paper are given as *days of the year* or *DOY* between DOY 130 and 283).

Surface snow samples, from the previous year's melted out firn layer, were collected in October 2013 at 16 sites on Vatnajökull (Dragosics et al. 2016). The samples contain dust deposited at these sites during the summer of 2013. The top ~8 cm of snow including impurities were brought to the laboratory, where they were melted, evaporated and the mass of the dust was weighed. Additionally, two ~8 m long firn cores including dust layers from Brúarjökull (NE Vatnajökull), were drilled at B15 in 2015. The dust layers in the cores were dated depending on their depth and compared with mass balance measurements ($h_w \times \rho_w = h_f \times \rho_f$; where h_w is mass balance given as thickness of water, ρ_w is the density of water, h_f is the thickness of a firn layer and h_f is the density of firn). Dust deposition rates were estimated by measuring the mass of the dust content in the annual layers, and compared to model results (Table 1).

2.3. Surface energy balance calculations

The total energy balance (M) for a melting glacier surface is expressed as

$$M = R + H + Hp, \tag{1}$$

where $R = Q_i(1 - \alpha) + I_i - I_o$ is the net radiation obtained from the observed shortwave and longwave radiation components, and $H = H_d + H_l$ is the net turbulent flux of sensible (H_d) and latent (H_l) heat calculated from the observed temperature, humidity and wind speed within the boundary layer. A one-level model with stability factor and different roughness lengths for wind-speed, temperature and humidity, described in Guðmundsson et al. (2009) was used to calculate H_d and H_l. Heat supplied by precipitation (H_p) is considered negligible and the melt (ablation) m is calculated as

$$m = \begin{cases} \frac{M}{\rho_w L_f}; M \geq 0 \\ 0; \quad M < 0 \end{cases} \tag{2}$$

where L_f is the latent heat of fusion ($L_f = 3.34\ 10^5$ J kg^{-1}) and ρ_w the density of water (1000 kg m^{-3}) (e.g. Guðmundsson et al., 2006).

Albedo is a key variable in the surface energy balance and it is used to calculate ice melting. If the energy balance is positive, this indicates an energy gain to the surface; if it is negative, it means an energy loss. The accuracy of the instruments (Kipp & Zonen CNR1, 2000) measuring longwave and shortwave radiation fluxes at AWSs was 3% (Guðmundsson et al., 2009).

To quantify the enhanced melt rates due to dust on the surface, the development of surface albedo for a dust free surface must be estimated at specific locations and meteorological conditions. This albedo estimate and in situ AWS data is used to calculate the energy balance

at the AWS sites. The results can be compared to energy balance calculated from only the AWS data including the observed albedo. The development of surface albedo of snow is depending on meteorological processes in the surface boundary layer, the energy budget of the surface, snowfall events etc. A regional climate model, which is forced with reanalysis data from a general circulation model at the lateral boundary and simulates the boundary layer meteorology and surface energy balance, can be used to simulate the clean surface albedo. Here we use the HIRHAM5 climate model. The HIRHAM5 model combines the dynamical core of the HIRLAM7 numerical forecasting model (Eerola, 2006) with the physical schemes from the ECHAM5 general circulation model (Roeckner et al., 2003). Model simulations have been validated over Greenland using AWS and ice core data (e.g. Lucas-Picher et al., 2012; Langen et al., 2015). Using the same method described in Langen et al. (2015), we run the surface scheme in HIRHAM5 by forcing it with atmospheric parameters from a previous model run. This method allows us to implement an improved albedo scheme (Nielsen-Englyst, 2015) without running the full model. This is described in more detail in the appendix and Schmidt et al. (submitted).

2.4. Evaluation of modelled albedo by HIRHAM5

As there was no ice at the surface at either of the two AWS's, we allowed the modelled clean surface albedo to drop to the value of clean firn, which we assumed to be 0.55. This value is based on the recommended value by Cuffey and Paterson (2010), but also represented in observed albedo in the years 2002, 2009 and 2014 (Appendix Fig. A1). For those years, measured albedo remained mostly above 0.55 for the whole measuring period. Under dry conditions the modelled albedo can only drop to 0.77. The albedo of fresh snow was assumed to be 0.9. Based on albedo measurements this value is assumed to be realistic after new snow events as seen in Fig. A1 in the Appendix. Sometimes measured albedo values especially in autumn can reach high values, even above 1. This can be explained due to the high solar zenith angle, multiple reflections and instrumental error (Kipp & Zonen CNR1, 2000).

The time scale τ_m, which determines how fast the albedo reaches its minimum value, was chosen to be 4 days, as it gives the best fit with the measurements without dropping below the measured values. In addition, this value gave the best fit when comparing with albedo measurements for other years with higher albedo (Appendix, Fig. A1 and Fig. A2), where the rate of the albedo decreased after a snow fall was realistic. Measured albedo might drop faster after a new snow event than predicted by the HIRHAM5 model because metamorphosis of fresh snow is fast at relatively high air temperatures (Oerlemans, 2001); light might also penetrate through the new snow and since the albedo of a thin snowpack depends on the albedo of the underlying surface (Wiscombe and Warren 1980) it could reach the dust surface below.

The AWS B16 is situated in the accumulation area, but B13 is close to the equilibrium line of the glacier. This means that only in some years, as e.g. in 1997, 2004, 2005 and 2012 (Appendix Fig. A3) the mass balance was negative and the previous years' surface melted out at B13 and exposed firn with dust. Since 2012 was a year of very warm temperatures and negative mass balance, not only deposition during dust events influenced the albedo and energy balance. At station B13 between days 206 and 225 simulation values have been manually set to the minimum value of 0.55 because HIRHAM5 simulated a snowfall event, which was not observed.

3. Results

   3.1. Spatial distribution of dust deposition 2013 and total deposition rates 2012 and 2013

The annual dust deposition distribution for the surface of Vatnajökull for 2013 showed a similar pattern in the model simulation and in the observations (Figure 2). The model simulated the highest concentrations in the south western part of Vatnajökull (Tungnaárjökull, Skaftárjökull, Síðujökull), followed by the north western and northern parts (Brúarjökull). This distribution is due to the major dust mobilization areas around Vatnajökull, such as Dynjgusandur, Tungná- and Skaftáöræfi (the area with severe erosion SW of Vatnajökull (Figure 1), as well as the prevailing winds. The measurements of Dragosics et al. (2016) are shown as circles superimposed upon the modelled dust distribution in Figure 2. The average dust deposition for the 16 measurement locations was 2 g m^{-2}. The standard deviation of the measurements, 4 g m^{-2}, was quite high due to one outlier with a deposition value of 16.6 g m^{-2} in the SW on Tungnaárjökull. The average modelled deposition for the same locations as in the measurements is 6 g m^{-2}, with a standard deviation of 1 g m^{-2}. Thus, the model overestimated measured dust deposition by a factor of three and generated smaller dust variability. The latter was not surprising, given the relatively coarse resolution of the model compared to the point measurements. Furthermore, variability in observed dust amounts was not only caused by the patterns of dust deposition on the glacier, but also due to windblown transport over an undulating surface, or surface melt streams washing away surface dust. Such processes were not accounted for in the modelled dust patterns. Regarding the mean concentrations, at least part of the model high bias may, in fact, be due to a location bias in the measurements. Most of the measurement locations are in the accumulation zone of the glacier. Model grid cells of the measurements often extend to the glacier edges, where deposition amounts are higher. Regardless of whether the model bias can be explained or not, the comparison shows that the order of magnitude of dust deposition on Vatnajökull is captured by the model.

In Table 1, the measured and modelled dust deposition during the years 2012 and 2013 for stations on Brúarjökull, our main area of investigation, were reported. Again, the model tended to overestimate dust deposition.

   3.2. Dust events on Brúarjökull 2012

FLEXPART results for both dust concentrations in the air and dust deposition on the glacier surface were reported for the dust events for the year 2012 at station B13 (Table 2) and B16 (Table 3). Albedo, temperature and wind at 2 m elevation were measured at the AWSs, while precipitation data were taken from the ECMWF model. At station B13 there were ten modelled dust events during the measuring period (9 May to 14 October 2012), and all of them were associated with an observed albedo drop during the event at the AWS. Four events had high dust concentrations and depositions (bold in Table 2), and six smaller events occurred as well (Figure 3). The highest deposition values were simulated during event 6 with 6.6 g m^{-2} of dust deposited during a period of 14 days with an albedo drop of 0.65 from the maximum to the minimum albedo value during that period. In contrast, at station B16 (Table 3) the largest deposition (5.2 g m^{-2}) occurred during event 1 with an albedo drop of 0.17. Two events, one occurred during sub-freezing temperatures, and the other during melting temperatures, were described in detail in section 3.3.

The albedo was almost always lower at site B13 than at site B16, due to the lower elevation and thus higher temperatures and increased melting at this site, and probably also because of its proximity to a major dust source area (Dyngjusandur). The biggest dust events happened in

spring (mid-May) and autumn (end of August and October), especially at station B16. Dust event 5 coincided with warm summer temperatures and exposure of the ablation area, where albedo at B13 reached its lowest value, 0.08, on day 223. At the lower elevation site B13 (~1210 m a.s.l.), dust deposition and concentration values during dust events were always larger than at the higher site B16 (~1525 m a.s.l.), except for event 1 (section 3.3). The duration of the events was also often longer at B13 than at B16. Furthermore, no dust was simulated at station B16 during event 8 (Table 3).

3.3. Case studies

Two dust events have been chosen for a detailed description. Event no. 1 (Figure 4) was by far the biggest event at B16 and temperatures were below freezing all the time, and event no. 2 (Figure 5) happened, as was often the case, during melting temperatures. The analysis of event no. 2 was supported by the availability of a clear-sky MODIS image showing the dust cloud and deposition.

3.3.1. Dust event 1

Dust event 1 is one of four major modelled dust storms on Brúarjökull in 2012 (Figure 4) and the only event for which total simulated dust deposition was higher at station B16 (3.7 g m^{-2}) than at B13 (2.6 g m^{-2}). This explains why the albedo reached a lower value between day 134 and 139 at B16 than B13, which is very atypical. During the event, albedo dropped by 0.15 from 0.9 to 0.75 at B13 (Table 2) and by 0.17 from 0.88 to 0.72 at B16. Albedo peaked on day 133 at B16 and on day 134 at B13 because of snow fall. Simulated dust deposition started on day 134 at midday and lasted until day 136 (afternoon). This was the largest wet deposition event at both stations. At B13 (B16) there were 1.6 g m^{-2} (1.3 g m^{-2}) dust deposited as dry deposition and 2.1 g m^{-2} (3.9 g m^{-2}) as wet deposition, which at B16 was by far the largest deposition in a single event.

Near-surface dust concentration reached values of 193 μg m^{-3} at B13 and 121 μg m^{-3} at B16. Temperature decreased during the event and remained well below the freezing point, excluding the possibility that melt processes were responsible for the albedo drop. This strongly supports our hypothesis that the dust deposition caused the albedo reduction. Since dust was deposited during snowfall, the albedo drop is probably smaller than if the dust were deposited entirely by dry deposition. In fact, normally albedo increases during snowfall, so the dust deposition must have more than compensated this effect. Wind was blowing from the north during days 134-138, with high wind speeds on day 134 and 135 (B16 16 m s^{-1}, B13 11 m s^{-1}), indicating that dust was transported most likely from Dyngjusandur.

55

3.3.2. Dust event 2

Dust event 2 is the second largest modelled dust event in terms of dust concentration and fourth biggest in terms of total deposition at station B13 (2.5 g m^{-2}) but it was much smaller at B16 (0.1 g m^{-2}) and started later (day 146). Dust concentrations at B13 (B16) reached 225 μg m^{-3} (19 μg m^{-3}). Dust deposition started in the afternoon on day 145 and albedo dropped on day 146 (from 0.73 to 0.60). During the whole dust event albedo dropped by 0.36 (from 0.86 to 0.5) at B13 and by 0.28 (from 0.87 to 0.59) at B16. Temperature rose above the freezing point on day 143 and this may partly explain the albedo reduction. However, the strongest albedo reduction coincided closely with the time period of the dust deposition. In particular, notice that the albedo did not decrease significantly after the end of the deposition event, even though temperatures (at least during daytime) remained above the freezing point.

Notice also that the albedo reduction was stronger at B13 than at B16, in agreement with the higher dust deposition at B13. Precipitation occurred until day 146, so mainly before dust deposition, suggesting that dust deposition was the main factor in this albedo drop. Wind was strongest on day 146 (13.6 m s^{-1} at B13) and from SW (glacier wind), but changed to WNW until day 149.

3.3.3. Average dust event at B13 in 2012

Using the values reported in Table 2, we calculated averages to characterize an *average* dust event at the B13 site. On average a dust event at station B13 in 2012 lasted for 6 days, had a maximum dust concentration of 122 μg m^{-3} and a total deposition of 2 g m^{-2}. Dry deposition in all cases except the first event exceeded wet deposition. This is due to the proximity of the measurement site to the source area and gravitational settling of larger particles, which dominated the removal near the source. The albedo is on average lowered by 0.18 in a dust event. This large reduction had a strong impact on the radiation and energy balance of the glacier. The average temperature during dust events was -2°C (at ~1210 m elevation) and the prevailing wind direction in 80% of the events was northerly, in 20% it is SW (the direction of the glacier wind on Brúarjökull). Average ECMWF precipitation during events was ~23 mm.

3.4. Surface energy balance impact of dust deposition

Deposition of dark dust particles on a glacier surface lowers the surface albedo, thus also the surface energy balance and in general increases the energy available for melt. In order to estimate the contribution of this effect, the surface energy balance (and the surface melt from energy balance) at the two AWS sites B13 and B16 was estimated from the AWS data in 2012. To estimate the effect, the regional climate model HIRHAM5 was used to simulate a clean glacier surface for the weather conditions occurring at the AWS B13 and B16 in 2012. The simulated clean surface albedo (black line in Figure 7) is compared to the observed albedo including impurities (red line in Figure 7). Generally, the model captures the measured albedo variability; however, the observed albedo is more variable and reaches lower values between events of snowfall**.** Since this is a simple model, we are not expecting the model to capture all details. The statistical fit for HIRHAM5 compared to the AWS data showed a better fit for years with higher albedos where the previous summer surface did not melt out. The average bias, taken as the difference between HIRHAM5 and AWS data, is 0.08 for the years 1997-2014 whereas for the year 2012 it is 0.18 which means an overestimate by the model. The correlation coefficient for measured and simulated albedo data for the year 2012 is 0.77, which is higher than the average value for other years of 0.68.

The difference between the modelled clean surface and the real surface is greater at B13 than B16. This was expected since dust concentration is much higher at the lower site B13 and snowfall more common at the upper site B16. We also know from mass balance measurements, that at B13 all the winter snow melted, exposing firn and surface dust from previous years (this happened at day ~205). With addition of dust from dust events starting on days 202 and 220 (Figure 8) the albedo values dropped very low at B13 between days 220 and 236. The simulated energy balance did not predict the snow from the previous winter to have been melted away completely, exposing the firn layer.

High temperatures at B13 up to ~5 °C coincide with dust event 5, which caused peaks in snow melt of 8.13 cm w.e. d^{-1} on day 222. In the autumn, after day ~240, the energy balance was mostly negative. Low net radiation is caused by low solar radiation due to shorter days and high albedo caused by snow fall. This is accompanied with negative turbulent heat fluxes (due to air temperatures below zero and strong winds) and resulted in negative total energy, i.e. no energy available for melting in 2012.

The total summer melt at B13 in 2012 estimated from the energy balance calculated for a dust free surface was 1.7 m w.e., whereas for the measured albedo the melt was estimated at 2.8 m w.e. From this we conclude that the melt increased by 1.1 m w.e., or by ~60%, due to dust deposition, and melting out of the dusty firn surface below. Other impurities such as black carbon were expected to be negligible (Dadic et al., 2013, Fig. 12a; Meinander et al., 2014). At the higher site, B16, 1.0 m w.e. of snow melt was calculated for the modelled dust free surface and 1.6 m w.e. when using the measured albedo, which results in 0.6 m more snow melt caused by dust on the surface. The increase in melt is similar to that in B13, i.e. additional 60%.

4. Discussion and conclusion

In this paper, we have shown that dust events modelled by FLEXDUST correspond to reductions in the observed albedo at two AWS sites on Vatnajökull. This indicates that the model is able to capture the occurrence of individual dust events. Furthermore, we showed that the model captures both the observed spatial distribution of dust on the glacier as well as the magnitude of the total annual deposition amounts. This suggests that the model can be used for longer-term studies, to quantify the dust deposition on Vatnajökull, including its interannual variability. Table 2 shows the dust events of the year 2012 at station B13 on Brúarjökull, where in total 10 dust events occurred; four main events and six smaller events. The AWS measurements show a drop in albedo in connection to all dust events predicted by FLEXPART within the AWS's survey period. The prevailing wind direction during dust events at site B13 is from a northerly direction, while for the whole period downslope (SW) winds dominate. The wind direction during dust events corresponds to the main dust source Dyngjusandur, north of Vatnajökull. At site B16, situated further upglacier, 9 dust events occurred (Table 3) where the first dust event with ~5 g m^{-2} of dust deposited within 3 days was by far the largest.

In Arnalds et al. (2014) average deposition of dust on Icelandic glaciers is estimated as ~400 g m^{-2} yr^{-1} which seems to be overestimated. Their estimate includes periodic tephra deposition and large dust events based on a country average and it does not adequately account for topographic differences and that much of the glacial areas are upwind for dry winds from the main dust sources at the glacial margins. With FLEXPART, we calculated much lower annual deposition rates for Vatnajökull and its surroundings in 2013 (Figure 2), up to 34 g m^{-2} in the

SW of the glacier. Moreover, modelled values for dust deposition rates on Brúarjökull of 20 g m^{-2} (B13) and 10 g m^{-2} (B16) for 2012 were much lower.

Firn core B drilled on Brúarjökull showed a dust layer of ~8 g m^{-2} for 2012 (Table 1), in very good agreement with the simulated dust of 8.5 g m^{-2}. At firn core (A), drilled in the immediate vicinity of core B, observed deposition rate was much smaller (1.7 g m^{-2}), showing the large spatial variability and consequent uncertainty in comparing point measurements to model simulations. We thus consider the model results satisfactory if they are in the same order of magnitude as observed dust amounts in ice cores or snow samples.

To estimate the impact of dust on the surface energy balance and melt rates, the regional climate model HIRHAM5 was used to simulate the surface albedo for a dust free, i.e. clean snow surface during the summer 2012. The surface energy balance (and melt rate) was calculated using the simulated albedo and the albedo observed from the AWS data. At the lower site, B13, the difference between dust free and real surface is 1.1 m w.e. of more snow melt (1.7 m w.e. snow melt for the clean surface and 2.8 m w.e. for the real surface). This does not only include dust events lowering surface albedo, but also dust and tephra that was deposited during previous years melting out from below. At the upper site B16 the difference results in 0.6 m of more snow melt (1.0 m w.e. for the clean surface and 1.6 m w.e. for the AWS). Since B16 is situated in the accumulation area, no dust expected to melt out from below. It cannot be excluded that small amounts of organic material or black carbon are deposited on the snow surface and influence albedo, but from in situ investigations this has not been observed in this area.

The year 2012 was a year of intensive summer melt. At site B13 on Vatnajökull the measured summer mass balance was 2.3 m w.e. mass loss, which means 0.5 m more mass loss than the average since 1993 (1.7 m w.e.). Summer mass balance measurements on Vatnajökull show 2.3 m w.e. of total mass loss at B13 which is 0.5 m less melt compared to calculated energy balance converted into snow melt (2.8 m w.e.). Most of these differences are assigned to summer snow fall that melts, and was not captured with the mass balance measurements.

Oerlemans et al. (2009) reported that decreased albedo at Vadret da Morteratsch glacier caused an additional removal of about 3.5 m of ice for the 4 year period 2003–06. This means 0.9 m more melt on average per year. Gabbi et al. (2015) compared a glacier surface with deposits of black carbon and Saharan dust to pure snow conditions for a 100 year period (1914-2014). They found that the mean annual albedo decreased by 0.04–0.06, therefore the mean annual mass balance was reduced by about 28–49 cm. These alpine melt rates due to impurities are in the same order of magnitude as our results.

Albedo comparisons for other years (Appendix, Fig. A3) have shown very low albedo values for 1997, 2004, 2005 and 2012. The surface dirt causing the low albedo in 1997 is related to the Grímsvötn eruption in 1996, and the following huge jökulhlaup with deposition of fine grained particles on Skeiðarársandur sandur plain. This was a vast source of dust in the dry and warm 1997 summer. The low albedo in 2005 and 2012 most likely also related to the 2004 and 2011 Grímsvötn eruptions (e.g. Guðmundsson et al. 2004, Möller et al. 2013). In 2004 increased melt rates due to high wind-driven turbulent heat fluxes in the end of July followed by exceptionally warm and sunny weather in August sped up melting into old firn (Guðmundsson et al. 2006).

The results in this paper shows positive radiative forcing impact on snow melt of Icelandic glaciers caused by deposition of dust that strongly enhances absorption of light. The duration

of dust radiative effects on glacier surfaces is extended compared to purely atmospheric effects because of the short lifetime of dust in the atmosphere.

Acknowledgements

References:

AMAP Assessment 2015: Black carbon and ozone as Arctic climate forcers. Arctic Monitoring and Assessment Programme (AMAP), Oslo, Norway. vii + 116 pp, 2015.

Arnalds, O., Olafsson, H., Dagsson-Waldhauserova, P.: Quantification of ironrich volcanogenic dust emissions and deposition over ocean from Icelandic dust sources. Biogeosciences 11, 6623–6632. http://dx.doi.org/10.5194/bg-11-6623-, 2014.

Arnalds, O.: The soils of Iceland, 160 pp., Springer, Dordrecht, The Netherlands, 2015.

Arnalds, O., Dagsson-Waldhauserova, P., & Olafsson, H.: The Icelandic volcanic aeolian environment: Processes and impacts—A review. Aeolian Research, 20, 176-195; 2016.

Arnalds, O., Gisladottir, F.O., Sigurjonsson, H: Sandy deserts of Iceland: an overview. Journal of Arid Environments 47, 359–371, 2001.

Benn, D. and Evans, D. J.: Glaciers and glaciation. Second edition. 802 pp. Routledge, 2010.

Björnsson, H., & Pálsson, F.: Icelandic glaciers. Jökull, 58, 365-386, 2008.

Björnsson, H., F. Pálsson, S. Gudmundsson, E. Magnússon, G. Adalgeirsdóttir, T. Jóhannesson, E. Berthier, O. Sigurdsson, and Th. Thorsteinsson, 2013. Contribution of Icelandic ice caps to sea level rise: Trends and variability since the Little Ice Age. Geophysical Research Letters, Vol. 40, 1-5, doi:10.1002/grl.50278.

Budyko, M. I.: The effect of solar radiation variations on the climate of the earth. Tellus, 21(5), 611-619, 1969.

Cuffey, K. M., & Paterson, W. S. B.: The physics of glaciers, 693pp, Academic Press, 2010.

Dadic, R., Mullen, P. C., Schneebeli, M., Brandt, R. E., & Warren, S. G. Effects of bubbles, cracks, and volcanic tephra on the spectral albedo of bare ice near the Transantarctic Mountains: Implications for sea glaciers on Snowball Earth. Journal of Geophysical Research: Earth Surface, 118(3), 1658-1676, 2013.

Dagsson-Waldhauserova, P., Arnalds, O., & Olafsson, H.: Long-term frequency and characteristics of dust storm events in Northeast Iceland (1949–2011). Atmospheric Environment, 77, 117-127, 2013.

Dagsson-Waldhauserova, P., Arnalds, O., Olafsson, H., Skrabalova, L., Sigurdardottir, G. M., Branis, M., et al.: Physical properties of suspended dust during moist and low wind conditions in Iceland. Icelandic Agricultural Sciences, 27, 25-39, 2014.

Dagsson-Waldhauserova, P., Arnalds, O., Olafsson, H., Hladil, J., Skala, R., Navratil, T., ... & Meinander, O.: Snow–dust storm: unique case study from Iceland, March 6–7, 2013. Aeolian Research, 16, 69-74, 2015.

Di Mauro, B., Fava, F., Ferrero, L., Garzonio, R., Baccolo, G., Delmonte, B., & Colombo, R.: Mineral dust impact on snow radiative properties in the European Alps combining ground, UAV, and satellite observations. Journal of Geophysical Research: Atmospheres, 120(12), 6080-6097, 2015

Dragosics, M., Meinander, O., Jónsdóttir, T., Dürig, T., De Leeuw, G., Pálsson, F., Dagsson-Waldhauserová, P., and Thorsteinsson, Th.: Insulation effects of Icelandic dust and volcanic ash on snow and ice. Arab. J. Geosci., 9, 126, 2016.

Eerola, K.: About the performance of HIRLAM version 7.0. HIRLAM Newsletter, 51:93–102, 2006.

Flanner, M. G., Zender, C. S., Randerson, J. T., & Rasch, P. J.: Present-day climate forcing and response from black carbon in snow. Journal of Geophysical Research: Atmospheres, 112(D11), 2007.

Flanner, M. G., Gardner, A. S., Eckhardt, S., Stohl, A., and Perket, J.: Aerosol radiative forcing from the 2010 Eyjafjallajökull volcanic eruptions. J. Geophys. Res. 119, 9481-9491, doi:10.1002/2014JD021977, 2014.

Gabbi, J., Huss, M., Bauder, A., Cao, F., & Schwikowski, M.: The impact of Saharan dust and black carbon on albedo and long-term mass balance of an Alpine glacier. The Cryosphere, 9(4), 1385-1400, 2015.

Gölles, T., Bøggild, C. E., & Greve, R.: Ice sheet mass loss caused by dust and black carbon accumulation. The Cryosphere, 9(5), 1845-1856, 2015. doi:10.5194/tc-9-1845-2015

Greuell, W., C. Genthon: Mass Balance of the Cryosphere: Observations and Modelling of Contemporary and Future Changes, eds. Jonathan L. Bamber and Antony J. Payne. Published by Cambridge University Press. Cambridge University Press, 2003.

Groot Zwaaftink, C. D., H. Grythe, H. Skov, and A. Stohl: Substantial contribution of northern high-latitude sources to mineral dust in the Arctic, J. Geophys. Res. Atmos., 121, doi:10.1002/2016JD025482, 2016.

Guðmundsson, S., Björnsson, H., Pálsson, F. and Haraldsson, H. H.: Energy balance of Brúarjökull and circumstances leading to the August 2004 floods in the river Jökla, N-Vatnajökull (Vol. 55, pp. 1-18). Jökull, 2006.

Guðmundsson, S., Björnsson, H., Pálsson, F., & Haraldsson, H. H.: Comparison of energy balance and degree-day models of summer ablation on the Langjökull ice cap, SW-Iceland. Jökull, 59, 1-18, 2009.

Hansen, J., & Nazarenko, L.: Soot climate forcing via snow and ice albedos. Proceedings of the National Academy of Sciences of the United States of America, 101(2), 423-428, 2004.

Hock, R.: Glacier melt: a review of processes and their modelling. Progress in physical geography, 29(3), 362-391, 2005.

IPCC: Climate change 2013: The physical science basis. In: Working Group I, Contribution to the IPCC 5th Assessment Report – summary for policy makers, 2013.

Kipp&Zonen Instruction Manual for Pyranometer/Albedometer CM11 and CM14. (2000)http://www.kippzonen.com

Kok, J. F.: A scaling theory for the size distribution of emitted dust aerosols suggests climate models underestimate the size of the global dust cycle. Proceedings of the National Academy of Sciences, 108(3), 1016-1021, 2011.

Langen, P. L., Mottram, R. H., Christensen, J. H., Boberg, F., Rodehacke, C. B., Stendel, M., van As, D., Ahlstrøm, A.P., Mortensen, J., Rysgaard, S., Petersen, D., Svendsen, K. H. , Aðalgeirsdóttir, G. and Cappelen J.: Quantifying Energy and Mass Fluxes Controlling Godthåbsfjord Freshwater Input in a 5-km Simulation (1991–2012). Journal of Climate, 28(9), 3694-3713, 2015.

Lucas-Picher, P., Wulff-Nielsen, M., Christensen, J. H., Adalgeirsdóttir, G., Mottram, R. H. and Simonsen, S. B.: Very high resolution regional climate model simulations over Greenland: Identifying added value. Journal of Geophysical Research, 117:2108, 2012.

Marticorena, B. and Bergametti, G.: Modeling the atmospheric dust cycle: 1. Design of a soil-derived dust emission scheme. Journal of Geophysical Research: Atmospheres, 100(D8), 16415-16430, 1995.

Meinander, O., Kontu, A., Virkkula, A., Arola, A., Backman, L., Dagsson-Waldhauserová, P., ... & Leppäranta, M. Brief communication: Light-absorbing impurities can reduce the density of melting snow. The Cryosphere, 8(3), 991-995, 2014.

Meinander, O., Dagsson-Waldhauserova, P. and Arnalds, O.: Icelandic volcanic dust can have a significant influence on the cryosphere in Greenland and elsewhere. Polar Research, 35, 2016.

Möller, R., Möller, M., Björnsson, H., Guðmundsson, s., Pálsson, F., Oddsson, B., Kukla, P. A., Schneider, C.: MODIS-derived albedo changes of Vatnajökull (Iceland) due to tephradeposition from the 2004 Grímsvötn eruption. International Journal of Applied Earth Observation and Geoinformation 26, 256-269, 2013.

Myhre, G., Shindell, D., Bréon, F. M., Collins, W., Fuglestvedt, J., Huang, J., ... & Nakajima, T.: Anthropogenic and Natural Radiative Forcing. In: Climate Change 2013: The Physical Science Basis. Contribution of Working Group 1 to the Fifth Assessment Report of the Intergovernmental Panel on Climate Change. Table, 8, 714, 2013.

Nielsen-Englyst, P.: Impact of albedo parameterizations on surface mass balance and runoff on the Greenland Ice Sheet. Master's thesis University of Copenhagen, unpublished, 2015.

Oerlemans, J., & Knap, W. H.: A 1 year record of global radiation and albedo in the ablation zone of Morteratschgletscher, Switzerland. Journal of Glaciology, 44(147), 231-238, 1998.

Oerlemans, Johannes (2001). Glaciers and climate change. CRC Press.

Oerlemans, J., Giesen, R. H., & Van den Broeke, M. R.: Retreating alpine glaciers: increased melt rates due to accumulation of dust (Vadret da Morteratsch, Switzerland). Journal of Glaciology, 55(192), 729-736, 2009.

Painter, T. H., A. P. Barrett, C. C. Landry, J. C. Neff, M. P. Cassidy, C. R. Lawrence, K. E. McBride, and G. L. Farmer: Impact of disturbed desert soils on duration of mountain snow cover, Geophys. Res. Lett., 34, L12 502, doi:10.1029/2007GL030284, 2007.

Painter, T. H., Flanner, M. G., Kaser, G., Marzeion, B., VanCuren, R. A., & Abdalati, W.: End of the Little Ice Age in the Alps forced by industrial black carbon. Proceedings of the national academy of sciences, 110(38), 15216-15221, 2013.

Quinn, P. K., Bates, T. S., Baum, E., Doubleday, N., Fiore, A. M., Flanner, M., ... & Shindell, D.: Short-lived pollutants in the Arctic: their climate impact and possible mitigation strategies. Atmospheric Chemistry and Physics, 8(6), 1723-1735, 2008.

Roeckner, E., Bäuml, G., Bonaventura,L., Brokopf, R., Esch, M.,Giorgetta, M., Hagemann, S., Kirchner, I.,Kornblueh, L., Manzini, E., Rhodin, A., Schlese, U., Schulzweida, U. and Tompkins , A.: The atmospheric general circulation model ECHAM 5 PART I: Model description. Technical Report 349, Report / MPI für Meteorologie, 2003.

Schmidt, L.S., Aðalgeirsdóttir, G., Pálsson, F., Björnsson, H., Guðmundsson, S., Langen, P.L., Mottram, R., Gascoin, S.: Evaluating the Surface Energy Balance in the HIRHAM5 Regional Climate Model Over Vatnajökull, Iceland, Using Automatic Weather Station Data, submitted to the cryosphere.

Stohl, A., Hittenberger, M., and Wotawa, G.: Validation of the Lagrangian particle dispersion model FLEXPART against large-scale tracer experiment data. Atmospheric Environment, 32(24), 4245-4264, 1998.

Stohl, A., Forster, C., Frank, A., Seibert, P., and Wotawa, G.: Technical Note : The Lagrangian particle dispersion model FLEXPART version 6.2. Atmos. Chem. Phys. 5, 2461-2474, 2005.

Wiscombe, W. J., & Warren, S. G.: A model for the spectral albedo of snow. I: Pure snow. Journal of the Atmospheric Sciences, 37(12), 2712-2733, 1980.

Yoshida, A., Moteki, N., Ohata, S., Mori, T., Tada, R., Dagsson-Waldhauserová, P., & Kondo, Y.: Detection of light-absorbing iron oxide particles using a modified single-particle soot photometer. Aerosol Science and Technology, 50(3), 1-4. DOI: 10.1080/02786826.2016.1146402, 2016.

Zhao, C., Hu, Z., Qian, Y., Ruby Leung, L., Huang, J., Huang, M., ... & Yan, H.: Simulating black carbon and dust and their radiative forcing in seasonal snow: a case study over North China with field campaign measurements. Atmospheric Chemistry and Physics, 14(20), 11475-11491, 2014.
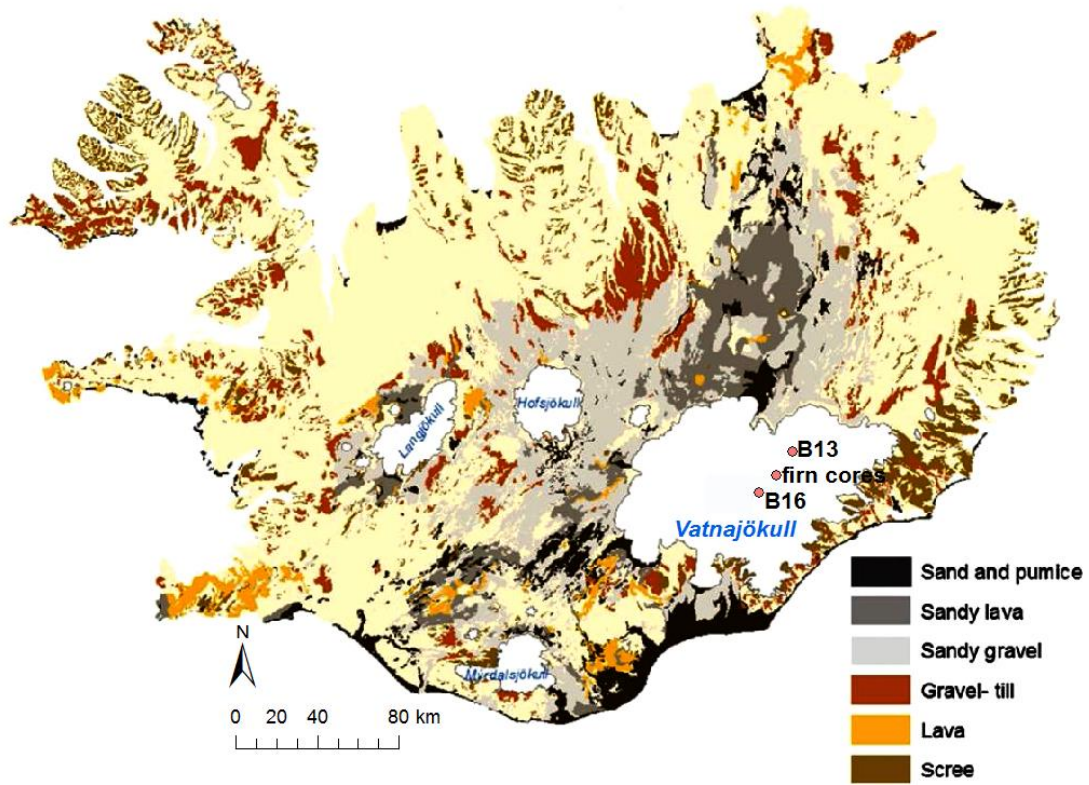
Figure 1: Iceland with glacier outlines and soil map adapted from Arnalds (2015). The two AWSs at B13 and B16 as well as the firn core drill site on Brúarjökull are highlighted
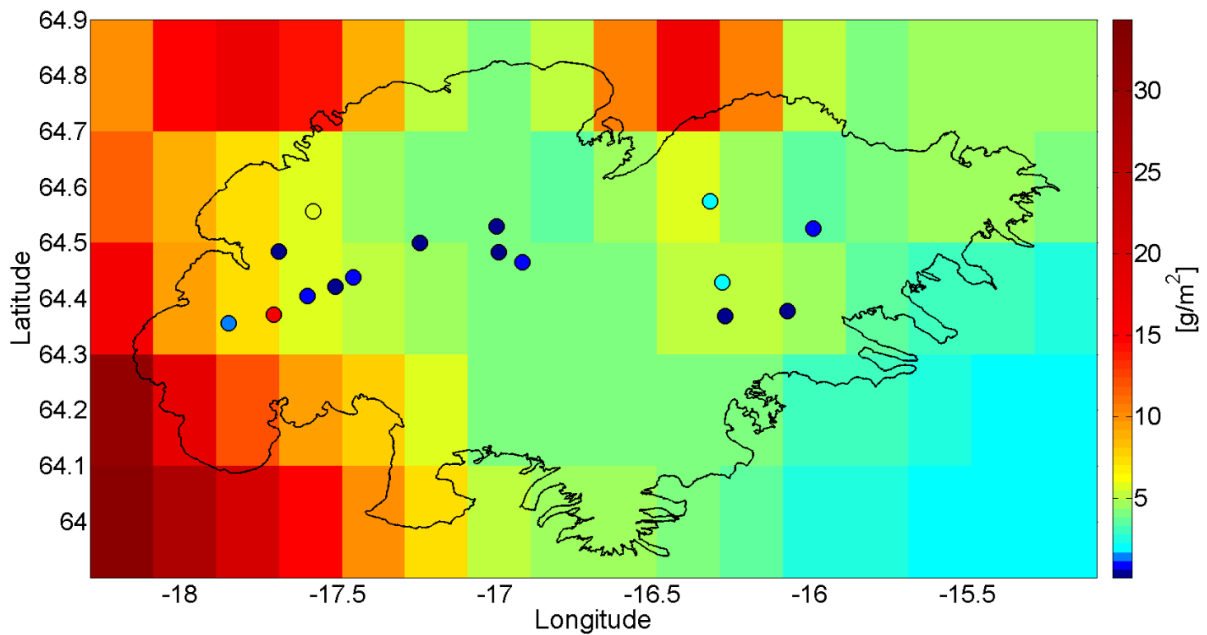

Figure 2: FLEXPART model simulation of the spatial dust distribution on Vatnajökull during 2013. The circles show the location of snow sample sites with dust deposition for the same year.
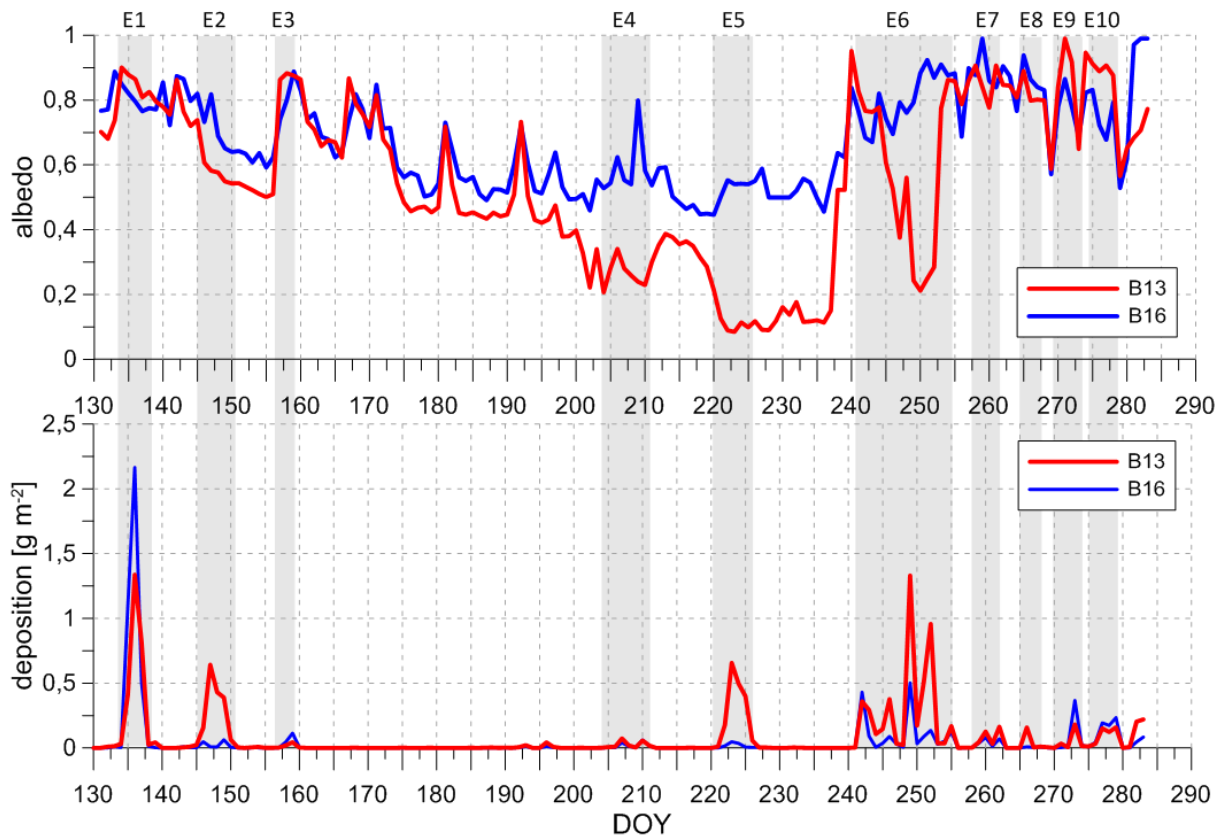
Figure 3: Upper graph: Albedo measurement from the AWS at B13 in red and B16 in blue for the measurement period in 2012. Lower graph: Daily dust deposition showing dust events modelled by FLEXPART. Dust events are highlighted in grey and named E1-E10.
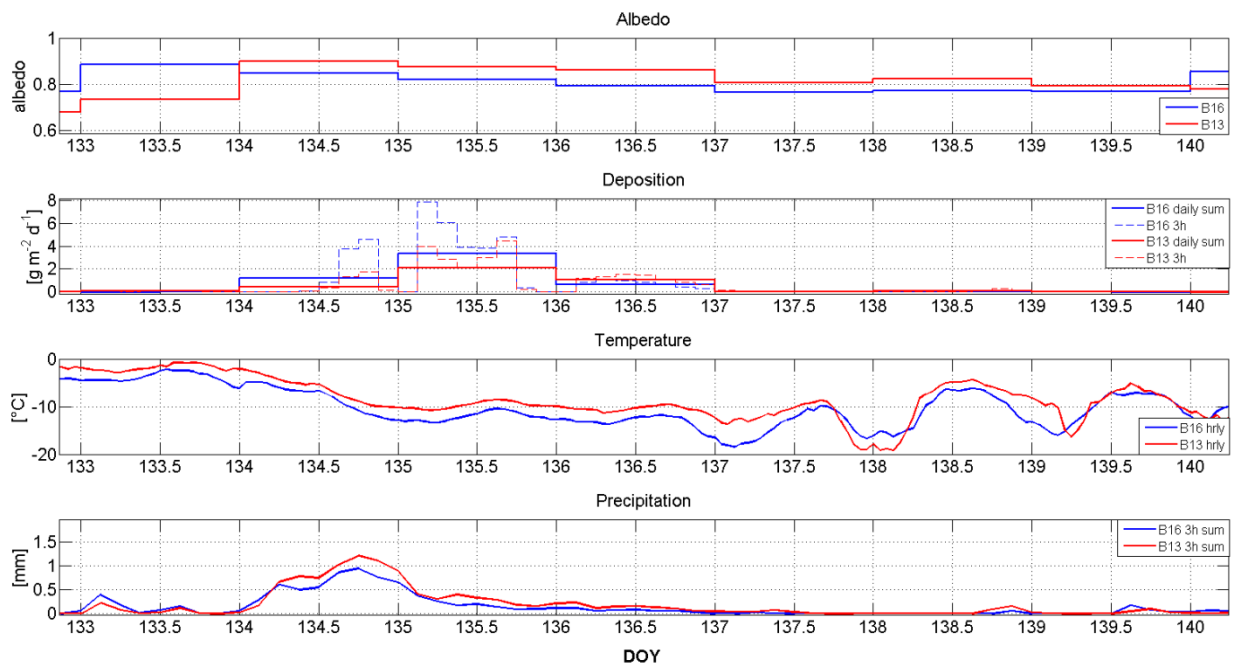

Figure 4: Observed albedo, simulated dust deposition, observed temperature and simulated precipitation dust event no. 1 at stations B16 (blue) and B13 (red). Modelled deposition is shown for 3-hourly and daily averages.
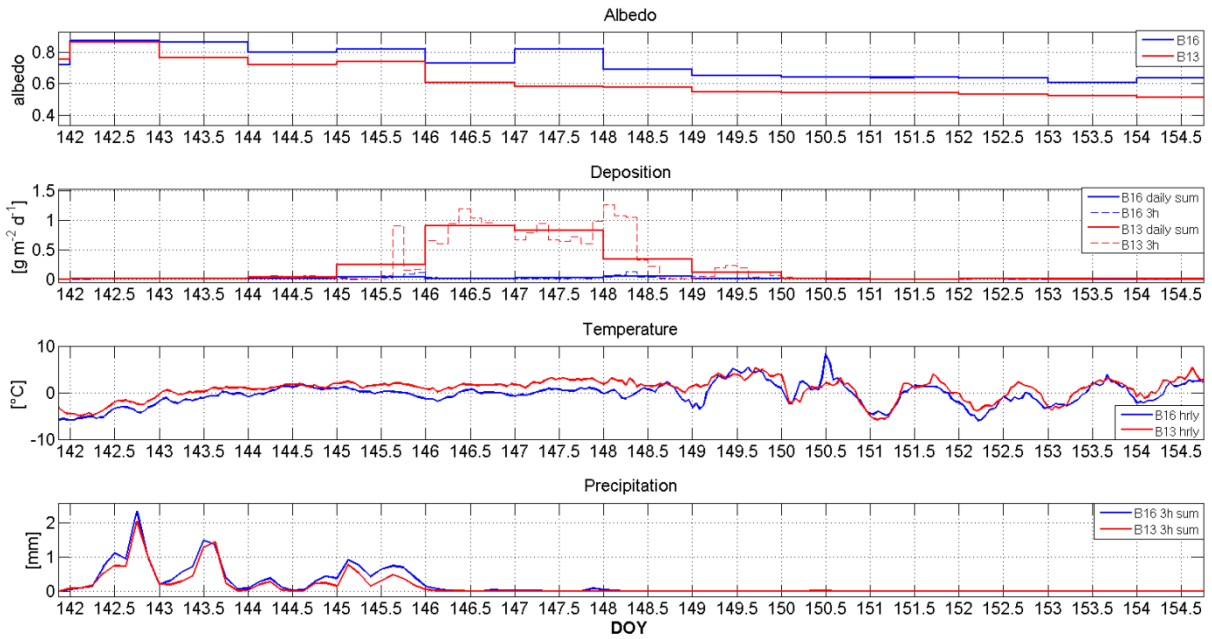
Figure 5: Observed albedo, simulated dust deposition, observed temperature and simulated precipitation dust event no. 2 at stations B16 (blue) and B13 (red). Modelled deposition is shown for 3-hourly and daily averages.
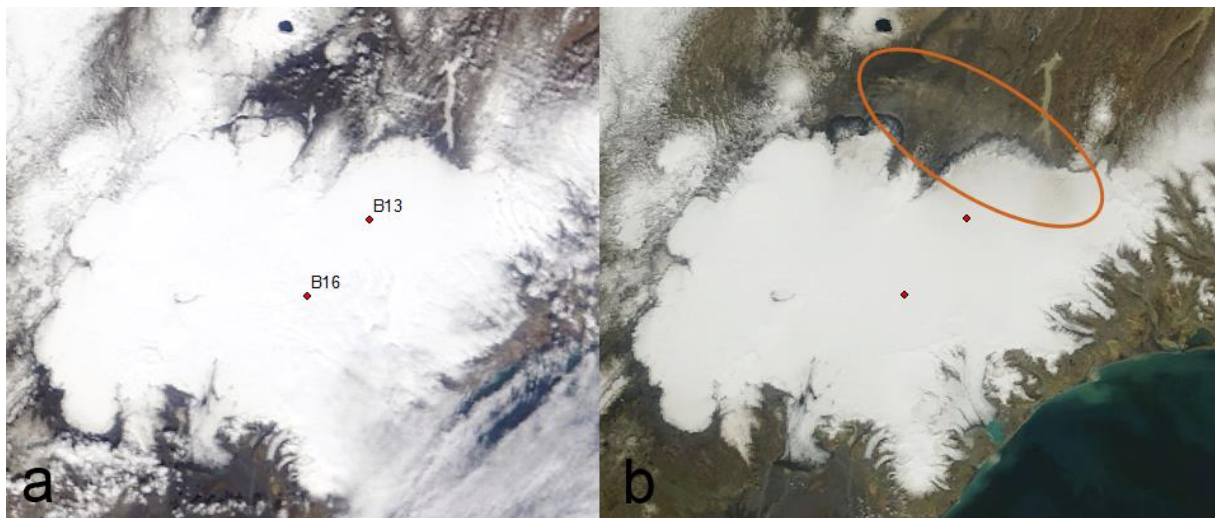

Figure 6: MODIS images of Iceland on a) 20 May 2012 (day 141) and b) 28 May 2012 (day 149). Notice the brownish hues (orange circle) on Brúarjökull outlet (north-Vatnajökull) after the dust event, which indicate that dust was deposited on the glacier. Image courtesy of MODIS Rapid Response System at NASA/GSFC. http://rapidfire.sci.gsfc.nasa.gov/
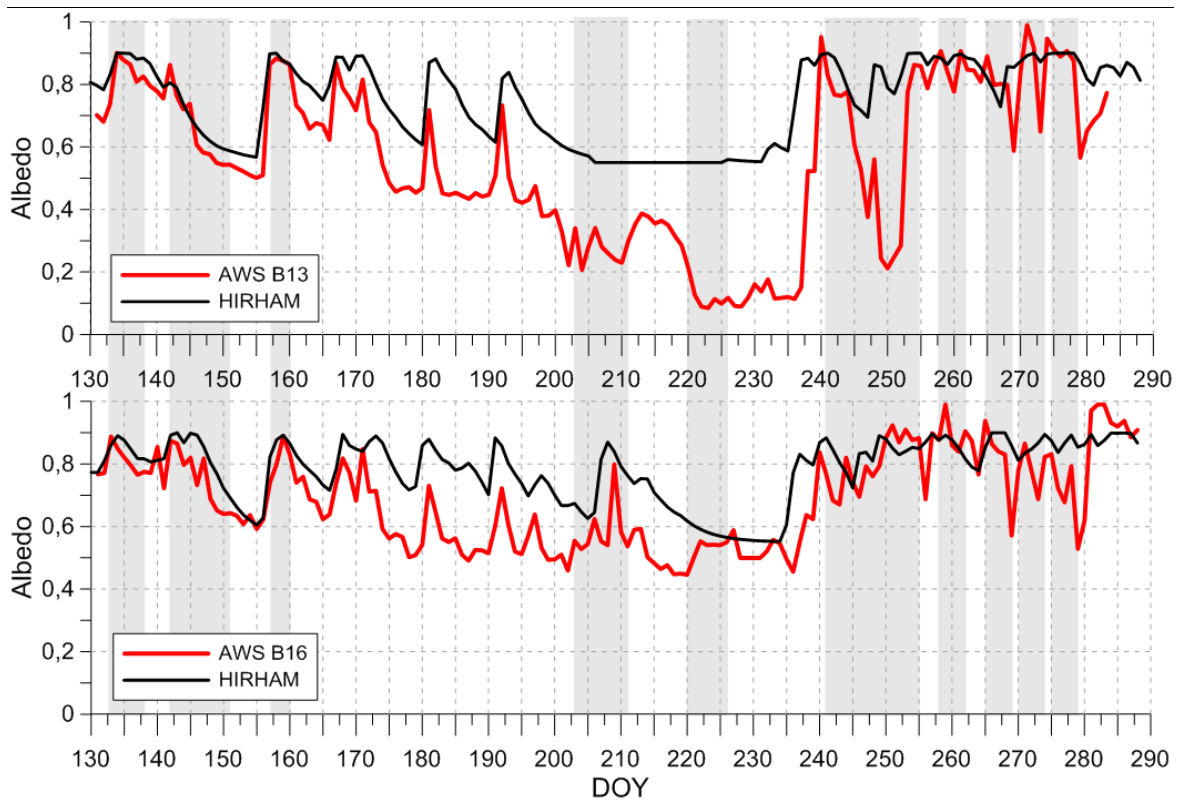
Figure 7: Measured albedo (red line) and albedo simulated with HIRHAM5 (black line) for a clean glacier surface without dust at the stations B13 (upper graph) and B16 (lower graph). Highlighted in grey are modelled dust event periods by FLEXPART.
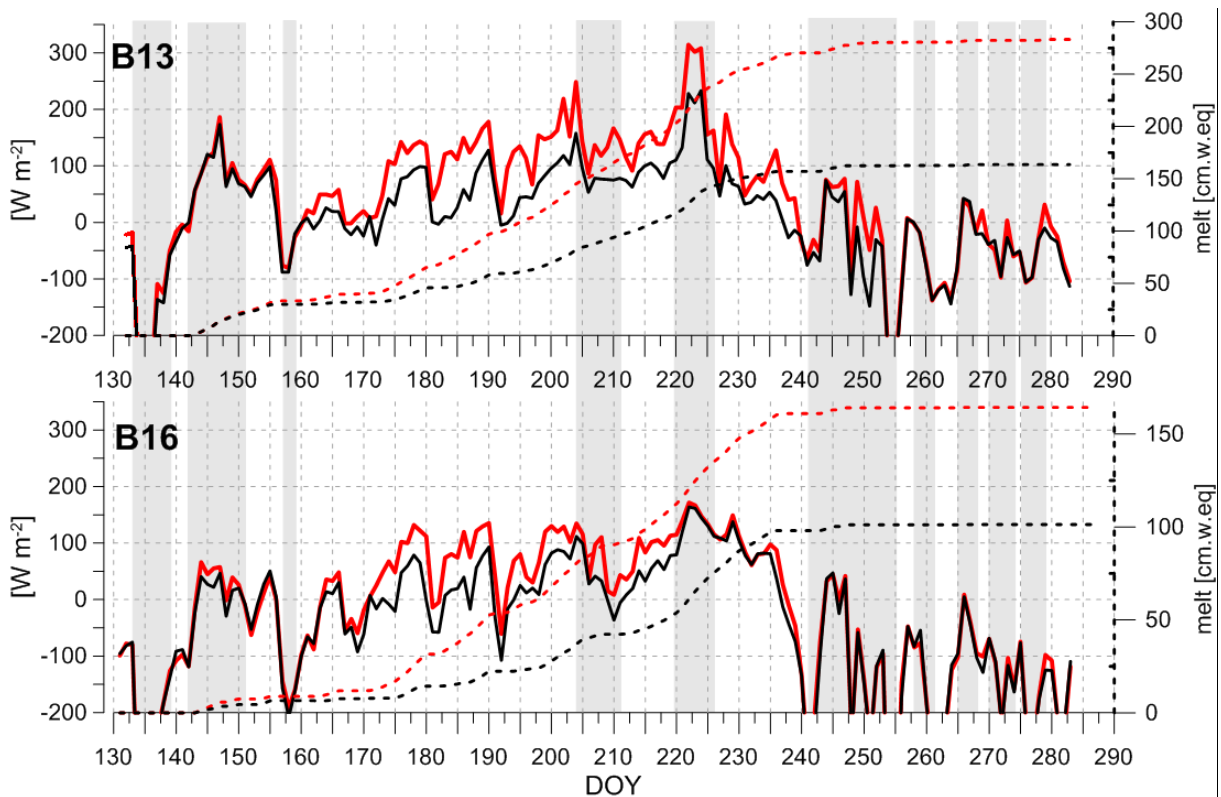
Figure 8: Measured energy balance (red line) and energy balance with simulated albedo with HIRHAM5 (black line) for a clean glacier surface without dust at the stations B13 (upper graph) and B16 (lower graph). Cumulative snow melt is shown in dotted lines for AWS in red and HIRHAM5 in black. Highlighted in grey are modelled dust event periods by FLEXPART.

Table 1: Total dust deposition [g m^{-2}] at stations on Brúarjökull in 2012 and 2013. Drill site A Figure 1is situated at station B15, drill site B 650 m below B15 at ~1400 m elevation.

2012	Measurements	Model
B16		10.4
B13		20.5
firn core 2015 A	1.7	9.1
firn core 2015 B	7.9	8.5
2013		
B13	2.0	9.4

Table 2: Dust events at station B13. Reported are the modelled maximum and minimum dust concentration, the maximum simulated daily deposition as well as the total deposition during the event, the measured albedo change, maximum and minimum temperature and wind direction from the AWS, and the precipitation sum from the ECMWF model.

			Model			AWS					Precipitation ECMWF [mm]
Event Nr.	DOY	Duration [days]	Concentration [μgm^{-3}]	Deposition [gm^{-2}]		Albedo change		Temperature [°C]		Wind	
			max	max	sum	max-min	start-end	min	max	main direction	sum
1	**133-138**	6	192.84	2.09	**3.70**	0.15	0.15	-12.7	-4.8	N	31
2	**142-150**	9	225.12	0.90	**2.48**	**0.36**	0.36	-2.9	3.4	E.S to NW	24
3	157-158	2	13.75	0.06	0.09	0.26	0.26	-3.8	-0.3	NNE	11
4	204-210	7	49.38	0.10	0.23	0.13	0.11	-0.1	2.4	S to N	19
5	**220-225**	6	212.07	1.02	**2.68**	0.04	0.04	2.0	4.8	SW	0
6	**241-254**	14	298.29	1.77	**6.60**	**0.65**	0.09	-6.2	2.4	SW to N.SE	114
7	258-261	4	44.89	0.19	0.37	0.13	0.13	-4.9	-2.4	NW to N	14
8	265-267	3	49.87	0.21	0.23	0.30	0.30	-5.1	1.4	SW.SE	48
9	270-272	3	67.86	0.29	0.33	0.34	0.34	-4.0	-1.8	W.NE.N	32
10	275-278	4	67.34	0.22	0.64	0.35	**0.35**	-10.3	-2.5	NNE	29

68

Table 3: Same as Table 2 but for station B16.

| Event Nr.	DOY	Duration [days]	Model Concentration [µgm⁻³]	Model Deposition [gm⁻²]		AWS Albedo change		Temperature [°C]		Wind	Precipitation ECMWF [mm]
			max	max	sum	max-min	start-end	min	max	main direction	sum
1	**134-136**	3	120.96	3.36	**5.22**	0.17	0.17	-14.3	-6.0	N	25
2	**145-149**	6	19.39	0.05	**0.12**	**0.28**	0.28	-4 1	2.5	once around clockwise	2
3	157-158	2	15.33	0.12	**0.17**	**0.27**	0.27	-5.1	-0.3	NNE	16
4	206-210	5	21.14	0.06	0.15	0.26	0.04	2.5	7.6	N .SW .N	4
5	221-223	3	15.01	0.07	0.15	0.01	0.01	2.2	2.9	SW	2
6	**241-254**	14	71.44	0.66	**2.34**	**0.25**	-0.04	-8.4	0.7	N .SW	110
7	258-259	2	27.92	0.07	**0.10**	0.13	0.13	-6.8	-3.7	W	4
8	no event										
9	270-273	3	51.31	0.53	0.55	0.18	0.18	-5.4	-4.7	SW .E .N	22
10	**275-278**	4	45.27	0.22	**0.64**	**0.30**	0.30	-8.7	-4.2	N	14

69

Appendix
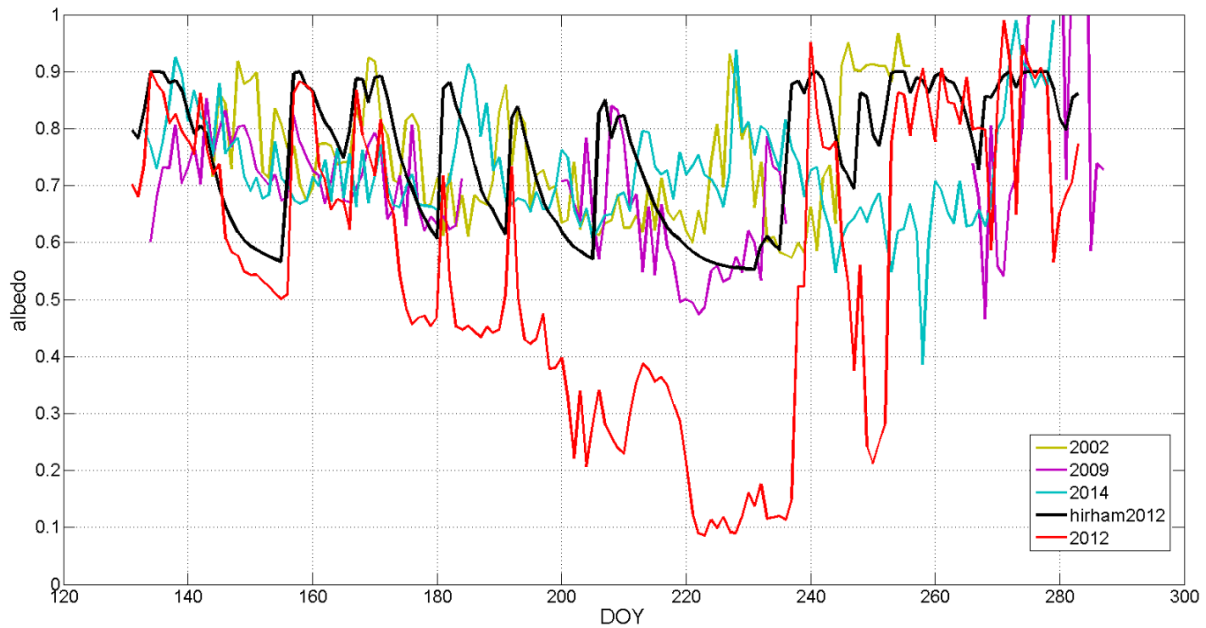
Figure A1: Albedo measurements for the AWS station B13 for the years 2002, 2009, 2012, 2014 (2002, 2009, 2014 are years of little or none surface dust) compared to the modelled surface albedo by Hirham5 (no surface dust assumed in the model) for 2012.

Albedo at station B13, which is close to the ELA is shown in Figure A1. The year 2012 was modelled by HIRHAM5 (in black) and compared to the AWS (in red) and to 3 other years of albedo measurements showing high albedo, but no melt out of the previous summer surface and a similar speed of albedo drop after a snow event. Also interesting is that after snowfall events the albedo usually peaks up to 0.9 even in the summer. If there is dust on the surface, prior to snowfall, light penetrates through the fresh thin snow cover, thus some light is absorbed by the dust and albedo will be lower than 0.9. This may help explain the low (~0.7) value of albedo in 2012 after snowfall events between days 180 and 200.
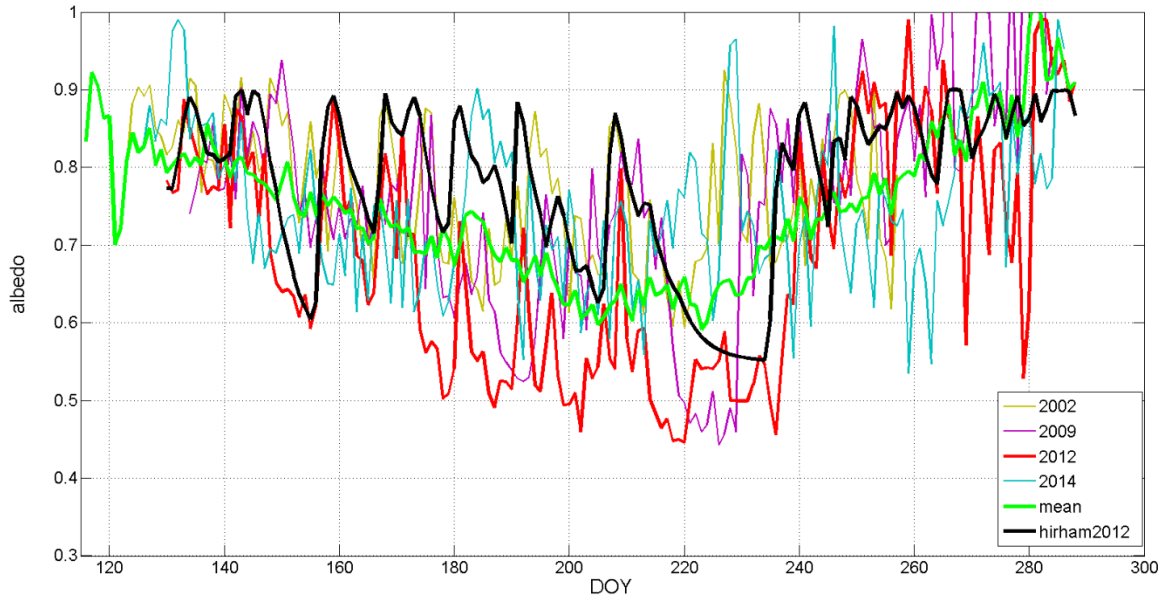
Figure A2: Albedo measurements at the AWS station B16 in the years 2002, 2009, 2012, 2014 (years of clean surface) compared to the modelled surface albedo by Hirham5 for 2012 (black curve) and the measured albedo mean for all years since 1997 (green curve).

The average measured albedo at B16 (Figure A2 in green) since 1997. In black the albedo estimate from HIRHAM5 model run for 2012 is shown (no dust on surface assumed), showing similar character as the measured albedo for the other years.
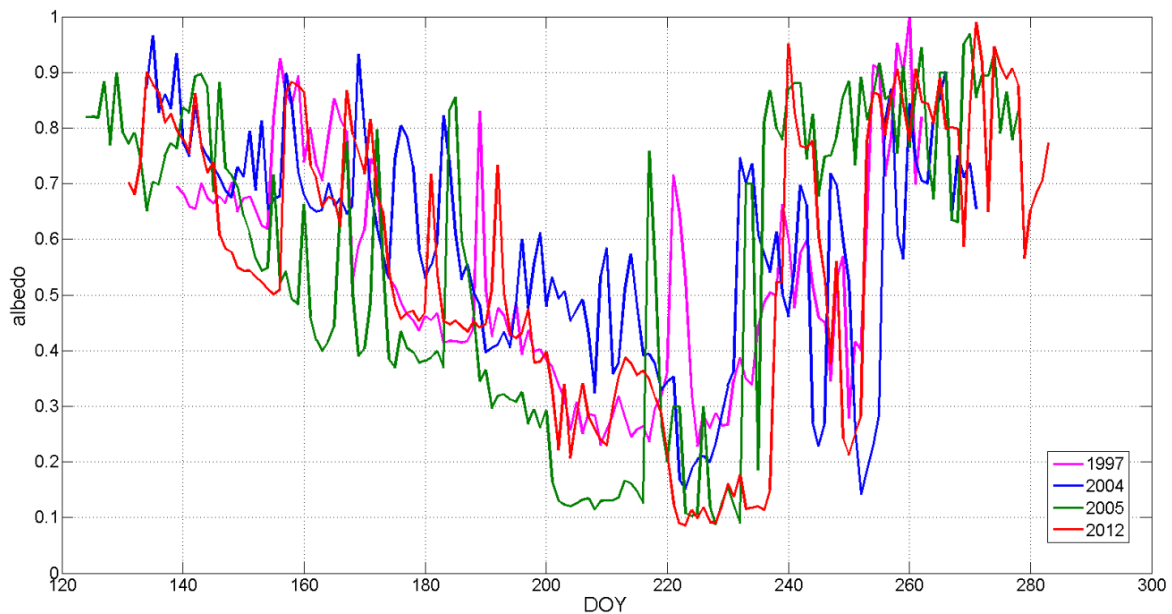

Figure A3: Albedo measurements at the AWS station B13 for selected years of very low albedo, 1997, 2004, 2005 and 2012.

Figure A3 shows years with very low albedos like in 2012 (red). The surface dirt causing the low albedo in 1997 is related to the Grímsvötn eruption in 1996, and the following huge jökulhlaup with deposition of fine grained particles on Skeiðarársandur sandur plain. This was a vast source of dust in the dry and warm 1997 summer. The low albedo in 2005 and 2012 is related to the 2004 and 2011 Grímsvötn eruptions (e.g. Guðmundsson et al. 2004, Möller et

71

al. 2013.) In 2004 increased melting rates due high wind-driven turbulent heat fluxes in the end of July followed by exceptionally warm and sunny weather in August sped up melting into old firn (Guðmundsson et al. 2006).

- Modelling of albedo evolution in dust free conditions with HIRHAM5

HIRHAM5 combines the dynamical core of the HIRLAM7 numerical forecasting model (Eerola, 2006) with the physical schemes from the ECHAM5 general circulation model (Roeckner et al., 2003). Model simulations have been validated over Greenland using AWS and ice core data (e.g. Lucas-Picher et al., 2012; Langen et al., 2015). Using the same method described in Langen et al. (2015), we run the surface scheme in HIRHAM5 by forcing it with atmospheric parameters from a previous model run. This method allows us to implement an improved albedo scheme (Nielsen-Englyst, 2015) without running the full model. One drawback of this method is that it neglects feedbacks between the surface and the atmosphere. However, since we are only interested in the albedo, and the temperature of the glacier surface of Vatnajökull in the summer is typically around the melting point, the error due to neglected feedbacks is likely small. The simulated albedo was interpolated to the AWS positions using bilinear interpolation of the four nearest grid points. The albedo parameterization is similar to that described in Oerlemans and Knap (1998), with the albedo decaying exponentially after a fresh snow fall depending on the age of the snow at the surface. However, unlike in Oerlemans and Knap (1998), the decay rate and the minimum albedo of the model depend on the surface temperature. If the surface temperature is -2°C or lower, no melt occurs and we characterise the snow as dry.

For each model time step, the albedo is updated using

$$\alpha_{snow}^{n+1} = \left(\alpha_{snow}^n - \alpha_{\{d,m\}}\right) \exp\left(\frac{-\delta t}{\tau_{\{d,m\}}}\right) + a_{\{d,m\}} \tag{3}$$

where α^n is the albedo from the previous day, $\alpha_{\{d,m\}}$ is the minimum albedo, which depends on whether the snow is under dry or melt conditions; δt is the model time step, and $\tau_{\{d,m\}}$ is a timescale which determines how fast the albedo reaches its minimum values under dry or melting conditions.

Under both melting and dry conditions, the albedo can only be refreshed to a higher value due to snowfall. In order to take the effect of rain into account, the albedo is refreshed if a certain amount of the total precipitation is snow. The model has a partial refreshment scheme, where the value of the albedo is refreshed and depends on the amount of snow. The refreshment rate is

$$rate = \min\left[1, \frac{S_f}{\delta t \cdot S_0}\right] \tag{4}$$

where S_f is the snowfall in metres and S_0 is the critical snowfall in metres per time step, equal to 0.3 m, which is needed to refresh the albedo to its maximum value. The albedo will be updated at each time step using

$$\alpha_{snow}^{n+1} = \alpha_{snow}^n + rate \cdot (\alpha_{max} - \alpha_{snow}^n). \tag{5}$$

In the case of small snow depths, the surface is affected by the underlying surface and an Oerlemans-Knapp transition (Oerlemans and Knap, 1998) is used to ensure a smooth transition between snow and ice.

Paper III

Ground based measurements of dust deposition on Vatnajökull; Firn core analysis and surface dust samples

Wittmann, M., Vogel, A., Groot Zwaaftink, C. D., Butwin, M., Pálsson, F., Thorsteinsson, Th.

Ground based measurements of dust deposition on Vatnajökull;

Firn core analysis and surface dust samples

Wittmann, M.[1], Vogel, A.[2,3], Groot Zwaaftink[3], C. D., Butwin[1,4], M., Pálsson[1], F., Thorsteinsson, Th.[1]

[1] Institute of Earth Sciences, University of Iceland, Reykjavik, Iceland; [2] University of Oslo, Department of Geoscience, Meteorology and Oceanography Section, Norway, [3] Norwegian Institute for Air Research (NILU), Atmosphere and Climate, Kjeller, Norway, [4] Icelandic Meteorological Office, Reykjavik, Iceland

Correspondence to: Monika Wittmann (mod3@hi.is)

Abstract

Icelandic glaciers are exposed to dust storms originating from sandur planes surrounding them. Small amounts of dust suspended in the atmosphere, e.g. during dust storms, amplify snow and ice melt, therefore, we wanted to investigate and quantify deposition of dust on the ice caps, specifically on the surface of Vatnajökull, Iceland's largest ice cap. Surface snow samples with dust inclusions from locations widely distributed over the glacier were collected in autumn of 2013 and 2015. The samples were investigated and the results show a generally larger dust concentration for 2013 compared to 2015. To investigate the variability of annual dust amounts, two firn cores, 650m apart, were drilled in the accumulation area of Brúarjökull in 2015 (NE-Vatnajökull outlet glacier); this was to receive many annual dust layers. The ~4.5 m long cores reached down to the summer surface of the year 2006. Analyses of the cores show clear dust layers for the years 2014, 2012, 2011 and 2008, but only very small amounts (~0.2 g m^{-2}) were detected for the years 2007 and 2013. The prominent dust/volcanic ash layers from 2011 were not located at the same depth in both cores but chemical analysis and a ground penetrating radar profile confirmed that this can be explained by the local variability of the surface/undulation even in close vicinity. Dust deposition on the surface has a negative impact on surface albedo, and this study shows a good correlation of dust amounts and minimum albedo.

1. Introduction

Located in the North Atlantic Iceland has the largest volcanoclastic desert on Earth, covering 22,000 km^2. The sand in this desert has been mainly created by glacio-fluvial processes and the volume of sand increases with the frequent volcanic eruptions. Pyroclastic materials also land directly onto glaciers and ice caps during eruptions as the volcanoes and ice are in close proximity to each other. Due to its location along the North Atlantic Storm track and its mesoscale features, Iceland frequently receives high winds. With loose dust available at the surface (particulate matter) and the common high wind speeds Iceland is very active in aeolian dust transport; 68% of the sandy deserts have active aeolian surfaces (Arnalds et al., 2016). With roughly 30 million tons of dust emissions each year some of it will inevitably be deposited on the glaciers or ice caps in Iceland (Arnalds et al., 2014). Due to the basaltic nature of the ash in Iceland, when thin layers are deposited on glaciers the albedo decreases and melting rate increases (Hansen and Nazarenko, 2004; Myhre et al., 2013, Möller et al., 2016). Dust or ash that is deposited on snow and ice changes the radiation budget, making for greater absorption of shortwave radiation (Yoshida et al., 2016, Gölles et al., 2015). When dust is deposited on snow, the lifetime of snow is decreased due to the shortwave radiative

forcing, resulting in a positive feedback loop for the melting of glaciers (Painter et al., 2007). However, when dust layers are thick and continuous, the dust serves as an insulator and prevents solar radiation from reaching the snow/ice and melting it. These conditions are often resulting from explosive volcanic eruptions such as the 2010 eruption of Eyjafjallajökull (Brock et al., 2007, Dragosics et al., 2016).

The probability of dust events occurring is high in regions that have severe or extremely severe erosion; these areas typically have little or no vegetation. Surfaces that are covered with vegetation have little erosion occurring (Arnalds et al., 2001). Areas with high erosion are located mainly along the south coast, and along glacial margins in the volcanic zone (Arnalds et al., 2001). Traditional synoptic meteorological codes for monitoring dust events in deserts, that are based on wind speed/direction, relative humidity and temperature coupled with mesoscale dust observations such as "re-suspended volcanic ash" and "blowing dust and snow" show that Iceland is one of the dustiest places on Earth. Iceland has over 135 dust days annually, where a dust day is classified when at least one report of dust is recorded (Arnalds et al., 2016). Direct measurements for severity of dust events are not made, however severity can be a function of visibility (Baddock et al., 2014). The mean visibility during a dust event in Iceland is 25 km, and there is an annual mean of six large dust events that create visibilities less than 5 km. Most of these events are classified as minor but have total annual emissions of roughly 7.6 million tons. With 50 events a year medium dust events are responsible for most emissions totalling 15.8 million tons. Major dust events have the capability to emit 1 million tons per event; major events are estimated to be responsible for 7.8 million tons annually (Arnalds et al., 2014). After volcanic eruptions that are rich in pyroclastic material these annual emissions can differ greatly from the annual averages. For example, after the Eyjafjallajökull eruption in 2010 it was recorded that over 11 million tons of ash passed over a 1 m wide transect, and events such as these continued over extensive areas (Arnalds et al., 2013, Thorsteinsson et al., 2012). However, after eruptions such as the Bárðarbunga-Holuhraun in 2014-2015 where 85 km^2 was covered in new lava possibly causing dust emissions to decrease, because the new lava covered an area that was mainly a sandur delta in an extreme erosion area (Arnalds et al., 2016).

As a result of being on the predominantly leeward side of Vatnajökull, the northern side receives less than 400 mm of rain annually. This side of the ice cap lies above an extreme erosion site, so no matter what the wind direction is, there is a possibility that dust is being transported to and deposited on the northern side of Vatnajökull. Dyngjusandur (Figure 1) is the most extensive source of dust where the Jökulsá á Fjöllum river originates, creating a large flood plain of fine grained sediment which remains mostly dry during the summer (Mountney and Russell, 2004, O. Arnalds, 2010, Baratoux et al., 2011). Between the months of May and October is the optimal time for dust to be transported to the glacier as the sandur arears are snow free and often dry. Wind data was taken from the weather station Brú á Jökuldal, northeast of Vatnajökull by about 45 km from the edge of the ice sheet (Figure 1). Wind speeds in this location can typically be between 5-15 m s^{-1} however have the potential to be 30 m s^{-1} during storms and greater than 50 m s^{-1} near mountains (see Icelandic Meteorology Office web page, www.vedur.is).

2. Methods

2.1. Surface snow samples

Snow samples from 16 locations widely distributed over the surface of Vatnajökull (Figure 1) were obtained in October 2013 (Dragosics et al. 2016). These samples were used to estimate the dust amount deposited during the glaciological year 2012/13 on the snow and ice surface.

The snow samples contained the top ~8 cm of the snow from the summer surface from an area of ~570 cm^2 (about 1-2 kg of snow) for each sample. The snow samples were transported to the laboratory of the Institute of Earth Sciences in Reykjavik frozen in plastic bags. In the laboratory the samples were melted, evaporated and the mass of the dried dust was weighed in beakers. To detect small dust layers, turbidity was measured in ppm with a MONITEK turbidity meter (galvanic.com).

In October 2015, 12 locations on the surface of Vatnajökull were sampled with a similar method. The collected surface snow samples had a mass ranging between 1.3 - 7.2 kg from a surface of 30x30 cm^2 or 40x40 cm^2. The snow was melted in the laboratory and turbidity was measured as before. Then the samples were filtered through quartz filters and the mass of the dust on the filter weighed. The locations did not all overlap with those from 2013; nine of the 12 samples were at the same locations as in 2013. However, the focus in 2015 was on Brúarjökull, therefore mass balance survey sites B13 to B16 were sampled (Figure 1).

2.2. Firn cores

During the spring expedition of the Icelandic Glaciological Society (www.jorfi.is), on 3 June 2015, two firn cores were acquired in the accumulation area of Brúarjökull outlet glacier. Core A was drilled in the close vicinity (10 m) of the mass balance survey site B15, and core B was taken 650 m down slope of the glacier from B15, towards B14 (Figure 2). At the location of core A, 590 cm of winter snow had accumulated on top of the 2014 summer layer, and 530 cm at core B. This was the thickest winter snow accumulation rates since mass balance surveys started. The sampling started from the summer surface of 2014 (chosen as the reference zero depth) indicated by a denser layer and as often characterized of summer surfaces, as well as some dust. The total lengths of cores A and B were 454 cm and 455 cm respectively; with both having the summer surface of 2014 as depth zero. The cores were drilled with an engine driven snow corer, used for mass balance measurements (3" snow corer, Engineering & Science Research Support Facility, College of Engineering, University of Nebraska-Lincoln, USA) and broke into segments during the drilling process (Figure 3). These snow and firn segments were weighted, measured (length, diameter), and labeled at the drilling site. They were transported frozen to the laboratory in Reykjavik where they were cut in half longitudinally and smaller pieces by a band saw; their dimensions were measured again, and they were melted. In their liquid state, turbidity of the meltwater was measured in a similar manner as the surface snow samples. If the turbidity was above 10 ppm, the sample was considered as dusty and filtered through a quartz filter. The dust remaining on the filter was weighted by a scale with an uncertainty of 0.1 mg.

The dust layers in the cores were dated depending on their depth and compared with mass balance measurements. The mass balance measurement of station B15 for each year was multiplied by the measured density of the firn to calculate the thickness of the firn for a certain year.

2.3. Dust transport modelling with FLEXDUST

A recently developed scheme for dust mobilization, called FLEXDUST is used to estimate dust emission and is described in detail by Groot Zwaaftink et al. (2016). For the spatial distribution of dust deposition specifically on and around Vatnajökull only dust emissions from Icelandic sources have been used. Dust emissions by FLEXDUST can be imported into the Lagrangian particle dispersion model FLEXPART developed by Stohl et al. (1998, 2005). FLEXDUST uses meteorological data from the European Centre for Medium-Range Weather Forecasts (ECMWF), land cover data by the Global Land Cover by National Mapping

Organizations (GLCNMO) and additionally, for Iceland, a high-resolution (~1 arcsec) land cover data set that identifies sandy deserts (Dagsson-Waldhauserova et al., 2014; Arnalds, 2015). Since snow cover limits dust emission this has been considered. We set a threshold friction velocity based on a set of measurements presented by Arnalds et al. (2001). As described in Dragosics et al. (submitted), contrary to FLEXDUST (Groot Zwaaftink et al., 2016), dust mobilization was assumed not to be influenced by soil moisture, but it is inhibited in case of precipitation. The model resolution uses a grid with 0.1°x0.1°, and a time resolution of 3 hours. The dispersion of dust emission rates calculated by FLEXDUST was simulated with FLEXPART version 10. The simulations were driven with ECMWF operational analysis data with a resolution of 1°x1° globally and a nest over Iceland with 0.2°x0.2° resolution. Dust was transported in 10 different size classes and was subject to both wet and dry removal. Dust has been simulated by FLEXDUST for the whole year in 2012 and 2013. Due to a change in the vertical resolution of the ECMWF data in June 2013 approximately 3 days are missing in the simulation.

2.4. Ground penetrating radar (GPR)

A Ground Penetrating Radar (GPR) profile was surveyed in May 2012 with a GSSI SIR3000 with 400 MHz transceiver geo radar. The path of the GPR profile in vicinity of the coring sites is shown in Figure 2. The drill sites of the firn cores were chosen after investigating the mass balance record for sites B14 and B15 and the GPR profile. The aim was to drill close to the average equilibrium line altitude (ELA) of the glacier to catch as many annual layers as possible with minimal spacing. The ELA varies from year to year but has been close to site B14 in the past decade. Due to the negative mass balance at B14 in 2010 and 2012 the coring sites were chosen at higher elevation, towards station B15, so no annual layers would be lost completely. As already mentioned, to calculate the year and depth of the annual layers, the mass balance (in m water equivalent) for station B15 was used for both core sites and multiplied by the firn density, taken from the measured cores and adapted with depth.

2.5. Analysis of chemical composition

To confirm the connection between the dust layers for the year 2011 found in the firn cores A and B, the chemical compositions of the bulk material from sample A20a (firn core A) and samples B14b (firn core B) were analyzed using field-emission gun scanning electron microscopy (FEG-SEM) including an integrated energy dispersive spectrometer (EDS) (Figure 4). The measurements were performed on a Nova NanoSEM650 microscope (FEI corp., Hillsboro, Oregon, USA) and the EDS analysis on an X-Max50 spectrometer (Oxford instruments, Abingdon, UK) at the SINTEF Materials and Chemistry characterization laboratory (Oslo, Norway). The SEM microscope captured the microstructure of the samples, whereas the backscatter detector recorded average elemental compositions of the powder samples. Prior to the measurements the powder samples were dried at 60 °C and mounted on a sample holder with a carbon tape before inserted into the instruments. The measurements were performed in a low-vacuum mode and analyzed using 5 kV accelerating voltage at a working distance of 6.8 mm.

2.6. Analysis of albedo and wind data

Wind measurements were analyzed on an hourly basis from the automatic weather station Brú á Jökuldal, located in the forefield of Brúarjökull, 373 m a.s.l. and ~45 m northeast from the glacier edge (Figure 1). Since the main dust source transporting material towards Brúarjökull is the dust hot spot Dyngjusandur, an area of extremely severe erosion north of Vatnajökull (Arnalds et al. 2016), wind measurements from a northerly direction were analyzed. A wind

event from a northerly direction was defined by a direction from 300-50° and a minimum speed of 5 m s^{-1} for at least two hours within the event. The analysis was done for the whole season starting from the day when the area north of Vatnajökull is at least partly snow free. The snow free conditions were inferred from inspection of MODIS images.

Surface albedo can be estimated from measured incoming and reflected short wave radiation as $\alpha = Q_o/Q_i$. Here we used data collected at the AWS stations on Brúarjökull at sites B13 and B16. Daily albedo values were calculated from measured short wave radiation at a 10 minute interval collected between 13 and 14 UTC, when the solar zenith angle is smallest. The incoming and reflected short wave radiation was measured at the AWS B13 and B16 at ~2 m elevation above the surface (Guðmundsson et al., 2006). At station B13 there are errors in the albedo measurements in 2007, therefore this year is not included in the data set. The measurement period ranges from day of the year (DOY) 120 until 300.

3. Results

3.1. Surface snow samples in 2013 and 2015, a comparison

The dust distribution on Vatnajökull, based on the surface snow samples taken in 2013 is shown in Figure 6 (modified from Dragosics et al. 2016). The 16 point samples were interpolated and in an attempt to show the spatial distribution of the dust concentration over the whole glacier. The interpolation was made with the geostatistical analyst method Inverse Distance Weighting (IDW) in ArcMap. As mentioned in Dragosics et al. (2016), topography was not accounted for in the interpolation. The sample sites are not evenly distributed over the glacier area and the southern part of Vatnajökull was not included in the interpolation due to too large distance from the measurement stations. The maximum value of dust deposited was at station T05, on Tungnaárjökull (SW Vatnajökull), with 16.6 g m^{-2} (Figure 6). Due to varying local topography, dust accumulation is not expected to be even and can collect in patches as visible in Figure 5 or gets transported somewhere else by wind or melt streams.

Surface snow samples for 2015 analyzed for dust concentration were interpolated using the same methods as for 2013 (Figure 7). It is obvious that dust depositions were overall smaller in 2015, but the spatial distribution pattern is similar, with most dust deposited on Tungnaárjökull followed by Brúarjökull.

For the two years sampled, not all of the same stations have been sampled in both years. Comparing the annual deposition (Figure 8) for the stations it is shown that only 2 of 9 had higher deposition rates in 2015 when compared to 2013.

3.2. FLEXDUST: spatial dust distribution 2012 and 2013

Figure 9 shows the dust deposition modelled by FLEXDUST for the whole year of 2012 and 2013. The modelled dust is only dust mobilized by wind, while the ground based measurements can include all sorts of material from eruptions, organic material or BC. The general dust distribution pattern shown from surface samples can be seen again with most dust deposition southwest of Vatnajökull and north of Brúarjökull. Overall, the output for 2012 has higher amounts of dust than 2013, especially in the following areas: the southwest portion of Vatnajökull, as well as away from Vatnajökull, on and north of Brúarjökull and on Dyngjujökull. However, dust deposition was higher in 2013 for some locations, e.g. on the southwestern parts of the ice cap such as on Tungnaárjökull, Skaftárjökull and Síðujökull as well as on Skeiðarárjökull and Öræfajökull.

3.3. Dust layers in firn cores

The two firn cores, cores A and B, were taken at and close to station B15 (Figure 2) in spring 2015. The oldest firn is from 2006 in the two cores. Figure 10 shows dust layers analyzed by mass of dust remaining on filters (left graph) and corresponding peaks in turbidity (right graph).

The measured dust amounts and turbidity correlates well; dust layers were found for the years 2014, 2012, 2011 and 2008. Only very small amounts of 0.2 g m^{-2} were measured in 2007 and 2013. The largest dust layer was found in 2011; 12.4 g m^{-2} of dust was measured in core B. In core A there were two layers for 2011, a smaller one at depth of 250 and a bigger dust layer in at 286 cm. The two layers sum up to 10.1 g m^{-2} (0.5 and 9.6 g m^{-2}). Also the dust layers in 2011 in core A and B were not located at the same depth, in core A they were located deeper down compared to core B (202 cm depth). This differing depth of the 2011 layer is investigated in the GPR discussion in section 3.4 and chemical analysis of samples for the 2011 layer in section 3.5. Dust layers in 2012 and 2008 are at the same depth in both cores. Since the mass balance was very negative in 2010 (-1.3 m at B13), the surface has melted down to the previous layer of 2009.

3.4. Ground penetrating radar

Figure 11 shows the profile of the GPR on Brúarjökull taken in May 2012 with a standard GSSI SIR3000 instrument. The profile is recorded from station B13 (0 distance) to B15 (ca. 13,800 m distance). The pink crosses in Figure 11 show the proximity of drill sites for cores A and B. Since the profile was recorded in spring 2012, the first layer's prominent interface below the winter snow is the summer surface of 2011 (highlighted in red) at ~3 m depth. The radar profile shows very well that the annual layers are submerging below a depth of 5 m from core B towards core A. In the layer 2011 we see fluctuation (not a straight line) and a general immersion towards core A. It has to be stated that neither one of the cores are exactly located on the radar profile. Core A is 10 m next to station B15 and core B 140 m west of the radar profile (Figure 2). From undulation of annual layers in the profile, we don't expect the two firn cores to be identical in layer depth and related dust contents.

3.5. Chemical composition of samples

To compare the samples A20a and B14b to each other, the elemental data of the samples measured by EDS were first converted in weight percent of the corresponding oxides (oxide wt. %) and subsequently averaged using a Gaussian filter function (2-sigma ranges). The major oxides found in both samples are SiO_2, Al_2O_3, FeO, MgO, CaO, Na_2O, K_2O, TiO and MnO in varying concentrations. By comparing the two samples, it can also be seen that the chemical compositions of both samples are very similar with only minor deviations in each oxides (Table 1). Furthermore, the SiO_2 (around 50 wt. %) and total alkali content indicate that the samples are basaltic origin. Only Na_2O and SiO_2 in sample A20a is slightly depleted and increased, respectively, potentially due to dissolution of the external Na layer by corrosive mixed gaseous/aqueous fluids (Delmelle et al., 2007; Vogel et al., 2016). However, the ratios between other components and SiO_2 are nearly identical in both samples.

Moreover, the chemical composition of the two samples were compared with the composition of a reference sample (REF) that was sampled ~80 km SW of Grímsvötn (near Skógar), directly after the 2011 eruption (Vogel et al. 2016, submitted). The two samples, A20a and B14b, show a very good agreement, both in chemical composition and in microstructure, to the reference sample as shown in Table 1 and Figure 4. Similar chemical composition were

also found by Kerminen et al. (2011) and Lieke et al. (2013), both for Grímsvötn ash collected in Finland and Denmark, respectively and confirm this finding. The microstructure of the samples is very compact and comparable to each other. Therefore, the two samples can be clearly assigned to dust from the 2011 eruptive event.

3.6. Albedo measurements

In Figure 12 surface albedo for the years 2007 until 2015 is shown for sites B13 and B16. At station B13 the lowest albedo was reached in 2010, followed by 2012. The year 2010 was characterized by the ash producing summit eruption of Eyjafjallajökull lasting from 14 April until 22 May (e.g. Gudmundsson et al., 2012a, Dellino et al., 2012). Ash was transported by wind to Vatnajökull, which was the main factor for darkening the glacier surface. In the firn cores no ash remained from that eruption, it is thought that the surface runoff removed the material from the surface at the core sites. The second lowest albedo year 2012 is well represented with 1.7 and 7.9 g m^{-2} of dust found in core A and B, respectively. The largest amount of dust was found in the firn cores for the year 2011, when the albedo was lower at B16 (0.32) compared to B13 (0.37). This is rather unusual that the upper station B16 has lower albedos than B13 since dust usually accumulated closer to the source areas around the glacier. The low albedo values in 2011 were caused by direct precipitation of tephra particles from the eruption plume from the Grímsvötn eruption in May 2011, lasting for a week (e.g. Petersen et al. 2012).

Figure 13 shows the MODIS image of Vatnajökull on day 224 (12 August 2011), where the lowest albedo value at B16 and B13 was recorded. It is visible that ash is not evenly distributed on Brúarjökull, and there are brighter patches around and below station B13 compared to close to B16.

The third lowest albedo (0.12) at B13 was reached in 2008, which is also the year with the third most dust found in the firn cores (3.2 and 4.6 g m^{-2}). To compare the albedo of the year 2013 and 2015 (years with dust in surface snow samples), it has to be stated that the albedo in 2015 was generally very high in both stations. Lowest values in 2015 only reach 0.58 in B13 and 0.66 at station B16. In 2013 the minimum albedo value for station B13 is 0.19 and 0.51 for station B16, which is much lower than the values for 2015.

3.7. Analysis of wind data

Northerly wind events occurred most frequently in 2012 with a total number of 71 events, 2009 had the second most frequent northerly wind events with a total of 59 events. A wind event is defined as minimum two hours consecutive wind from a northerly direction ≥5 m s^{-1}. Continuous northerly winds for at least 10 hours in a row occurred most often in 2011 and 2012 (36 and 39 times, respectively), which are also the years with most dust deposition in the analysed firn cores (Table 2). Five or more hours of continuous northerly winds with at least 10 m s^{-1} gusts occurred 18 times in 2011. Precipitation thresholds of >1 mm and >2 mm were analysed within the long events (over 10 hours of continuous northerly winds).

In the years of surface dust measurements, 2013 and 2015, there were about the same number of total northerly winds. The higher dust amount in 2013 could be explained by more total hours of strong gusts (>10 m s^{-1}) in 2013 than 2015 (152 and 73 respectively).

In Figure 14 amounts of dust found in firn core A and B are compared to the sum of hours per year with more than 10 m s^{-1} gusts. The minimum number of hours of gusts > 10 m s^{-1} was 2 hours in a row. A total of 395 hours of > 10 m s^{-1} gusts occurred in 2011. Years with more

dust amounts such as 2008, 2011 and 2012 in ice core B correlate well with a rising sum of hours of gusts. The trend line for core A (in blue) in Figure 14 lies below the one for core B which is realistic, since the location of core A is a bit higher upglacier, so the same number of events should transport less dust to the site. The same was compared with dust amount and the frequency of at least 5 hour long northerly gusts with speeds of at least 10 m s^{-1} which shows a very similar correlation pattern. However, there is high uncertainty in all measurements and a high spatial variability on a small scale as can be seen on Figure 5.

4. Discussion and conclusion

Dust on Brúarjökull is expected to get deposited during strong northerly winds originating mostly from Dyngjusandur, northwest of the glacier. There is no clear correlation between wind and dust amount because for some years firn cores show no or almost no dust, but there sometimes is still a high occurrence of northerly winds. This could be explained due to high uncertainty of dust amounts because of local variations and melt streams washing away surface dust as e.g. in 2010. In the year 2010 the eruption of Eyjafjallajökull caused a thin tephra layer in the western portion of Vatnajökull and intensified the melt rates significantly due to the absorption of shortwave radiation (Gudmundsson et al. 2012b and Pálsson et al. 2013). Gudmundsson et al. (2012a) reported the thickness of the ash layer from the Eyjafjallajökull 2010 eruption deposited on south western Vatnajökull to be a 0.1 mm thick tephra layer covering the ice. Due to the eruption in Grímsvötn 2011, this was a large source of ash deposited on and around the glacier. Therefore dust amounts in ice cores have been the largest in 2011 (12.4 g m^{-2} in firn core B) and it is very likely that ash redistribution in the following year was the reason for the second largest dust amounts found in firn cores.

The likelihood of dust getting deposited on the glacier increases with the frequency of northerly winds. However, very few wind events can be efficient enough to deposit a lot of dust from the sandur to the glacier. Dagsson-Waldhauserova et al. 2014 showed that wet surfaces were mobilized within <4 hours after a precipitation event driven by direct solar radiation and consequent surface heating to make dust airborne again. Dust amounts analysed in surface samples and firn cores have possibly have large uncertainties because dust can be washed away from the surface by rain or melt in the ablation area, gets redistributed by wind or mixed with snow. Dust often is not deposited evenly on the surface, but appears patchy or gets deposited in standing waves of the wind because of varying surface drag over an undulated surface. Also we only look at dust sources from the north; It is possible that in some cases dust can be blown over the glacier from local sources as Grímsvötn surroundings (especially at the SW boundary), other sources in the north such as Brúaröræfi (highland north of Brúarjökull), Mývatnsöræfi (highland south of lake Mývatn), in the north west and west of Sprengisandur, Tungnaáröræfi (the "desert" around Tungnaá), in the south the large sandur plains like Skeidarársandur or from further away Mýrdalssandur. However, this work proofs that in many cases the hypothesis of a northern source and certain weather conditions are likely to transport dust to the glacier surface.

Chemical analysis shows that the two firn cores in 2011 at differing depths have the same composition and belong to the eruption of Grímsvötn in the same year. The two analysed firn cores were drilled only 650 m apart from each other, and for the year 2011 the dust layers were measured at 202 (core B) and 286 cm (core A) depth. This shows that dust and other factors (e.g. wind, blowing snow or melt) can cause uneven surface smoothness and dust distribution on the surface. Therefore albedo and melt rates can differ very locally. In summary we cannot expect a perfect correlation between frequency of northerly winds and dust amount.

The comparison with minimum albedo and dust amount found in firn cores fit well together, except for 2010 with very low albedos but no dust, where we assume that dust has been washed away by surface streams due to heavy melting. Lower albedo values in 2013 than 2015 confirm the distribution of surface dust for these years with less dust in 2015.

References

Arnalds, O., 2010: Dust sources and deposition of aeolian materials in Iceland. Icel. Agric. Sci., 23, 3-21.

Arnalds, O., 2015: The soils of Iceland, 160 pp., Springer, Dordrecht, The Netherlands.

Arnalds, O., Olafsson, H., Dagsson-Waldhauserova, P., 2014. Quantification of iron rich volcanogenic dust emissions and deposition over ocean from Icelandic dust sources. Biogeosciences, 11, 6623–6632.

Arnalds, O., P. Dagsson-Waldhauserova, and H. Olafsson, 2016: The Icelandic volcanic aeolian environment: Processes and impacts — A review. Aeolian Research, 20, 176-195.

Arnalds, O., Thorarinsdottir, E.F., Metusalemsson, S., Jonsson, A., Gretarsson, E., Arnason, A., 2001a. Soil erosion in Iceland. Soil Conservation Service and Agricultural Research Institute, Reykjavik (original edition in Icelandic 1997).

Arnalds, O., Thorarinsdottir, E.F., Thorsson, J., Dagsson-Waldhauserova, P., Agustsdottir, A.M., 2013. An extreme wind erosion event of the fresh Eyjafjallajökull 2010 volcanic ash. Nat. Sci. Rep. 3, 1257. http://dx.doi.org/10.1038/srep01257

Baddock, M.C., Strong, C.L., Leys, J.F., Heidenreich, S.K., Tews, E.K., McTainsh, G.H., 2014. A visibility and total suspended dust relationship. Atmos. Environ. 89, 329–336.

Baratoux, D., Mangold, N., Arnalds, O., Bardintzeff, J.-M., Platevoet, B., Gregorie, M., Pinet, P., 2011. Volcanic sands of Iceland – diverse origins of aeolian sand deposits revealed at Dyngjusandur and Lambahraun. Earth Surf. Proc. Land. 36, 1789–1808.

Brock B., Rivera A., Casassa G., Bown F., Acuñn C., 2007. The surface energy balance of an active ice-covered volcano: Villarrica volcano, southern Chile. Ann Glaciol 45(1):104–114

Dagsson-Waldhauserova, P., Arnalds, O., Olafsson, H., Skrabalova, L., Sigurdardottir, G. M., Branis, M., 430 et al., 2014. Physical properties of suspended dust during moist and low wind conditions in Iceland. Icelandic Agricultural Sciences, 27, 25-39.

Dellino, P., Gudmundsson, M. T., Larsen, G., Mele, D., Stevenson, J. A., Thordarson, T., & Zimanowski, B., 2012. Ash from the Eyjafjallajökull eruption (Iceland): Fragmentation processes and aerodynamic behavior. Journal of Geophysical Research: Solid Earth, 117(B9).

Delmelle, P., Lambert, M., Dufrêne, Y., Gerin, P. and Óskarsson, N., 2007: Gas/aerosol-ash interaction in volcanic plumes: New insights from surface analyses of fine ash particles, Earth Planet. Sci. Lett., 259(1–2), 159–170, doi:10.1016/j.epsl.2007.04.052.

Dragosics, M., Groot Zwaaftink, Ch., Schmidt, L.S., Guðmundsson, S., Pálsson,F., Arnalds, O., Björnsson, H., Thorsteinsson, Th., Stohl, A.: Impact of dust deposition on the albedo of Vatnajökull ice cap, Iceland, submitted to the Cryosphere.

Dragosics, M., Meinander, O., Jónsdóttir, T., Dürig, T., de Leeuw, G., Pálsson, F., Dagsson Waldhauserová, P., and Thorsteinsson, Th., 2016. Insulation effects of Icelandic dust and volcanic ash on snow and ice. Arab. J. Geosci., 9, 126, doi:10.1007/s12517-015-2224-6

Gölles, T., Bøggild, C. E., & Greve, R.: Ice sheet mass loss caused by dust and black carbon accumulation. The Cryosphere, 9(5), 1845-1856, 2015. doi:10.5194/tc-9-1845-2015

Groot Zwaaftink, C. D., H. Grythe, H. Skov, and A. Stohl (2016), Substantial contribution of northern high-latitude sources to mineral dust in the Arctic, J. Geophys. Res. Atmos., 121, doi:10.1002/2016JD025482.

Gudmundsson, M. T., Thordarson, T., Höskuldsson, Á., Larsen, G., Björnsson, H., Prata, F. J., et al., 2012a. Ash generation and distribution from the April-May 2010 eruption of Eyjafjallajökull, Iceland. Sci Rep 2

Gudmundsson, S., Pálsson, F., Björnsson, H., Magnússon, E., Thorsteinsson, T., Haraldsson, H. H., 2012b. The impact of volcanic aerosols on the energy-and mass balance of Langjökull ice cap, SW-Iceland. In AGU Fall Meeting Abstracts (Vol. 1, p. 0659)

Guðmundsson, S., Björnsson, H., Pálsson, F. and Haraldsson, H. H., 2006. Energy balance of Brúarjökull and circumstances leading to the August 2004 floods in the river Jökla, N-Vatnajökull (Vol. 55, pp. 1-18). Jökull.

Hansen, J., & Nazarenko, L., 2004. Soot climate forcing via snow and ice albedos. Proceedings of the National Academy of Sciences of the United States of America, 101(2), 423-428.

Kerminen, V. M., Niemi, J. V., Timonen, H., Aurela, M., Frey, A., Carbone, S., Saarikoski, S., Teinilä, K., Hakkarainen, J., Tamminen, J., Vira, J., Prank, M., Sofiev, M. and Hillamo, R., 2011: Characterization of a volcanic ash episode in southern Finland caused by the Grimsvötn eruption in Iceland in May 2011, Atmos. Chem. Phys., 11(23), 12227–12239, doi:10.5194/acp-11-12227-2011.

Lieke, K. I., Kristensen, T. B., Korsholm, U. S., Sørensen, J. H., Kandler, K., Weinbruch, S., Ceburnis, D., Ovadnevaite, J., O'Dowd, C. D. and Bilde, M., 2013: Characterization of volcanic ash from the 2011 Grímsvötn eruption bymeans of single-particle analysis, Atmos. Environ., 79, 411–420, doi:10.1016/j.atmosenv.2013.06.044.

Möller, R., Möller, M., Kukla, P. A., Schneider, C., 2016: Impact of supraglacial deposits of tephra from Grímsvötn volcano, Iceland, on glacier ablation. J. of Glaciology 62.235, 933-943.

Möller, R., Möller, M., Kukla, P. A., Schneider, C., 2016: Impact of supraglacial deposits of tephra from Grímsvötn volcano, Iceland, on glacier ablation. J. of Glaciology 62.235, 933-943.

Mountney, N.P., Russell, A.J., 2004. Sedimentalogy of cold-climate aeolian sandsheet deposits in the Askja region of northeast Iceland. Sediment. Geol. 166, 223–244.

Myhre, G., Shindell, D., Bréon, F. M., Collins, W., Fuglestvedt, J., Huang, J., ... & Nakajima, T., 2013. Anthropogenic and Natural Radiative Forcing. In: Climate Change 2013: The Physical Science Basis. Contribution of Working Group 1 to the Fifth Assessment Report of the Intergovernmental Panel on Climate Change. Table, 8, 714.

Pálsson, F., Björnsson, H., Guðmundsson, S., Haraldsson, H., 2013. Vatnajökull: mass balance, meltwater drainage and surface velocity of the glacial year 2010-11. Institute of Earth Sciences, University of Iceland and National Power Company, December 2013, RH-24-2013

Petersen, G. N., Bjornsson, H., Arason, P., & Löwis, S. V., 2012. Two weather radar time series of the altitude of the volcanic plume during the May 2011 eruption of Grímsvötn, Iceland. Earth System Science Data, 4(1), 121-127.

Stohl, A., Forster, C., Frank, A., Seibert, P., and Wotawa, G., 2005. Technical Note : The Lagrangian particle dispersion model FLEXPART version 6.2. Atmos. Chem. Phys. 5, 2461-2474.

Stohl, A., Hittenberger, M., and Wotawa, G., 1998. Validation of the Lagrangian particle dispersion model 515 FLEXPART against large-scale tracer experiment data. Atmospheric Environment, 32(24), 4245-4264.

Thorsteinsson, Thr., Johannsson, T., Stohl, A., Kristiansen, N.I., 2012. High levels of particulate matter in Iceland due to direct ash emissions by the Eyjafjallajökull eruption and resuspension of deposited ash. J. Geophys. Res. 117, B00C05. http://dx.doi.org/10.1029/2011JB008756.

Vogel, A., Diplas, S., Durant, A. J., Azar, A., Rose, W. I., Sytchkova, A., Bonadonna, C., Krüger, K. and Stohl, S.: Reference dataset of volcanic ash physicochemical and optical properties for atmospheric measurement retrievals and transport modelling, J. Geophys. Res. Atmos., 2016, submitted.

Yoshida, A., Moteki, N., Ohata, S., Mori, T., Tada, R., Dagsson-Waldhauserová, P., & Kondo, Y., 2016. Detection of light-absorbing iron oxide particles using a modified single-particle soot photometer. Aerosol Science and Technology, 50(3), 1-4. DOI: 10.1080/02786826.2016.1146402.
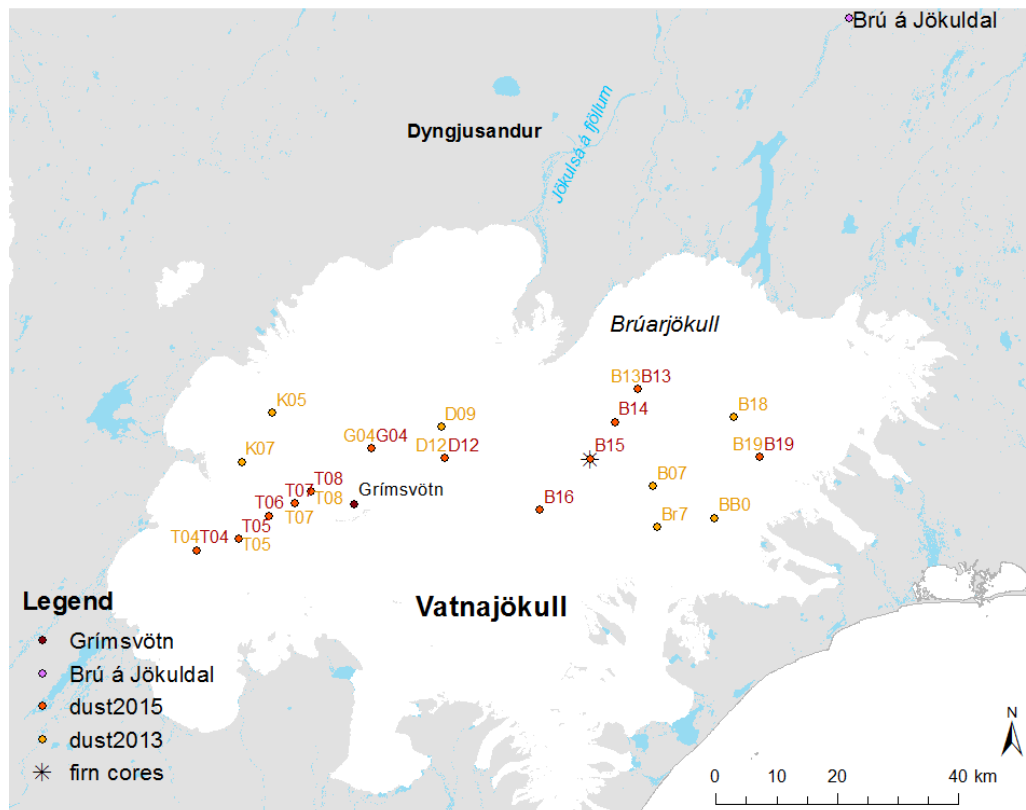
Figure 1: Locations of stations where amongst other things snow samples from Vatnajökull were taken in 2013 (yellow) and 2015 (red) to measure dust content. Wind data was used from the automatic weather station Brú á Jökuldal north east of Vatnajökull.
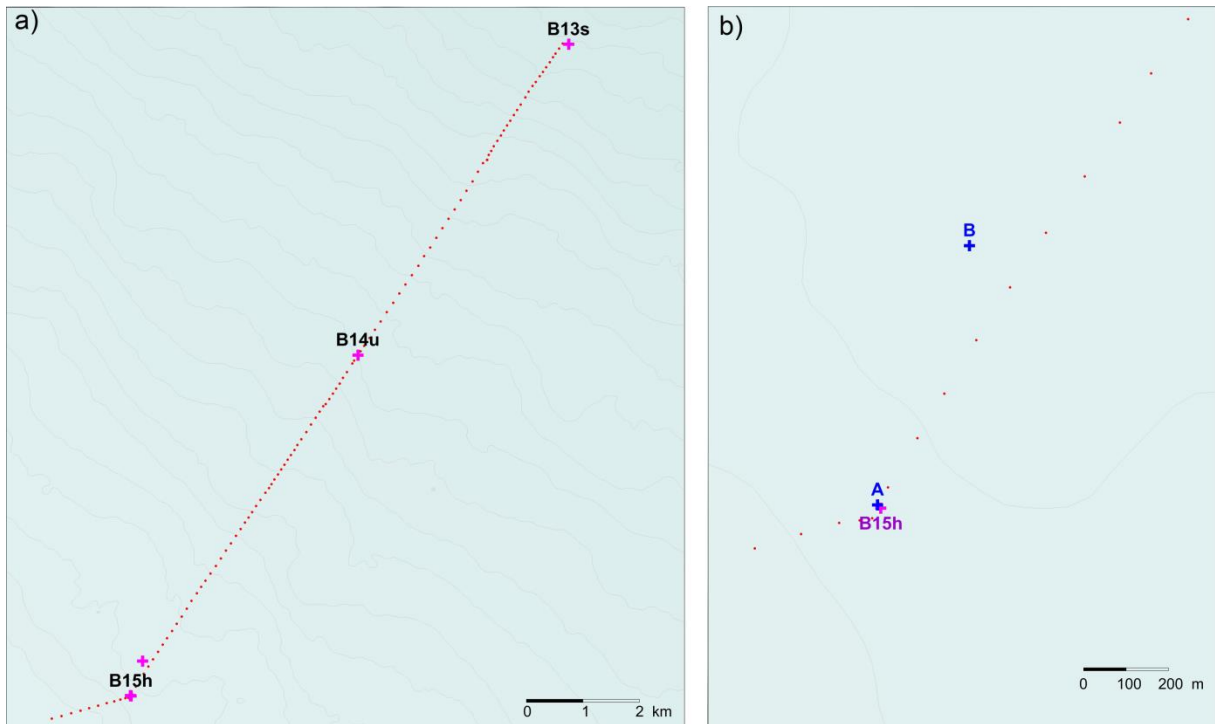
Figure 2: a) Ground penetrating radar profile on Brúarjökull ranging from stations B13 to B15 highlighted with a red dotted line. b) Location of the firn cores A and B in blue. Core A is 10m next to station B15 and core B 140m west of the radar profile.
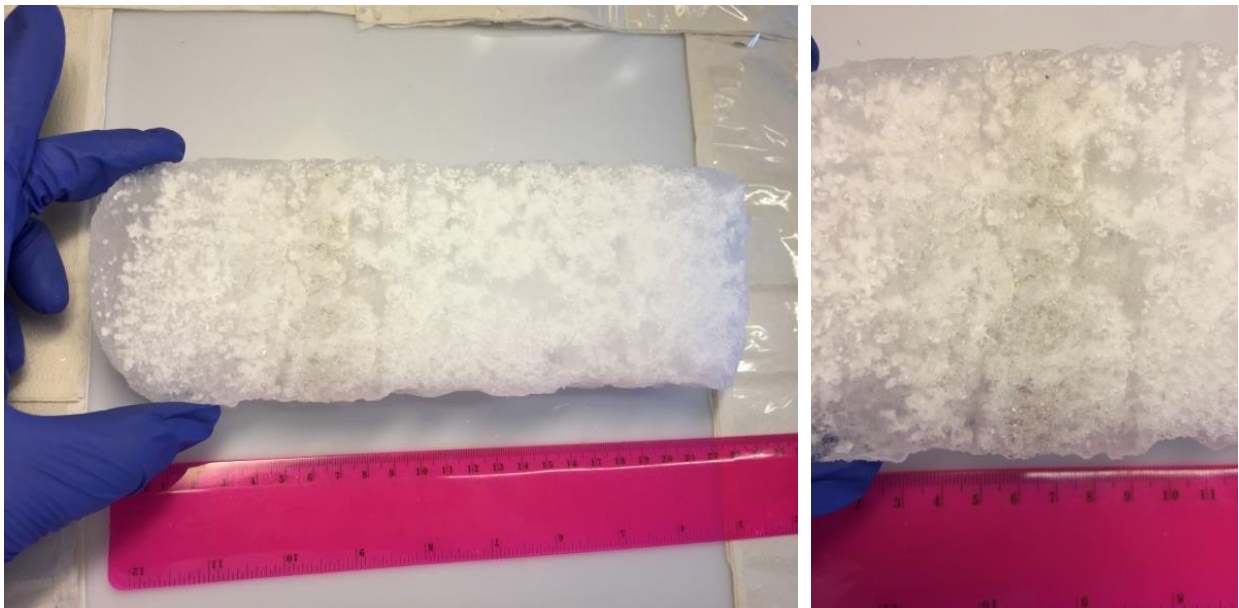

Figure 3: Dust layer 2011, firn core B 2015
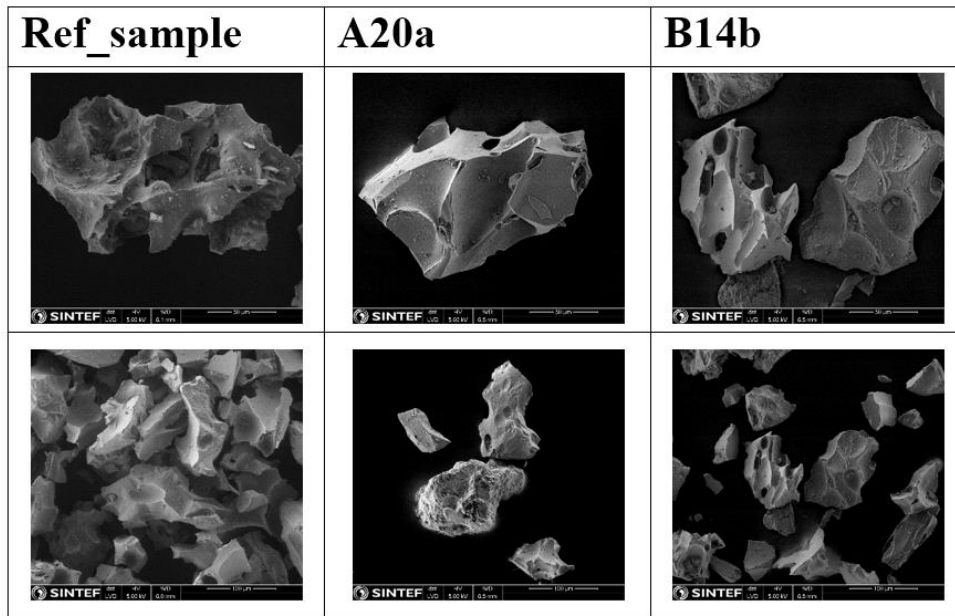
Figure 4: Microstructure of the two samples A20a and B14b in addition to the reference sample (Vogel et al. 2016)

Figure 5: Uneven surface dust collection with melt streams around station B1 (picture taken by F. Pálsson in September 2001)
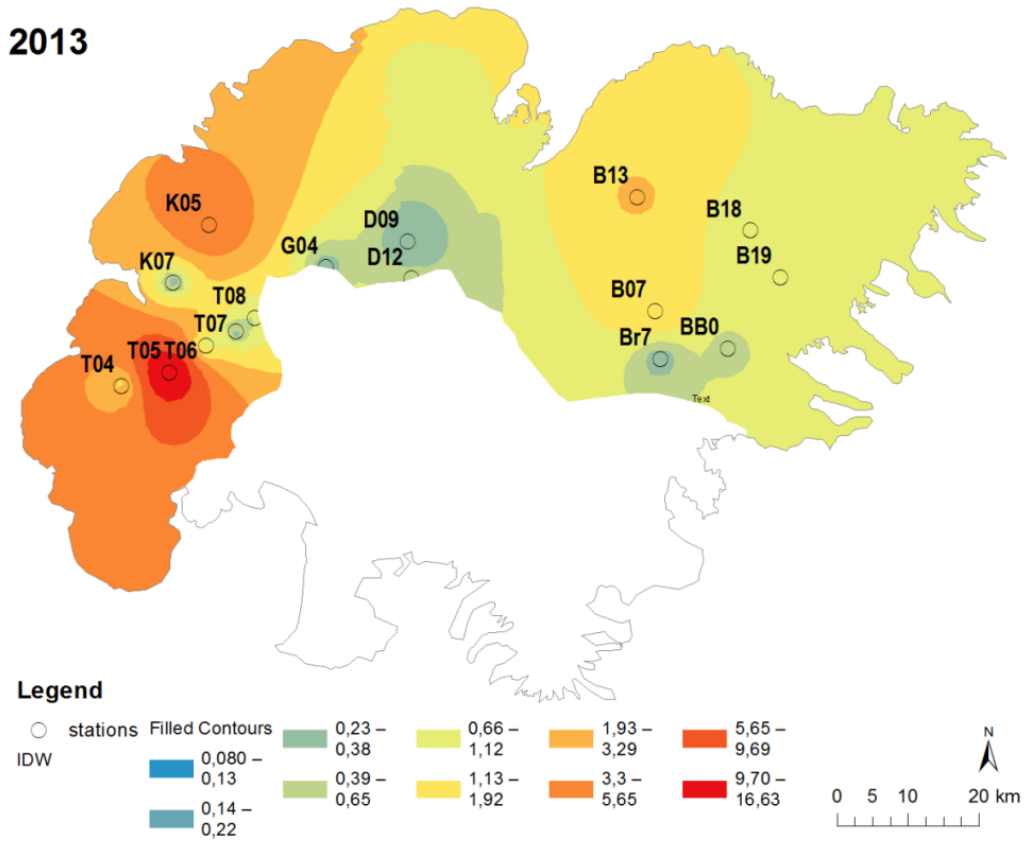
Figure 6: Surface dust interpolation based on samples in 2013
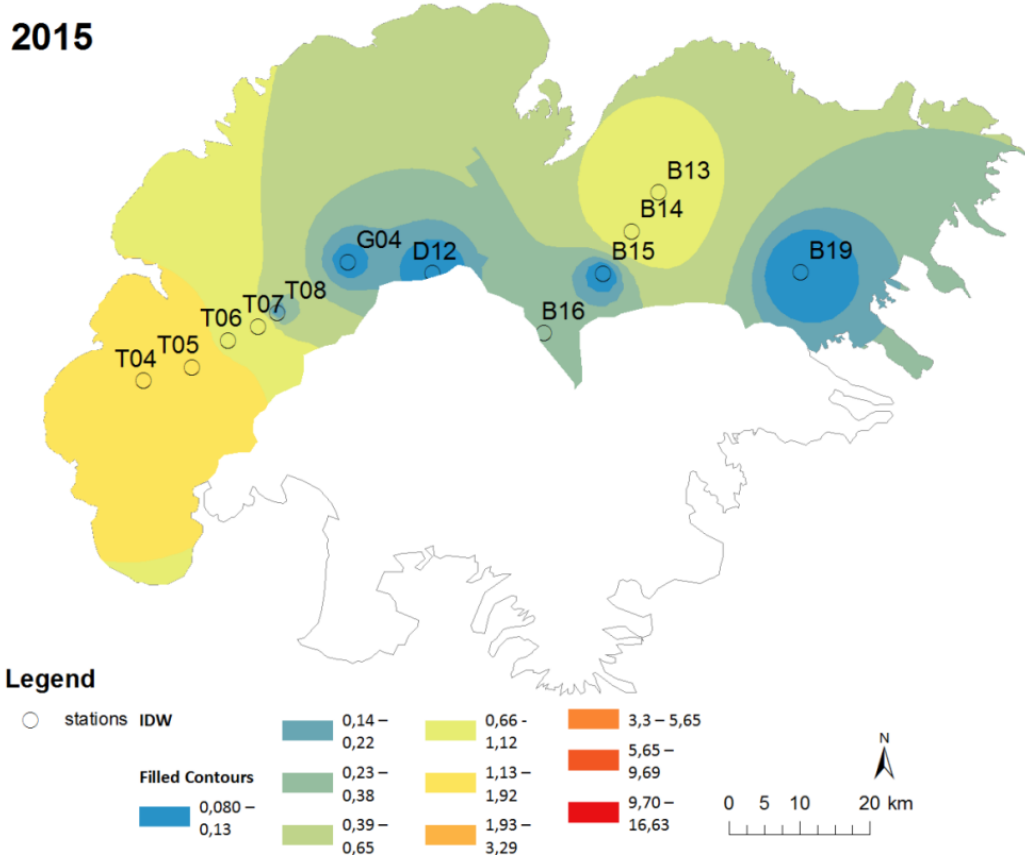
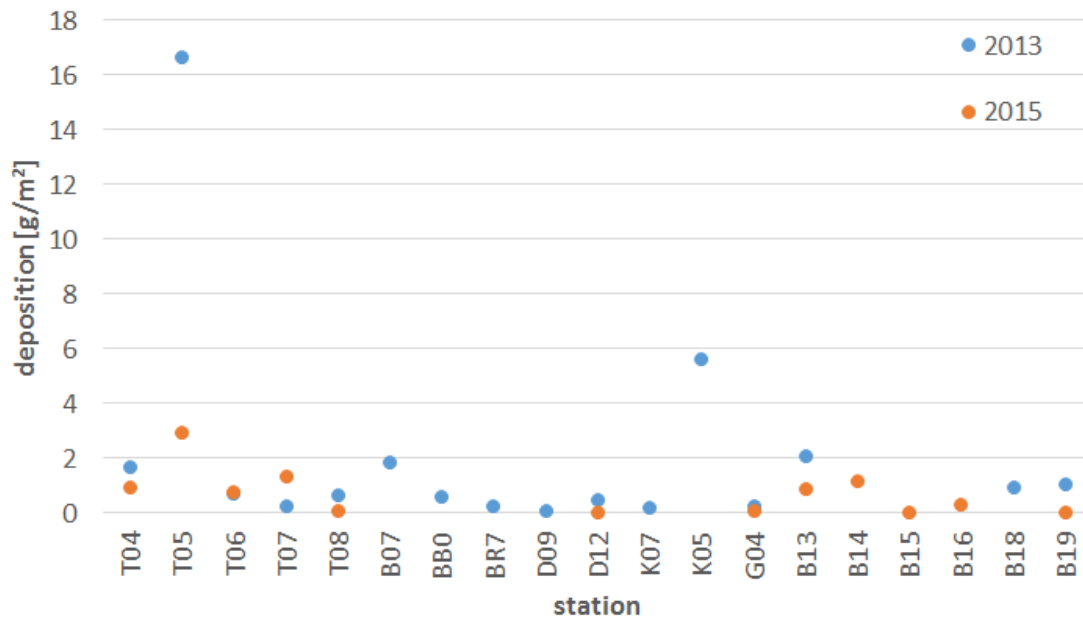*Figure 7: Surface dust interpolation based on samples in 2015*

Figure 8: Dust deposition rates for the years 2013 and 2015. Not all the same stations have been samples in both years.
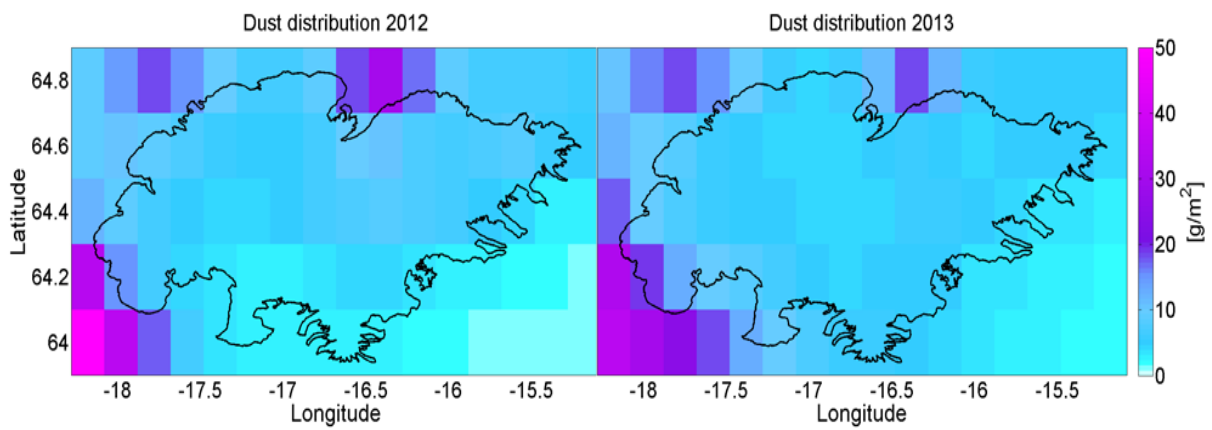

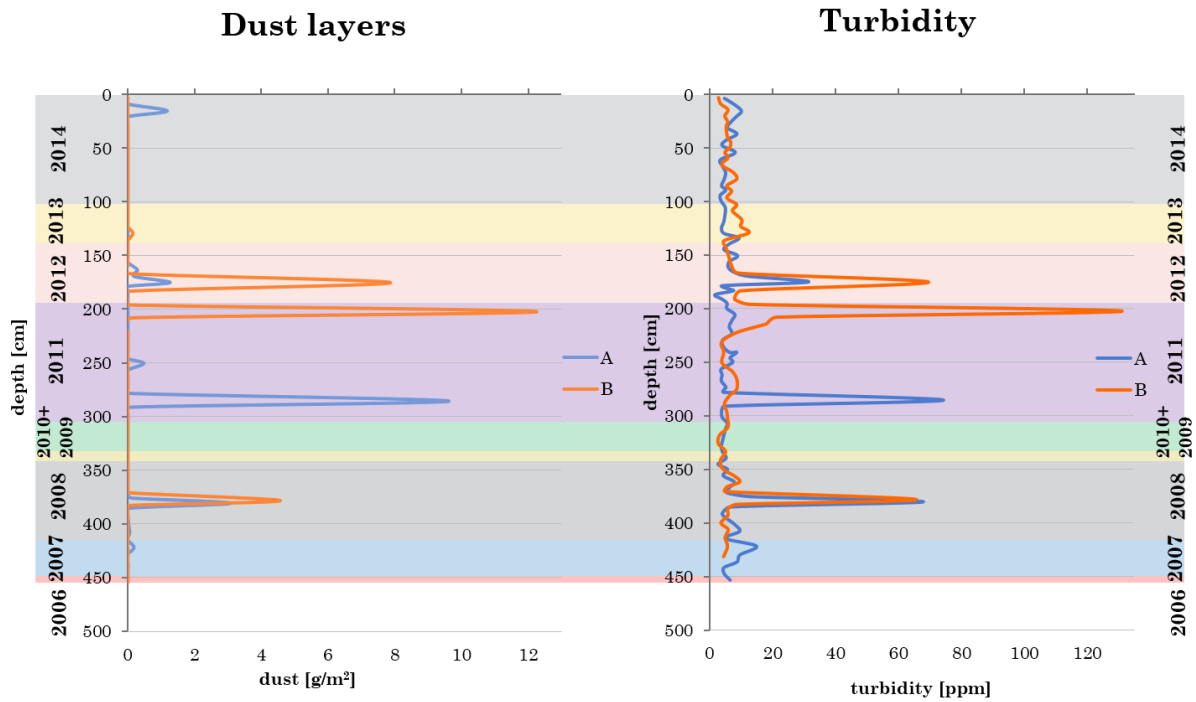*Figure 9: Modelled dust distribution by FLEXDUST for 2012 and 2013*

Figure 10: The left graph shows dust layers found in two firn cores, firn core A in blue and firn core B in orange. The different background colors indicated different years within the firn layer, from 2006 to 2014. The right graph shows the continuously measured
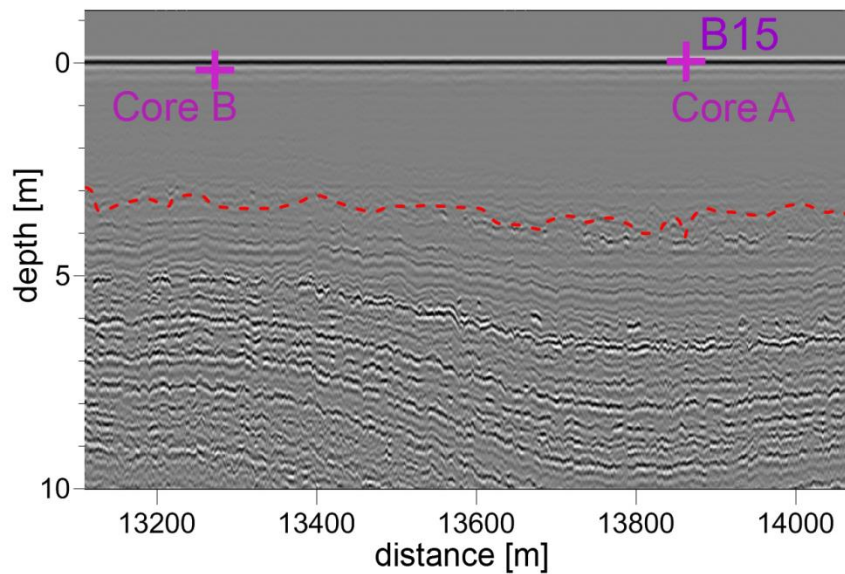

Figure 11: The ground penetrating radar profile from May 2012. The red line is highlighting the layer 2011. The darker lines are reflections by the radar and indicate annual surface layers where ice is denser. The distance on the y-axis is the distance to where the profile has started. The depth in meters starts on the x-axis at the snow surface 0. The figure is showing the position of the firn cores in the radar profile. The pink cross on the left shows the location of core B and the cross at B15 the location of core A. For this study we are zooming in the location where the cores have been taken.
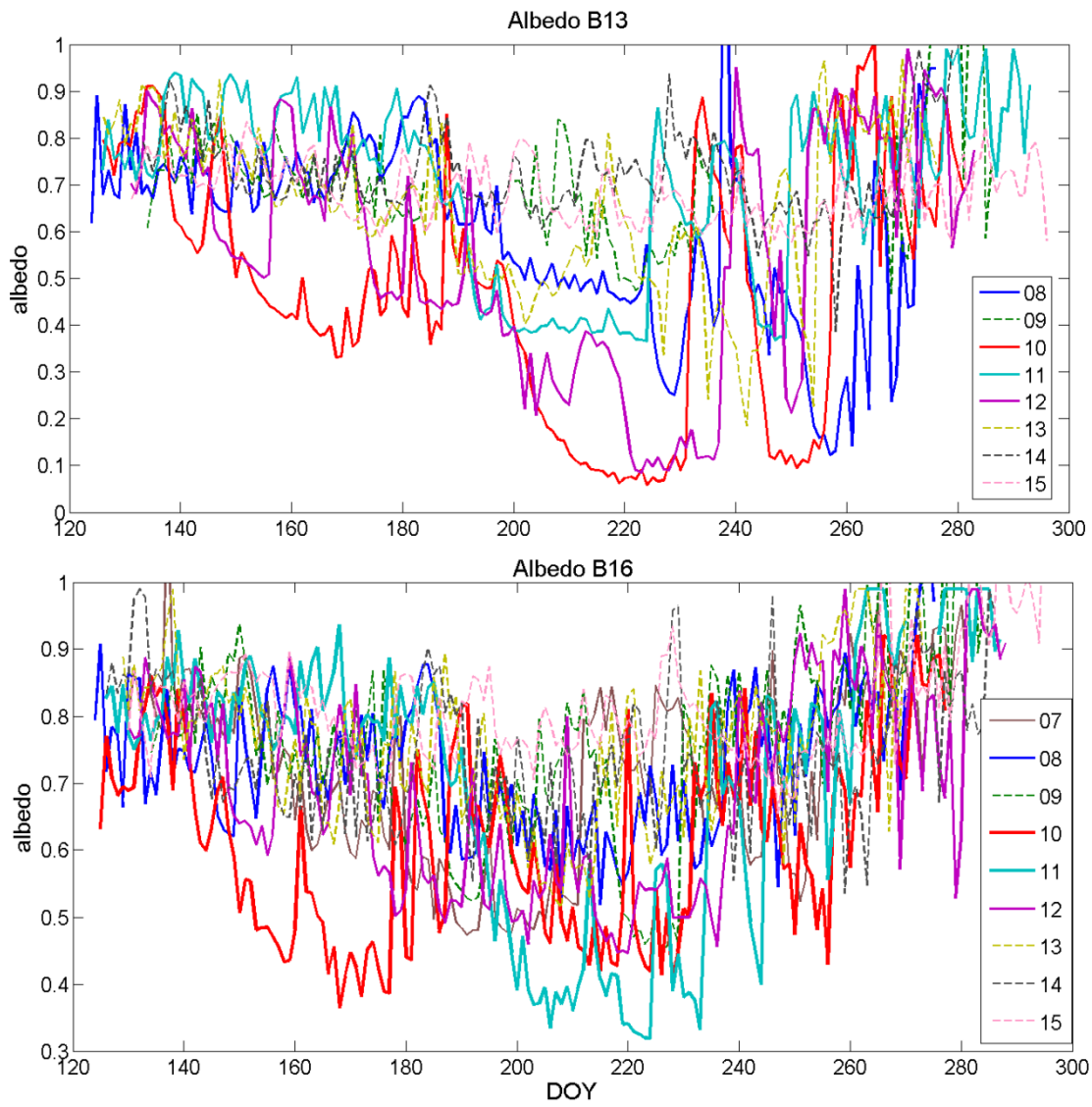
Figure 12: Albedo measured at the AWS B13 and B16 for the years 2007-2015.
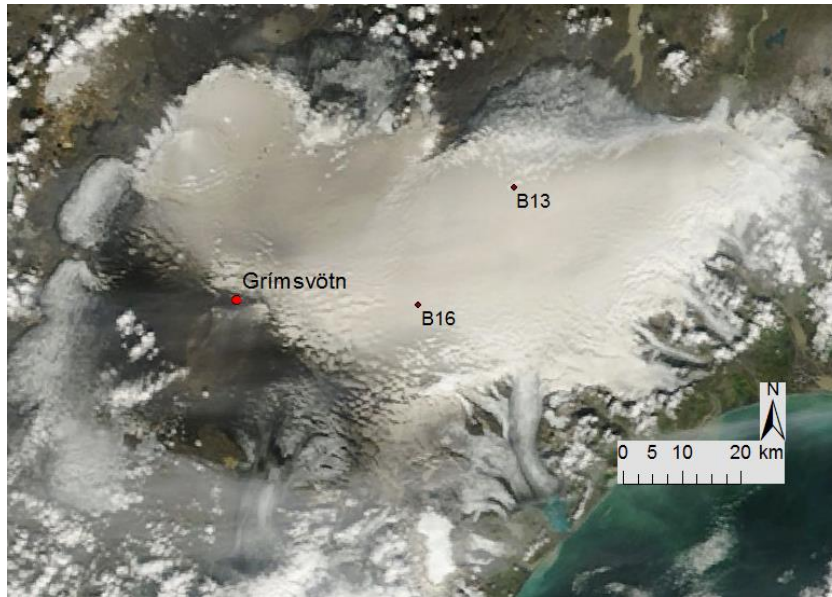
Figure 13: MODIS image after the Grímsvötn 2011 eruption showing the ash distribution over Vatnajökull on day 224 (12. August 2011) and the two AWS B13 and B16. Image courtesy of MODIS Rapid Response System at NASA/GSFC. http://rapidfire.sci.gsfc.nasa.gov/
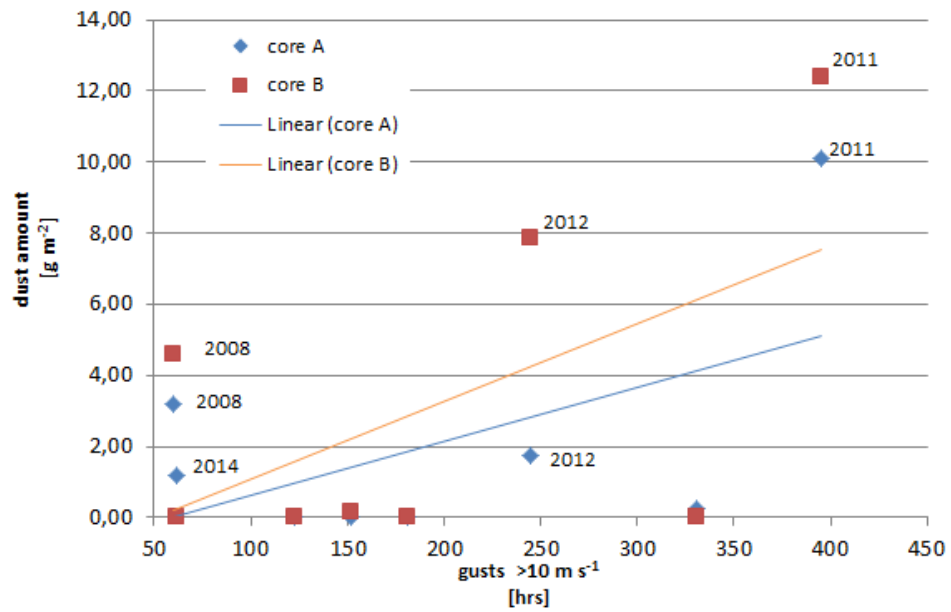

Figure 14: Correlation between dust amount in two firn cores A and B and the hours of wind gusts per year with at least 10 m s-1 speed with a linear trend line.

Table 1: Chemical composition in weight percent for the reference sample and the two samples A20a and B14b based on EDS data including composed alkali oxides and calculated ratios between individual elements and the SiO2 content.

	REF[*]	A20a	B14b
Major oxides			
SiO_2	51.7	52.0	52.5
Al_2O_3	13.6	13.5	13.0
FeO	13.3	13.5	13.4
MgO	5.83	5.77	5.40
Cao	9.54	9.74	9.60
Na_2O	3.01	2.56	3.20
K_2O	0.15	0.20	0.25
TiO_2	2.70	2.62	2.77
MnO	0.00	0.03	0.01
Total	99.8	100	100
Total Alkali (Na_2O+K_2O)	3.16	2.76	3.45
Composition ratios			
Al_2O_3/SiO_2	0.26	0.26	0.25
FeO/SiO_2	0.26	0.26	0.25
MgO/SiO_2	0.11	0.11	0.10
Cao/SiO_2	0.18	0.19	0.18
Na_2O/SiO_2	0.06	0.05	0.06
K_2O/SiO_2	0.00	0.00	0.00
TiO_2/SiO_2	0.05	0.05	0.05
MnO/SiO_2	0.00	0.00	0.00
$Alkali/SiO_2$	0.06	0.06	0.05

* Composition data of volcanic ash particles from the 2011 Grímsvötn eruption from Vogel et al. 2016 (submitted)

Table 2: Comparison of dust amounts in two firn cores and analysis of hourly wind data from the station Brú á Jökuldal for the years 2007 to 2015. Illustrated are the total events of winds from a northerly direction (300-50°, at least 2 hrs ≥5 m s^{-1} gusts per wind event), continuous northerly winds for ≥10 hrs, continuous winds for ≥ 5 hrs with speeds ≥ 10 m s^{-1} gusts,> 1 mm precipitation (P) during long wind events (continuous wind ≥ 10 hrs), > 2 mm precipitation during long wind events, and days of a (partly) snow free glacier forefield.

year	2007	2008	2009	2010	2011	2012	2013	2014	2015
dust amount core A [g m^{-2}]	0.2	3.2	0.0	0.0	10.1	1.7	0.0	1.2	-
dust amount core B [g m^{-2}]	0.0	4.6	0.0	0.0	12.4	7.9	0.2	0.0	-
surface sample B13							2.0		0.9
total N-winds events	54	31	62	42	59	71	39	22	40
N-Wind events ≥10hrs in row	29	15	26	27	36	39	24	11	28
events ≥5 hrs in row ≥10 m s^{-1} gusts	17	5	9	10	18	9	7	4	5
hrs >10 m/s gusts	331	60	123	181	395	245	152	62	73
>1mm P during long events	9	4	10	9	15	14	10	2	12
>2mm p during long events	8	5	9	4	13	10	7	1	8
days of snowfree season	212	149	192	173	214	185	171	136	172